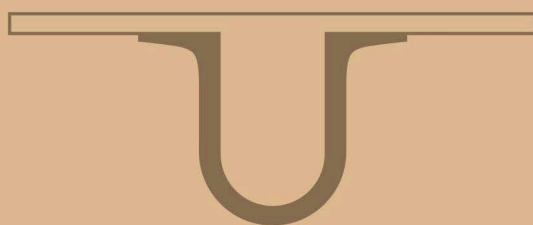


UNIVERSIDADE D
COIMBRA



João Carlos Salgueiro Simões

A NEW GENERATION OF
RING-FUSED FLUORINATED CHLORINS
AS PROMISING PDT AGENTS
FROM SYNTHESIS TO *IN VITRO* STUDIES

Dissertação de Mestrado em Química Medicinal,
orientada pela Professora Doutora Teresa Pinho e Melo
e apresentada ao Departamento de Química da Faculdade de Ciências e Tecnologia
da Universidade de Coimbra.

Setembro de 2018

Departamento de Química

A NEW GENERATION OF RING-FUSED FLUORINATED
CHLORINS AS PROMISING PDT AGENTS: FROM SYNTHESIS
TO *IN VITRO* STUDIES

João Carlos Salgueiro Simões

Dissertação no âmbito do Mestrado em Química Medicinal
orientada pela Professora Doutora Teresa Margarida de
Vasconcelos Dias Pinho e Melo e coorientada pelo Doutor Nélson
Pereira e apresentada ao Departamento de Química da
Universidade de Coimbra.

Setembro de 2018

“O caminho do conhecimento não tem fim...
é sempre mais um passo onde nunca estarás só”
- João Carlos Marques Simões (pai)

Agradecimentos

A primeira alcunha que alguma vez me foi dada foi “8 milímetros”, pois era esse o meu tamanho na primeira ecografia que a minha mãe fez. É engraçado pensar nisso porque desde esse momento várias foram as alcunhas que me foram dadas por aqueles que me foram mais importantes. De 8 milímetros passei a ser o Cuquita/Cuca, depois o Quincas, o Bão, o Joãozito, o JC, o Joca/Jocacarlitos, o Jonas Macarroni, o Jon-jon, o Joní, o Simões, o Puto, a Pessoa, entre tantos outros até ser o João ou o João Carlos. Cada um especial pelo carinho que traz consigo, pela amizade que encerra, pelas memórias que carrega. Assim, neste pequeno espaço que me é reservado para poder retribuir, decidi agradecer a todas essas pessoas que de alguma maneira tornaram esta existência em vida, colorindo-a de significado, de vontade de mais... mais noites, mais dias, mais tristezas e alegrias, mais momentos... porque no fim, fazendo as contas, não somos mais do que a soma de tantas parcelas, das quais, sem dúvida, as pessoas que encontramos pelo caminho são a maior delas todas.

Por isso, começo por agradecer aos meus pais. Obrigado por me ensinarem o que é ser amado incondicionalmente, por fazerem das tripas coração, pelas noites perdidas, por me darem mais do que me podiam, por nunca me faltar nada, mesmo que isso significasse que faltasse para vocês. Lembro-me de me chamarem o vosso herói desde pequenino, quando ainda nada havia feito para merecer esse título. Agora é a minha vez de vos dizer que os meus heróis são vocês por todos os valores que vos fazem: a caridade, a gentileza, a paciência, o sacrifício, o amor, a verdade e tantos mais, infundáveis. Obrigado por tudo, quando crescer quero ser como vocês.

Em segundo lugar, apenas porque a boa educação pede que assim seja, porque espero que saibas bem que vens sempre em primeiro, a ti, mana, o meu primeiro amor. Enquanto os pais me ensinaram o que é ser amado, tu ensinaste-me o que é amar alguém pela primeira vez. A minha melhor amiga, a minha confidente, a minha inspiração, a minha mais que tudo. Quando a vida se põe no caminho da felicidade, lá estás tu, a animar-me, a fazer-me rir, a fazer-me chorar, a fazer-me pensar e acreditar que sou muito mais do que sou. Tens este dom de fazer os outros felizes, de pões os outros à vontade de ser eles mesmos, e não há nenhum eu mais verdadeiro do que quando estou contigo... este é o maior elogio que posso dar a alguém e dou-to a ti. As

minhas melhores memórias têm apenas uma coisa em comum e és tu. Desde as férias de verão em que não havia mais ninguém para além de nós dois, às sessões de karaoke em que nos perdíamos completamente, aos bilhetes debaixo da porta quando nos zangávamos com os pais, mas não conseguíamos deixar de falar um com outro. Até as nossas zangas, e tantas que elas foram, até essas não quero esquecer só porque estás lá. Não sabendo o que nos espera, de uma coisa tenho a certeza, no meu coração encontrarás sempre um ninho, um porto de abrigo, uma pista de dança, para que possas ser tu mesma, para que possas gritar de raiva ou euforia, não importa, estarei sempre aqui. Se tivesse que te passar um último bilhete debaixo da porta diria apenas que te amo e que me terás como teu mano até ao fim dos meus dias.

A vocês, avós, pilares desta família, eternos lutadores, sonhadores, temas de mil histórias... A ti, madrinha, por estares sempre lá para mim quando preciso e por me teres dado os primos mais espetaculares do mundo.

Um pequeno parágrafo agora para os meus amigos, cada um diferente, cada um especial. A ti Joana, em primeiro, porque me ensinaste que a amizade existe fora da família, obrigado por tudo. Obrigado por seres a pessoa mais gentil, mais honesta, mais generosa e altruísta que conheci, a melhor coisa que me aconteceu naquele secundário. A ti Bruna, que juntamente com a Joana, fazem a minha família fora qualquer de laços de sangue. Obrigado por me acolheres na tua casa, no teu coração. Comigo levo as nossas maratonas de cinema, as nossas conversas na cozinha, as saudades que já tenho e a certeza de que estaremos na vida uns dos outros para sempre. A ti Cláudia, a minha companheira de laboratório, a coisa mais próxima de uma esposa que alguma vez terei, por todos os momentos que partilhámos. Contigo aprendi que deixar pessoas novas entrar na nossa pequena bolha só traz coisas boas, és um exemplo de dedicação, de força, de perseverança. Obrigado por todos os minutos que passámos juntos e como os gastámos até ao último segundo. O teu riso, se pudesse, tornava-o no meu toque de mensagens. A ti Patrícia, por seres o meu puto, por me gastares os minutos do telemóvel com dúvidas e novidades, por nunca me desiludires. A ti também Juliana, pelo teu sentido de humor e por me ensinares que é possível ficar feliz pelo sucesso dos outros sem ter inveja, apenas porque o sucesso dos outros é o nosso. Desejo-vos às duas o melhor que este mundo tem para vos oferecer e fico à espera de todas as coisas impressionantes que sei que irão alcançar. A vocês Cristiana, Andreia e Eduardo por me aceitarem, pelas horas de almoço, pelos jantares e noitadas

que sempre passaram depressa demais. Pudessem eu fazer uma hora durar dias e fazia-o para passar mais tempo com vocês. À Raquel, ao Luís e ao Filipe por serem eles mesmos, que é tudo o que peço. A todas as pessoas do laboratório que tornaram as manhãs e tardes a fazer colunas ou à espera do MTT mais toleráveis e divertidas: Vanessa, Francisco, Carla, Nélia, Américo Andreia, Ricardo, Rita, Beatriz, Catarina e, especialmente, ao Gonçalo por se ter disponibilizado para me ajudar enquanto estive no IBILI.

Por último, queria agradecer àqueles que tornaram esta tese possível, mais precisamente à Professora Teresa Pinho e Melo pela sua orientação e ensinamentos e por me ter dado a oportunidade de realizar este trabalho, ao Dr. Nélson, ao Dr. Bruno e à Professora Marta pelo seu tempo e conselhos, à Dra. Mafalda Laranjo pela sua ajuda e dedicação, à Dra. Ana Lúcia pelo seu carinho e paciência, e finalmente às doutoras Susana Lopes, Isabel Soares, Margarida Abrantes e Salomé Pires e às professoras Dina Murtinho e Elisa Serra pela sua atenção e disponibilidade.

Nada mais há a dizer para além de obrigado a todos os que me possa ter esquecido, e desejar que mais alcunhas venham se isso significar mais pessoas como vocês na minha vida.

Resumo

A terapia fotodinâmica (TFD) apresenta várias vantagens sobre as terapias convencionais contra o cancro. Combinando o uso de um fotossensibilizador (FS), irradiação de luz de um comprimento de onda específico para cada FS e oxigénio, esta alcança uma seletividade única pela produção localizada de oxigénio singleto e outras espécies reativas de oxigénio (ROS) dentro de células tumorais levando à sua destruição, traduzindo-se, conseqüentemente, em menos efeitos colaterais.

Relativamente aos fotossensibilizadores, os macrociclos porfirínicos em geral, e as clorinas em particular, têm as características fotofísicas ideais para serem usados na TFD, pois possuem um rico padrão de bandas de absorção na região espectral do vermelho e infravermelho próximo (NIR), entre 650 e 850 nm. Esta faixa é conhecida como janela fototerapêutica, e equilibra a penetração profunda dos tecidos com o fornecimento de energia suficiente para excitar o oxigénio para o seu estado singleto (comprimentos de onda mais efetivos inferiores a 800 nm). Contudo, as clorinas que resultam da simples redução de uma das ligações duplas do anel porfirínico apresentam desvantagens quanto à sua estabilidade e síntese em várias etapas. Uma vez que foi demonstrado que as porfirinas podem atuar como dienófilos em reações de Diels-Alder e como dipolarófilos em ciclo-adições 1,3-dipolar, uma forma mais simples de produzir clorinas mais estáveis é via reações de cicloadição com porfirinas que possuam dois grupos atratores de elétrons nas posições vicinais beta. Além disso, é bem conhecido que a incorporação de átomos de halogénios (-F, -Cl) nas posições orto dos anéis fenilo na posição *meso* do macrociclo melhoram as propriedades fotofísicas e apresentam propriedades citotóxicas melhoradas devido a alterarem o balanço entre a fluorescência e o cruzamento intersistema.

Esta dissertação foca-se, portanto, numa reação de cicloadição [$8\pi + 2\pi$] de 5,10,15,20-tetraquis(pentafluorofenil)porfirina (TPPP₂₀) com o anião metil diazafulvénio, gerado por extrusão térmica de SO₂ a partir de 2,2-dioxo-6,7-dimetil-1*H*,3*H*-pirazolo[1,5-*c*][1,3]tiazole-6,7-dicarboxilato. Esta reação produziu a 5,10,15,20-tetraquis(pentafluorofenil)clorina (TPPC₂₀) de um modo seletivo, a qual revelou ser um molde surpreendentemente versátil para novos derivados de clorina, uma vez que o substituinte pentafluorofenil reage facilmente com nucleófilos através, por exemplo,

de substituições nucleofílicas aromática (S_NAr) nos átomos de fluor da posição para, de forma altamente seletiva e frequentemente ocorre com alto rendimento.

Foi demonstrado, ainda, que a hidrofiliçidade dessas clorinas é crucial para garantir alta citotoxicidade contra as células cancerígenas. Sabendo que uma estratégia aplicada no design de fármacos para obter compostos com as propriedades ideais para serem utilizados em meios biológicos e para melhorar a permeabilidade celular é a incorporação de porções de polietilenoglicol (PEG), decidiu-se preparar um novo tipo de pentafluorofenilclorinas de anel fundido PEGuiladas, explorando essas mesmas reações nucleofílicas de substituição aromática. Desta forma, estas estruturas não só possuem estabilidade química e estrutural, melhorada pela introdução de um anel fundido, mas também aumentam a sua hidrofiliçidade. Estas características em associação com um padrão rico de bandas de absorção dentro da janela fototerapêutica, tornam estes compostos promissores agentes fotodinâmicos muito ativos.

O objetivo desta tese foi, em última análise, esclarecer sobre os detalhes sintéticos, a caracterização estrutural e a avaliação da citotoxicidade destes agentes muito promissores para a TFD contra linhas celulares de cancro do esófago (OE19) e de melanoma (A375).

PALAVRAS-CHAVE: *terapia fotodinâmica, macrociclos tetrapirrólicos, cancro, PEG, fluor, hidrofiliçidade.*

Abstract

Photodynamic therapy (PDT) presents several advantages over conventional cancer therapies. Combining the use of a photosensitizer (PS), light irradiation of a specific wavelength for each PS, and oxygen, it achieves a unique selectivity by the localized generation of singlet oxygen and other reactive oxygen species (ROS) inside tumor cells leading to their destruction, which, consequently, translates in less side effects.

When it comes to the PS, porphyrin type macrocycles in general, and chlorins, in particular, have the ideal photophysical characteristics to be used in PDT because they have a rich pattern of absorption bands in the red and near-infrared spectral region (NIR), between 650 and 850 nm. This is the range known as phototherapeutic window, which balances deeper penetration of tissues by providing enough energy to excite the oxygen to its singlet state (most effective wavelengths inferior to 800 nm). Their only drawback is the problems related to multi-step synthesis and stability. Since it has been demonstrated that porphyrins can act as dienophiles in Diels-Alder reactions and as dipolarophiles in 1,3-dipolar cycloadditions, a simple way to produce chlorins is via cycloaddition reactions over the porphyrins bearing two vicinal electron-withdrawing groups in beta positions, namely Diels-Alder 1,3-dipolar cycloadditions. In addition to that, it is well-known that the incorporation of a halogen atom (-F, -Cl) in the ortho positions of the phenyl rings in the *meso* position of the macrocycle improves the photophysical properties and changes the balance between fluorescence and intersystem crossing, enhancing its photo-induced cytotoxic properties.

Therefore, this dissertation focused on a $[8\pi + 2\pi]$ cycloaddition of 5,10,15,20-tetrakis(pentafluorophenyl)porphyrin (TPPP₂₀) with diazafulvenium methide, generated by thermal extrusion of SO₂ from 2,2-dioxo-1*H*,3*H*-pyrazol[1,5-*c*]thiazole.

This reaction afforded 5,10,15,20-tetrakis(pentafluorophenyl)chlorin (TPPC₂₀) in a selective fashion, which has revealed to be a surprisingly versatile template to new chlorin derivatives, since the pentafluorophenyl group easily reacts with nucleophiles through, for example, nucleophilic aromatic substitution (S_NAr) of the *para*-F atoms providing a simple and general access to functionalized *meso*-tetraarylchlorins

containing electron-donating substituents in the p-position of their *meso*-aryl groups in a highly selective way and frequently with high yield.

Furthermore, it was demonstrated that the hydrophilicity of these chlorins is crucial to ensure high cytotoxicity against cancer cells. A strategy applied in drug design to achieve compounds with the ideal properties to be used in biological media and to improve cell permeability is the incorporation of polyethylene glycol (PEGs) moieties.

For that reason, it was decided to prepare a new type of PEGylated ring-fused (pentafluorophenyl)chlorins by exploring these nucleophilic aromatic substitution reactions. This way, the obtained structures do not only show enhanced chemical and structure stability by the introduction of a fused ring but also increased hydrophilicity. All these characteristics make these compounds promising very active photodynamic agents.

The aim of this thesis was, ultimately, to offer synthetic details, structural characterization and cytotoxicity evaluation of these very promising PDT agents against oesophagus cancer cell line (OE19) and melanoma cells lines (A375).

KEYWORDS: *photodynamic therapy, tetrapyrrolic macrocycles, cancer, PEG, fluoride, hydrophilicity.*

Index

Agradecimentos	III
Resumo.....	IX
Abstract.....	XI
Index	XIII
Figure Index.....	XVI
List of Schemes	XIX
List of Tables.....	XX
List of Abbreviations.....	XXI
PREFACE	1
CHAPTER 1 – The Problem of Cancer and the Photodynamic Response.....	3
1. Introduction	Erro! Marcador não definido.
1.1. An historical background for Photodynamic Therapy.....	8
1.2. PDT mechanism of action.....	11
1.3. Active components on PDT.....	14
1.3.1. Light.....	14
1.3.2. Oxygen	16
1.3.3. PS.....	18
1.3.3.1. PS ideal characteristics	20
CHAPTER 2 – The Chemistry.....	23
1. Tetrapyrrolic Macrocycles	23
1.1. Natural Derivatives.....	24
1.2. Structure and Nomenclature.....	25
1.3. Properties.....	28
1.4. Reactivity.....	32
1.5. Synthetic Strategies for <i>meso</i> -substituted porphyrins	34
1.5.1. Rothmund/Adler-Longo’s Method.....	34
1.5.2. Lindsey’s Method.....	36
1.5.3. The Nitrobenzene Method.....	38
1.6. Synthesis of <i>meso</i> -substituted chlorins.....	39
1.6.1. Some strategies for the synthesis of chlorins.....	40

1.6.1.1.	Reduction.....	41
1.6.1.2.	Oxidation.....	Erro! Marcador não definido.
1.6.1.3.	Cycloaddition.....	42
1.6.1.4.	Diels-Alder.....	42
	✓ 1,3-dipolar cycloaddition reactions	43
	✓ 1,7- dipolar cycloaddition reactions	43
1.7.	Fluoride, more than a Hydrogen bioisostere	44
1.8.	The rationality behind the design.....	48
1.9.	So, what are the goals?.....	50
CHAPTER 3 – Experimental Section		51
1.	Experimental Section Part I – Synthesis and Characterization.....	53
1.1.	SYNTHESIS OF DIAZAFULVENIUM METHIDE 3.0 PRECURSORS.....	53
	✓ Synthesis of 1,3-thiazolidine-4-carboxylic acid (3.0a)	53
	✓ Synthesis of 3-nitrosothiazolidine-4-carboxylic-acid (3.0b)	54
	✓ Synthesis of 4,6-dihydrothiazolo[3,4-c][1,2,3]oxadiazol-7-ium-3-olate (3.0c)	54
	✓ Synthesis of dimethyl 4,6-dihydropyrazolo[1,5-c]thiazole-2,3- dicarboxylate (3.0d).....	55
	✓ Synthesis of dimethyl 4,6-dihydropyrazolo[1,5-c]thiazole-2,3- dicarboxylate 5,5-dioxide (3.0)	56
1.2.	SYNTHESIS OF PORPHYRINS	57
1.2.1.	Synthesis of 5,10,15,20-tetrakis(pentafluorophenyl)porphyrin (3.1a) 57	
1.2.1.1.	Alternative method	58
1.3.	SYNTHESIS OF THE DESIRED CHLORINS.....	59
1.3.1.	Synthesis of the diester ring-fused 5,10,15,20- tetrakis(pentafluorophenyl)chlorin (3.2).....	59
1.2.1.1	Alternative method	60
1.3.2.	Synthesis of the dihydroxymethyl ring-fused 5,10,15,20- tetrakis(tetrafluorophenyl)chlorin (3.3).....	61
1.3.3.	Synthesis of the PEGylated ring-fused 5,10,15,20- tetrakis(pentafluorophenyl)chlorin (3.4).....	63

Strategy A.....	63
Strategy B.....	64
2. Experimental Section Part II – In Vitro Studies	66
2.1. Cell Cultures	66
2.2. Cell Lines	66
2.3. Cell storage: cryopreservation	67
2.4. Cryopreservation of cells.....	68
2.5. Initiation of culture.....	68
2.6. Maintenance of culture	68
2.7. Trypan blue exclusion method.....	69
2.8. Photodynamic Treatment	71
2.9. Cytotoxicity studies.....	71
2.9.1. Metabolic Activity.....	72
2.10. Cell viability	74
2.11. Cellular uptake.....	75
CHAPTER 4 – Discussion of Results	77
1. Discussion of Results Part I – <i>Synthesis</i>	77
1.1. Synthesis of the precursors	78
1.2. Synthesis of the desired chlorins.....	81
1.2.1. The Nucleophilic Aromatic Substitution.....	83
2. Discussion of Results Part II - Aggregation and Photophysical Studies.....	91
3. Discussion of Results Part III - <i>In Vitro</i> Studies	98
3.1. Cytotoxicity Studies.....	98
3.2. Viability Studies	103
3.3. Uptake Studies	105
3.4. Comparison with the literature.....	110
Conclusions	115
Future Perspectives	117
References	123

Figure Index

Figure 1. 1 – Map of incidence (top) and map of mortality (bottom) for oesophageal cancer (left) estimated for 2012. Source: GLOBOCAN 2012 (http://globocan.iarc.fr/Pages/Map.aspx , 16 th of July of 2018).....	6
Figure 1. 2 – Map of incidence (top) and map of mortality (bottom) for melanoma estimated for the year 2012. Source: GLOBOCAN 2012 (http://globocan.iarc.fr/Pages/Map.aspx , 16 th of July of 2018).....	7
Figure 1. 3 – Molecular Structures of Photofrin, Verteporfin and Temoporfin	9
Figure 1. 4 – Modified Jablonski diagram depicting the process of photodynamic therapy. When PSs in cells are exposed to specific wavelengths of light, they are transformed from the singlet ground state (S ₀) to an excited singlet state (S ₁ –S _n), which is followed by intersystem crossing to an excited triplet state (T ₁). Abbreviation: IC: internal conversion; ISC: intersystem crossing; PS: photosensitizer; 1PS*: Singlet excited photosensitizer; T ₁ : Triplet excited state; R: biological substrate; R*: oxidized biological substrate; ¹ O ₂ : Singlet oxygen; H ₂ O ₂ : hydrogen peroxide; O ₂ *: superoxide; HO*: hydroxyl radical. (http://www.mdpi.com/journal/ijms/special_issues/photo_therapy , 16 th of July of 2018).....	11
Figure 2. 1 – Central nucleus of a porphyrin and its reduced derivatives: chlorin and bacteriochlorin.....	23
Figure 2. 2 – Structures for the heme group and chlorophyll	25
Figure 2.3 – Representation of porphyrin and porphyrinogen.....	26
Figure 2.4 – Representation of the aromatic distribution on chlorin, bacteriochlorin, and isobacteriochlorin	26
Figure 2.5 – Numeration of tetrapyrrolic macrocycles according to the Fischer Nomenclature (a) and IUPAC (b).....	27
Figure 2.6 – UV-vis spectrum of a porphyrin with an expansion of Q region between 480-720 nm.	29
Figure 2.7 – a) Axes system on the porphyrinic “backbone”; b) Representation of the orbitals and electronic transitions between the fundamental state and the excited state of complexed and “free” porphyrins according to the model proposed by Gouterman.....	29
Figure 2.8 – HOMO and LUMO energies.....	30

Figure 2.9 – Standard electronic absorption spectra for porphyrin, chlorin, and bacteriochlorin.	31
Figure 2.10 – Schematic representation of the electronic distribution on porphyrins and chlorins, according to Woodward.....	33
Figure 2.11 – Synthesis of 5,10,15,20-tetrakis(phenyl)porphyrin according to the reactional conditions established by (a) Rothmund's and (b) Adler-Longo's Method.	35
Figure 2.12 – Two-step method proposed by Lindsey in 1987 for the synthesis of <i>meso</i> -substituted porphyrins.	37
Figure 2.13 – Schematic representation of the mechanism of an aromatic nucleophilic substitution reaction.....	47
Figure 3. 1 – Chemical Structure of Trypan Blue.....	69
Figure 3.2 – Opening of the MTT's tetrazolium rings by mitochondrial reductase to form violet formazan crystals.....	72
Figure 3.3 – Chemical Structure of Sulforhodamine B.....	74
Figure 4.1 – Overview of synthesized photosensitizers.....	78
Figure 4.2.1 – Parallel dislocated faces porphyrin self-aggregates.....	92
Figure 4.2.2 – Absorbance spectra of the di-alcohol chlorin 3.3 in DMSO at different concentrations.....	93
Figure 4.2. 3 – Absorbance spectra of the di-alcohol chlorin 3.3 in water at different concentrations.....	94
Figure 4.2. 4 – Absorbance spectra of the di-ester chlorin 3.4 in DMSO and water at different concentrations.....	94
Figure 4.2. 5 – Representation of the orbitals involved in Gouterman four-orbital theory (adapted from Senge et al., 2014).....	95
Figure 4.2. 6 – Cartesian axes system for the study of free base porphyrins (D _{2h}) and representation of orbitals and electronic transitions between the ground state and the excited state, according to the Gouterman model (adapted from Nemykin et al., 2010).	96

Figure 4.2.7 – Absorption and fluorescence spectra of chlorins 3.2 and 3.4 in toluene.	97
Figure 4.3.1 – Chemical structures of the studied photosensitizers.	98
Figure 4.3.2 – Dose-Response curves for the human cell line of oesophagus carcinoma (OE19) 24 h after photodynamic treatment. The experimental values represent the mean and standard deviation of, at least, three experiments.....	100
Figure 4.3.3 – Dose-Response curves for the human cell line of skin melanoma (A375) 24 h after photodynamic treatment. The experimental values represent the mean and standard deviation of, at least, three experiments.....	100
Figure 4.3. 4 – Viability of oesophagus carcinoma cells (OE19) and melanoma cells (A375) 24 h after photodynamic treatment. The results represent the mean and standard deviation of, at least, three experiments.....	104
Figure 4.3. 5 – Uptake of the photosensitizers 3.3 (left) and 3.4 (right) at different time points and at different concentrations by cells of oesophageal carcinoma. The results represent the mean and standard deviation of, at least, two experiments.....	105
Figure 4.3. 6 – Uptake of the photosensitizers 3.3 (left) and 3.4 (right) at different time points and at different concentrations by cells of skin melanoma. The results represent the mean and standard deviation of, at least, two experiments.	106
Figure 4.3. 7 – Uptake of the photosensitizers 3.3 and 3.4 at different time points and at 1000 nM by cells of oesophageal carcinoma (left) and skin melanoma (right). The results represent the mean and standard deviation of, at least, two experiments.	107
Figure 4.4 1 – Chemical structure of the chlorin synthesized by Zhang et al.	110
Figure 4.4 2 – Chemical structure of O-chlorin	112
Figure 4.4 3 – Chemical structure of Photofrin® and Foscan®	1123
Figure 4.4 4 – Chemical structures of 4,5,6,7-tetrahydropyrazolo[1,5-a]pyridine-fused chlorins with photodynamic activity against melanoma cell line (A375).....	114
Figure 5. 1 – Chemical structures of investigated photosensitizers.	120
Figure 5. 2 – Some of the proposed structures	122

List of Schemes

Scheme 4.1.1 – Schematic route for the synthesis of porphyrin 3.1a.....	79
Scheme 4.1.2 – Schematic route for the synthesis of sulfone 3.0	80
Scheme 4.1.3 – Schematic route for the synthesis of chlorin 3.2.....	81
Scheme 4.1.4 – Schematic route for the synthesis of chlorin 3.3.....	82
Scheme 4.1.5 – Overview of the schematic route for the synthesis of porphyrin 3.1b..	86
Scheme 4.1.6 – Overview of the schematic route for the PEGylation of chlorin 3.2..	88
Scheme 4.1.7 – Overview of the schematic route for the synthesis of chlorin 3.4 from the cycloaddition reaction of porphyrin 3.1b with sulfone 3.0.....	90
Scheme 5.1 – Example of the proposed synthetic route for one of the compounds ..	122

List of Tables

Table 4.1.1 – Optimization of the reaction conditions for the synthesis of porphyrin 3.1b.....	86
Table 4.1.2 – Optimization of the reaction conditions for the PEGylation of chlorin 3.4.	89
Table 4.1.3 – Reaction conditions for the Cycloaddition of porphyrin 3.1b.....	90
Table 4.3. 1 – IC ₅₀ values of chlorins 3.2, 3.3 and 3.4 against OE19 and A375 cancer cell lines.	101
Table 4.3. 2 – IC ₅₀ in the absence of light (dark) and after irradiation (PDT) of chlorins 3.3 and 3.4 against OE19 and A375 cancer cell line, and respective PE values.....	102

List of Abbreviations

5-ALA – 5-aminolevulinic acid	GPx – Glutathione Peroxidase
5-FU – 5-Fluorouracil	GR – Glutathione Reductase
ABC – ATP Binding Cassette	GSH – Glutathione
AMD – Age-Related Macular Degeneration	Hb – Haemoglobin
ATCC – American Type Culture Collection	HIV – Human Immunodeficiency Virus
ATP – Adenosine Triphosphate	HOMO – Highest Occupied Molecular Orbital
CRT – Chemoradiotherapy	IC ₅₀ – Half Maximal Inhibitory Concentration
DDQ – 2,3-dichloro-5,6-dicyano-1,4-benzoquinone	LDL – Low-Density Lipoprotein
DFT – Density Functional Theory	LogD – Log of Partition of a Chemical Compound between the Lipid and Aqueous Phases
DLI – Drug-Light Interval	LUMO – Lowest Unoccupied Molecular Orbital
DMAD – dimethyl acetylenedicarboxylate	MCPBA – meta-chloroperoxybenzoic acid
DMEM – Dulbecco's Modified Eagle's Culture Medium	MTT – 3-(4,5-dimethylthiazol-2-yl)-2,5-diphenyltetrazolium bromide
DMSO – Dimethyl Sulfoxide	NADPH – nicotinamide Adenine Dinucleotide Phosphate Hydrogen
EBR – External Beam Radiotherapy	NCI – National Cancer Institute
ECCC – European Collection of Cell Cultures	NIR – Near Infrared
EDG – Electron-Donating Groups	NMP - N-methylpyrrolidone
EDTA – ethylenediaminetetraacetic acid	NMR – Nuclear Magnetic Resonance
EPR – Enhanced Permeability and Retention	PBS – Phosphate-Buffered Saline
ESD – Endoscopic Submucosal Degeneration	PDI – Photodynamic
EWG – Electron-Withdrawing Groups	PDT – Photodynamic Therapy
GCSG – Glutathione Disulphide	PE – Photodynamic Efficiency
GI – Gastrointestinal	PEG – Polyethylene Glycol

PET – Positron Emission Tomography

pKa – Acid Dissociation Constant At Logarithmic Scale

PPM – Parts Per Million

PS – Photosensitizer

ROS – Reactive Oxygen Species

RPMI – Roswell Park Memorial Institute 1640 Medium

S_nAr – Nucleophilic Aromatic Substitution

SOD – Superoxide Dismutase

SRB – Sulforhodamine B

TAPC – (4-(3-n,n-dimethylaminopropoxy)phenyl)chlorin

TCB - trichlorobenzene

TCNE – Tetracyanoethylene

TLC – Thin-Layer Chromatography

TMS – Tetramethylsilane

TPFPP – *meso*-Tetrakis(Pentafluorophenyl)Porphyrin

TPP – Tetraphenylporphyrin

UV-Vis – Ultraviolet–Visible

Tt – Lifetime Of The Excited Triplet State'

ΦT – Quantum Yield Of The Excited Triplet State

PREFACE

Humankind has been, is, and will forever be, the most interesting mystery, the problem that drives all answers, the infinite well of questions. From consciousness which leaves us wondering around philosophical questions, to the unit of life that all living things, of which we are included, are made from, we cannot escape the simple complexity of ourselves, and what seems to be two completely separate fields, is, in the end, the same, a bug of curiosity that has stuck its teeth on our skin and that we find ourselves in the need of scratching. Then, tickled by the charming unknown, as people in general, and as scientists in particular, all that is left to do is to find a reason, a reason to all of this, from the universe to the atom, a reason that explains why we are here, what are we doing here...

Over the years, there has been a constant progress in science, and especially on the field of life sciences that has allowed us to improve our understanding of the human organism and its pathologies, thereby giving us the chance to know ourselves and the world we live a little better. From all pathologies, there are some that because of their devastating consequences or their intricacy, have been on the frontline of investigation and cancer is one of those. Cancer is a fascinating subject, maybe because we're programmed to see growth as a natural and beautiful step of existence: a child that turns into a man, a seed into a flower, an idea into a book, they all start as small things that grow over time, and so, to find out that cancer is a group of diseases involving abnormal cell growth, with the potential to invade or spread to other parts of the body, shakes our pillars. Makes us uncertain of what we had learned so far and had taken as truth. It's very interesting to have our points of view, our beliefs, shaken, because it wakes in us a desire to strengthen ourselves, and the only way to do so is by knowledge.

This dissertation is, ultimately, added knowledge, added strength, and added power, not only to me but hopefully to the world. In its small contribution to the scientific state of the art, the main goal is to help to get closer to a solution on a problem that is undeniably in need of new blood and of a revolution of mindsets and work-strategies.

CHAPTER 1 – The Problem of Cancer and the Photodynamic Response

1. Introduction

The increase in overall incidence rates and non-response to current therapies has turned cancer into a growing worldwide socioeconomic concern. After all, regardless of the huge global research efforts, cancer remains a leading cause of death worldwide with 8 million deaths every year and the problem is not circumscribed: it is estimated that this number will double in the next 20 to 40 years, with a higher incidence in developing countries, with one in four people dying of cancer in Portugal, according to Eurostat. In addition, the cost of developing innovative drugs has increased dramatically, while new drug approval rates are moving in the opposite direction, also affecting the oncology segment (Ferlay *et al.*, 2013).

In the last decades, due to the scourge of this problem, scientific research has focused on the search for new antitumor agents, thus becoming a worldwide topic of interest. Although traditional therapeutic strategies have provided significant advances, offering high cure rates for some types of cancer, they are also responsible for the occurrence of serious adverse effects, and its effectiveness is somewhat questionable. This can be explained by the heterogeneity and genetic complexity of the tumors within the population and that is why all life-related fields, from medicine and medicinal chemistry to pharmaceuticals, have put so much effort to develop new, safer, more effective and specific therapies for cancer.

One of the major barriers when it comes to traditional cancer therapies is the development of drug resistance often attributed to the emergence of tumor cell populations that are insensitive to cytotoxic drugs. One of the well-known causes for this is the high mutation rate cancer cells are notable for. Other explanations might be: reduced drug absorption or increased drug efflux, drug target modifications or activation of alternative pathways of cell survival (Agostinis *et al.*, 2011). Another mechanisms usually associated with multiple drug resistance in chemotherapy is the

active transport of a large class of hydrophobic anticancer drugs from the cytoplasm to the extracellular medium, mediated by a membrane carrier family known as the ATP binding cassette (ABC).

Over the years, increasing understanding of the genesis, progression and dissemination mechanisms of cancer has allowed the development of several therapeutic strategies, such as angiogenesis inhibitors, active cytotoxic drug focus, gene therapy or immunotherapy. Photodynamic Therapy (PDT) has also presented itself as a promising cancer therapy, since it shows several advantages regarding tolerability profiles, absence of specific resistance mechanisms and the ability to stimulate the immune system, which is seen as a great differentiation factor, when compared with traditional oncology therapies (Serra *et al.*, 2008; Agostinis *et al.*, 2011).

Photodynamic therapy starts with the administration of a photosensitizer (PS), ideally a molecule with high tumor selectivity (Plaetzer *et al.*, 2009). The PS is then activated by light at an appropriate wavelength to initially form the excited singlet state, followed by a transition to the long-lived excited triplet state, which then can undergo photochemical reactions in the presence of oxygen to form reactive oxygen species (including singlet oxygen). The generated reactive oxygen species (ROS) induce malignant cell death, damage tumor-associated vasculature and activate the antitumor immune response. At the same time, the lifetime of singlet oxygen (1O_2) is very short, limiting its diffusion to only approximately 50 to 100 nm in cells. Thus, the photodynamic damage is likely to occur very close to the intracellular location of the PS (Pereira *et al.*, 2018). Since the PS only becomes toxic upon light-irradiation, it allows for selective targeting of the tumor cells without affecting healthy tissue. The dual-specificity of PDT, therefore, relies on the accumulation of the PS in diseased tissue and also on localized light delivery (Abrahamse *et al.*, 2016).

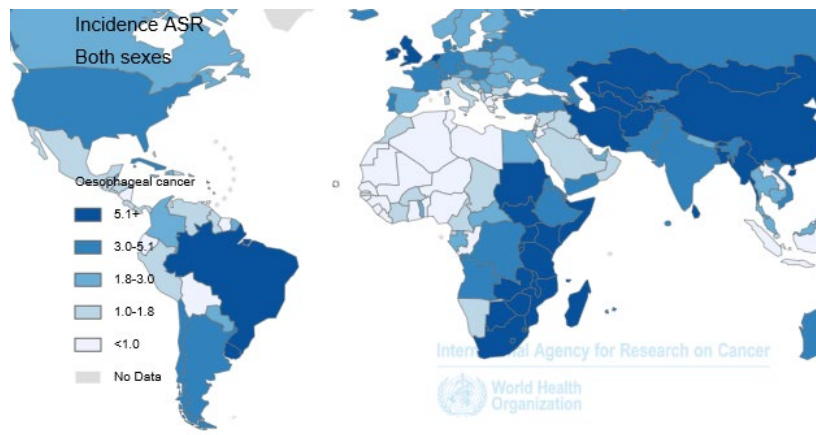
The generation of cytotoxic ROS near the target and the high selectivity of photosensitizers to solid tumors minimize the side effects usually observed with common systemic drugs, giving photodynamic therapy several advantages over the classic anticancer therapies. Alongside that, one of the recognized keys of PDT, and one of its major advantages over traditional therapeutic strategies is the ability to destroy tumors while preserving surrounding healthy tissue. Another advantage is

that PDT treatments can be repeated, in cases of recurrence or presence of multiple lesions, because of the absence of specific resistance mechanisms and the reduced side effects, a consequence of high selectivity (Allison, 2014).

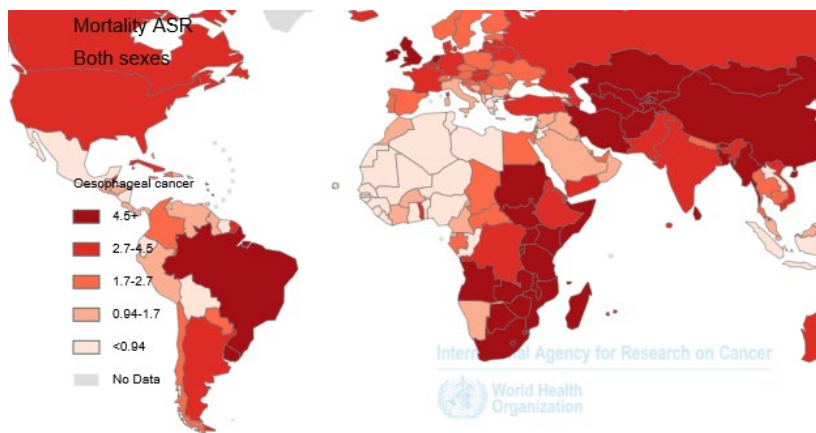
PDT can be extremely effective with only one treatment for localized and early-stage solid tumors (Agostinis *et al.*, 2011). However, because of the limited ability of light to penetrate through tissues, in advanced cases where tumors are generally larger, PDT has only been applied as a palliative treatment. In such cases, PDT can delay the progression of cancer and improve the quality of life of the patient (Agostinis *et al.*, 2011; Allison, 2014). Knowing this, PDT can also be used in combination with surgery, chemotherapy or radiotherapy as it does not interfere with these treatment modalities nor does it exhibit its typical side effects. Many PDT combinations with conventional anticancer drugs are also being studied to find synergistic effects. Furthermore, another notable advantage is the absence of significant sequelae, since there is no destruction of the connective tissue, allowing tissues to maintain their functional and anatomical integrity after PDT treatments (Agostinis *et al.*, 2011).

Nowadays, PDT has established itself as an effective treatment and is being tested to treat many cancers, such as those of the skin, head and neck, brain, lung, bladder, gastrointestinal (GI) tract, and others.

In the case of oesophageal cancer, between 40–50% of patients are deemed surgically unresectable and, of those resected, no more than 15–20% have a chance of cure of their disease or long survival (Davila, 2011; Anand *et al.*, 2012). Consequently, for the majority, the mainstay of treatment is palliation of symptoms which, for all practical purposes, means the relief of dysphagia. For this, bypass surgery, external beam radiotherapy (EBR), brachytherapy, chemotherapy, indwelling tube and stent placement, or a combination of these, have been advocated. However, more recently, endoscopic photo-irradiation has been used to relieve malignant obstruction of the esophagus, which led to PDT using porfimer sodium followed by excimer dye laser irradiation as an approved curative treatment for superficial oesophageal cancer (Davila, 2011; Allison, 2014). While endoscopic submucosal dissection (ESD) is currently more popular for oesophageal cancer, there is evidence to support PDT as an alternative treatment and as a salvage treatment for local failure after chemoradiotherapy (CRT) (Yano *et al.*, 2007; Allum *et al.*, 2011).



Source: GLOBOCAN 2012 (IARC)



Source: GLOBOCAN 2012 (IARC)

Figure 1. 1 – Map of incidence (top) and map of mortality (bottom) for oesophageal cancer (left) estimated for 2012. Source: GLOBOCAN 2012 (<http://globocan.iarc.fr/Pages/Map.aspx>, 16th of July of 2018).

On the other hand, melanoma imposes itself as another rising concern in terms of global health (**Figure 1.2**). Melanoma and non-melanoma skin cancers are the most common malignancies in Caucasians, with increasing incidence over the past years. According to the World Health Organization, 2 to 3 million non-melanoma skin cancers and almost 132,000 melanoma skin cancers occur every year. Albeit being one of the least common forms of skin cancer, it is also the most deadly type because of its potential to spread to other parts of the body. Each year, about 76,000 people are diagnosed with melanoma, and more than 10,000 people die from it. When one adds the rising rates of melanoma, especially among children and teens, with its resistance to conventional chemotherapy and radiotherapy, it becomes easy to understand the

increasing need of searching for alternative strategies of therapy. PDT has been successfully used in the treatment of skin cancers, however, the use of this therapy against melanoma can be compromised due to the natural resistance mechanism of some melanoma cancer cells (Huang *et al.*, 2014). In particular, high melanin levels in melanomas (pigmented tumors) can lead to an antioxidant effect due to optical interference via competition with the photosensitizer for the light absorption. Being a very aggressive form of skin cancer with a very unfavorable prognosis, particularly if advanced stages have been attained, it demands the search for new photosensitizers able to overcome the resistance of melanoma to photodynamic therapy.

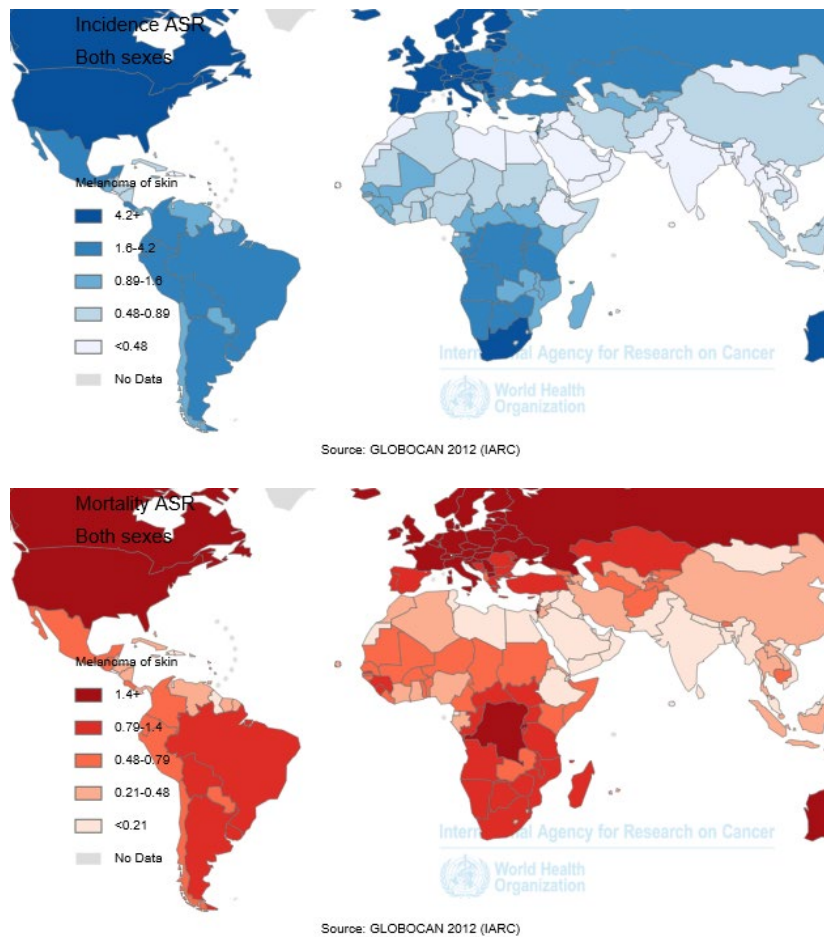


Figure 1. 2 – Map of incidence (top) and map of mortality (bottom) for melanoma estimated for the year 2012. Source: GLOBOCAN 2012 (<http://globocan.iarc.fr/Pages/Map.aspx>, 16th of July of 2018).

1.1. An historical background for Photodynamic Therapy

The idea of using light to cure diseases is not something new, in fact for over 5000 years, in India and ancient Greece, different forms of phototherapy have been used to treat psoriasis and vitiligo, by the combination of psoralens with sunlight. However, the current concept and clinical application of PDT were only described in the early years of the 20th century when a medical student, Oscar Raab, working in his Ph.D., made an accidental discovery that microorganisms such as paramecia that had been incubated with certain dyes, such as acridine, could be killed when exposed to light, but not when they were kept in the dark (Abrahamse *et al.*, 2016).

In 1903, when it was subsequently discovered that oxygen in the air was also necessary for this light-mediated killing effect to occur, Herman von Tappeiner, an advisor to Oscar Raab, called this light effect a "photodynamic effect" (Ackroyd *et al.*, 2001). It was not long after these discoveries that the first efforts were made to use this phenomenon as a cancer therapy, by painting dyes on to superficial skin tumors and then exposing them to light. Actually, it was von Tappeiner, himself, and Jesionek who conducted the first clinical trials of PDT (Triesscheijn *et al.*, 2006). In one of these tests, they observed that the topical application of the eosin compound, followed by exposure to light, was used to treat skin cancer. However, the following two world wars and the impressive rise of the pharmaceutical industry in the 1950s and 1960s delayed the further exploration of PDT by over 60 years (Abrahamse *et al.*, 2016).

The true potential of PDT was only realized after the extensive work of Dougherty and co-workers who, between 1975 and 1978, reported complete cure of malignant tumors by the combined application of HpD (Hematoporphyrin Derivative) and red light, initially in a breast cancer model, and later in patients with skin, prostate, breast and colon tumors. These promising results were later confirmed in clinical trials with improved versions of HpD in patients with skin and bladder cancer.

In 1976, Weishaupt and his colleagues postulated that singlet oxygen ($^1\text{O}_2$) generated in PDT was the cytotoxic agent responsible for the destruction of tumor cells.

Finally, in 1993, a landmark for PDT was achieved with the regulatory approval in Canada of porfimer sodium (Photofrin®), a semi-purified version of HpD, for the treatment of bladder cancer (Triesscheijn *et al.*, 2006; Allison, 2014).

Although still being the most frequently used PS worldwide at this time, Photofrin has many known disadvantages including a relatively small absorbance peak at 630 nm making it somewhat inefficient in use, especially for bulky tumours where light penetration is problematic and skin photosensitivity that can last for weeks or months and can be highly troubling for patients (Abrahamse *et al.*, 2016). Knowing this, the attention has shifted into the discovery and development of new and safer PS molecules, which led to the regulatory approval in 2000 of verteporfin (Visudyne®), a derivative of benzoporphyrin, for the treatment of age-related macular degeneration (AMD), and temoporfin (Foscan®) in 2001, a chlorin, for the treatment of head and neck cancer. The structures of all these compounds can be found in **Figure 1.3**.

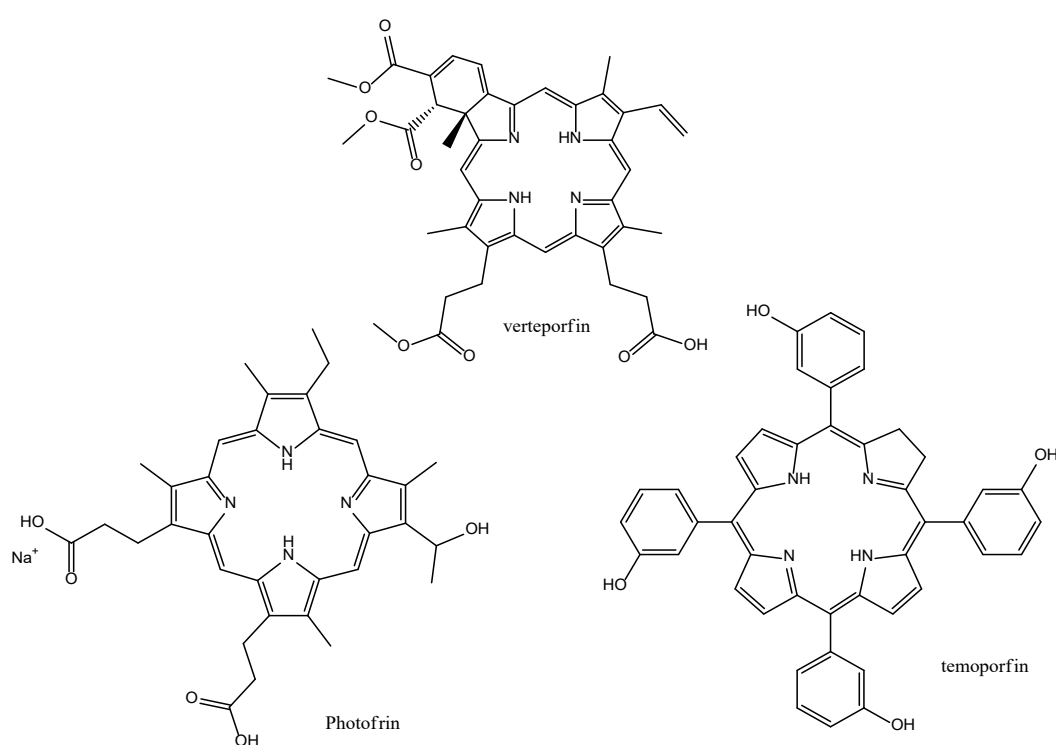


Figure 1.3 – Molecular Structures of Photofrin, Verteporfin and Temoporfin

The approval of the first photosensitizers represented significant advances in PDT for the treatment of cancer, but its wide clinical acceptance was hampered by its limited efficacy and adverse effects, mainly prolonged skin photosensitivity reactions, to the tendency of some PS to accumulate in the patient's skin after treatment and their possible activation by sunlight or strong artificial light, which can cause skin lesions. Thus, patients should avoid direct exposure to sunlight by staying home under moderate light several weeks after treatment until PS levels in the skin decrease to safe values. Although at first glance this limitation could be considered a small price to pay for the benefits of therapy, the risk of photosensitivity was responsible for a poor perception of PDT by patients and physicians and could have contributed to the slow penetration of PDT in clinical practice (Plaetzer *et al.*, 2009). Since then, medicinal chemists have attempted to synthesize and discover molecules that could act as improved PSs, and several hundred compounds have now been proposed as potentially useful to mediate PDT for tackling cancer, infections and many other diseases. (Yoo & Ha, 2012).

The last twenty years can be characterized by the advances in new, safer and more effective PS. At the same time, better, cheaper, and easier to use light sources have turned the PDT from a curiosity to a highly promising therapeutic strategy with applications in such fields as dermatology, ophthalmology, cardiology, rheumatology or infectious diseases, medical imaging, and oncology. In this regard, clinical applications of PDT have been shown to prolong survival time and improve quality of life in patients with advanced head and neck cancers and have demonstrated high cure rates for some types of early-stage tumors, most often in dermatology, as in the treatment of precancerous lesions and non-melanoma skin cancers (Abrahamse *et al.*, 2016).

1.2. PDT mechanism of action

PDT involves several steps, the first being the administration of the photosensitizer to the patient. After administration, the PS needs a period of time to arrive and preferably accumulate in the target tissue, the so-called drug-light interval (DLI), which depends on the route of administration and the type of PS, more specifically its pharmacokinetics and biodistribution properties. Once the appropriate concentration of the photosensitizer in the target cells is reached, the PS is activated (by excitation) with a suitable beam of light, passing into a triplet state of energy, which triggers a series of photochemical reactions that lead to the generation of ROS and, consequently, cell death (**Figure 1.4**).

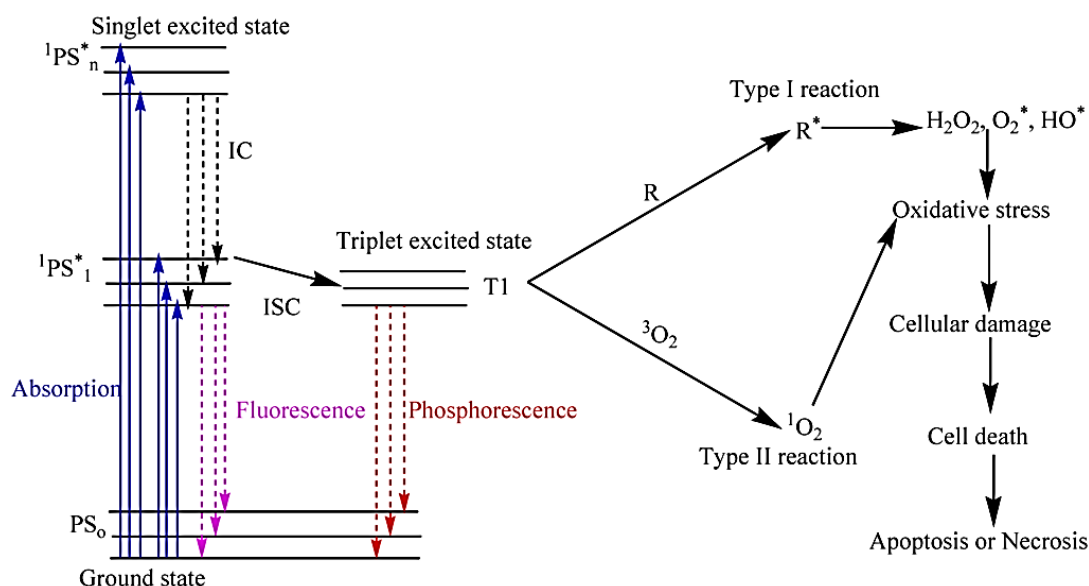


Figure 1.4 – Modified Jablonski diagram depicting the process of photodynamic therapy. When PSs in cells are exposed to specific wavelengths of light, they are transformed from the singlet ground state (S0) to an excited singlet state (S1–Sn), which is followed by intersystem crossing to an excited triplet state (T1). Abbreviation: IC: internal conversion; ISC: intersystem crossing; PS: photosensitizer; 1PS*: Singlet excited photosensitizer; T1: Triplet excited state; R: biological substrate; R*: oxidized biological substrate; 1O₂: Singlet oxygen; H₂O₂: hydrogen peroxide; O₂*: superoxide; HO*: hydroxyl radical.

(http://www.mdpi.com/journal/ijms/special_issues/photo_therapy, 16th of July of 2018)

Typically, the electronically excited oxygen molecule is in its lower energy singlet state - singlet oxygen ($^1\text{O}_2$) - which can cause extensive oxidative damage to biomolecules and cell structures, leading to cell death. Other ROS that can be generated in PDT are the superoxide ion ($\text{O}_2^{\cdot-}$), hydrogen peroxide (H_2O_2) and the hydroxyl radical (OH^{\cdot}), (Agostinis *et al.*, 2011; Ortel *et al.*, 2009; Anand *et al.*, 2012). Once the ground state PS (a singlet state) absorbs light and goes into an electronically excited state (also a singlet state), it can decay back to the ground state with fluorescence emission, or it can pass through intersystem intersection to a more stable excited state (a triplet state), by converting electron rotation into the higher energy orbital. The triplet state has a longer lifetime (up to tens of microseconds compared to some nanoseconds or less), allowing sufficient time for its interaction with molecular oxygen by two different routes, which will then lead to ROS generation:

- i) A type I reaction which can be by either photooxidation, the transfer of electrons to O_2 , with the formation of superoxide anions ($\text{O}_2^{\cdot-}$); or photoreduction, the transfer of electrons or protons from an organic substrate, resulting in a radical cation and a reaction of O_2 .
- ii) Or a type II reaction which consists of a direct transfer of energy to the ground state O_2 (a triplet state) to form oxygen singlet ($^1\text{O}_2$). This path is allowed only when the triplet energy PS is greater than the excitation energy, which is 94.5 kJ/mol.

The type II reaction tends to occur preferentially since it has a simpler mechanism and is generally thermodynamically favorable to the red absorbing PS. This explains why $^1\text{O}_2$ is considered the main mediator of PDT phototoxicity. The quantum yield of the $^1\text{O}_2$ ($\Phi\Delta$) formation is one of the most important characteristics of a PS, and is determined by the quantum yield (ΦT) and the lifetime (τT) of the excited triplet state (Juarranz *et al.*, 2008; Ortel *et al.*, 2009; Plaetzer *et al.*, 2009; Agostinis *et al.*, 2011; Yoo & Ha, 2012).

In the case of both mechanisms occurring competitively, which can happen for certain photosensitizers, an enlarged PDT response is observed. The characteristics of the PS, the PDT protocol and possibly the local oxygen concentration dictate the relative extent of type I and type II mechanisms. For example, the microenvironment of the tumor is often described as hypoxic, especially near the centre due to insufficient blood flow, this in combination with oxygen consumption by PDT can dramatically reduce local oxygen concentration and favour the occurrence of type I reaction.

It is thought that the subcellular localization of the PS in different organelles (mitochondria, lysosomes, endoplasmic reticulum, plasma membrane, etc.) also plays a major role in the type of cell death mechanism (apoptotic, necrotic and autophagy-associated cell death) that dominates, but other factors such as the overall PDT dose (PS concentration \times light fluence), DLI, the type of tumor, the characteristics of PS and the treatment protocol itself also play a role.

Overall, when cells are treated with PDT *in vitro*, apoptosis is accepted as the principal modality of cell death (Abrahamse *et al*, 2016). However, while less intense protocols seem to favour apoptotic cell death, some results suggest that in more aggressive PDT protocols (high doses of PS and light and short DLI) there is a tendency to cause extensive cell death by necrosis. The combination of the facts that oxygen concentration is not constant across the tumor tissue factors and light distribution in the tumor tissue is not homogeneous, due to the strong attenuation of the light by the tissues, will result in heterogeneous intra-tumor ROS production, with different areas of the tumor undergoing different levels of oxidative damage. This will certainly have a negative impact on the overall predictability of outcome and treatment effectiveness (O'Connor *et al*, 2009; Plaetzer *et al*, 2009; Robertson *et al*, 2009).

1.3. Active components on PDT

There are three PDT components (light, oxygen, and photosensitizer) which precise conjugation is key for the efficacy of PDT to selectively destroy target tissue. This represents a great challenge in the optimization of therapeutic protocols in clinical practice, because in order to obtain the desired therapeutic effect, one shall have in consideration a great number of factors such as the type of PS and the dose administered, the intracellular location, the DLI, the total light dose applied, its wavelength and fluence rate, tumor characteristics and local availability of oxygen. It is the combination of these elements innocuous *per se* that triggers the production of ROS responsible for the inactivation and destruction of tumor cells, and so to fully understand which role each one of them plays on PDT efficacy is crucial for drug and protocol design.

1.3.1. Light

The first light sources were conventional lamps, used mainly in the treatment of superficial lesions, and produced a heterogeneous light and a large thermal component, and the emitted energy was delimited by optical filters (Triesscheijn *et al.*, 2006; Mitton & Ackroyd, 2008), but over the years there has been a rapid evolution of light sources with clinical applications and nowadays, lasers (e.g., argon, diode) and LEDs, which produce a highly homogeneous monochromatic light, are the most commonly used light sources. The coupling of these light sources to fiber-optic technology revolutionized the PDT concept and expanded its applicability to hard-to-reach places (Juzeniene *et al.*, 2004; Mitton & Ackroyd, 2008; Agostinis *et al.*, 2011; Allison, 2014).

Light penetration into a human tissue is of major relevance since its intensity not only ensures a more or less efficient photoactivation of the PS inside a tumour, but also it is determinant of the type of antitumor response. Therefore, it is essential to understand that reflection, absorption and dispersion processes all affect the mode of propagation of light in tissues, to the extent that these processes occurrence depends

on the wavelength used. Alongside with the tissue properties and heterogeneities (e.g., macromolecules, organelles), the wavelength determines the depth of light penetration into the tissue (**Figure 1.5**). On one hand, to ensure that endogenous chromophores, namely hemoglobin (Hb), myoglobin, melanin, and cytochromes, are undisturbed, the efficient optical window is restricted, going from 600 to 1200 nm (Sibata & Colussi, 2000; Plaetzer *et al.*, 2009; Robertson *et al.*, 2009).

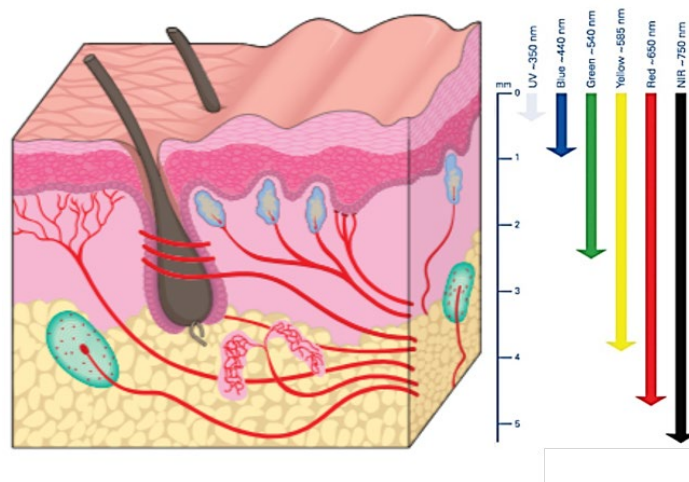


Figure 1. 5 – Light penetration into skin illustrating the depth to which wavelengths penetrate human skin. Red light is extinguished some 4–5 mm beneath the surface of the skin whereas ultraviolet hardly penetrates at all and blue barely 1 mm into tissue. (adapted from Ash, Caerwyn *et al.* (2017) “Effect of wavelength and beam width on penetration in light-tissue interaction using computational methods.” *Lasers in Medical Science*.)

On the other hand, wavelengths longer than 850 nm do not provide enough energy to produce singlet oxygen, which limits the “phototherapeutic window” to 600-850 nm. Thus, an important characteristic for a compound to be considered a potent PS is to have an intense absorption band within this wavelength range, the red and near-infrared (NIR) spectral region (Pereira *et al.*, 2018). The optimal wavelength for PDT should, therefore, result from a compromise between PS activation and depth penetration with minimal dispersion. For that, the selection should be based on both the absorption spectrum of the photosensitizer and the properties of the damaged tissue (location, lesion size, and accessibility).

1.3.2. Oxygen

Oxygen is a key element in PDT and its intracellular concentration has an undeniable effect on the success of the treatment. It is probably the component which importance is most often overlooked, especially if we take into account the fact that O₂ concentration can separate between tumors and even between different tumor regions, depending on the density of the vasculature, especially in deeper solid tumors, often characterized by their hypoxic microenvironment. Interestingly, the photodynamic treatment itself can induce acute tumor hypoxia, a condition attributed to the high oxygen consumption during the photochemical reaction, which will stop the production of ROS and reduce the render of treatment. In addition, destruction of the vascular system and occlusion of the peritumoral vasculature, resulting in a decrease of blood flow to the tumor tissue and preventing the oxygen supply in the tumor can also be caused by PDT causing more hypoxia (Kushibiki *et al.*, 2013). Tumor hypoxia is responsible for resistance to Photodynamic Therapy, chemo and radiotherapy, and is associated with malignant progression and poor prognosis. Furthermore, it has been documented that hypoxia can lead to angiogenic stimuli, contributing to tumor survival and tumor resurgence, which can be seen as a disadvantage of PDT. Several methodologies have been proposed to avoid hypoxia caused by the photodynamic reaction, such as, for example, reduction of fluence rate or irradiated fraction at alternating intervals of light. These techniques serve to promote tissue oxygenation and tumor reperfusion, and thus, to compensate for the depletion of oxygen caused by the photochemical reaction. Although some improvement in tumor response after tissue oxygenation control has been reported, some limitations have also been reported. The reduction of the fluence and the fractionation of the light dose only consider the depletion of O₂, not the preexisting hypoxic cells and, in addition, it forces the increase of the time of treatment (Anand *et al.*, 2012; Mitton & Ackroyd, 2008; Huang *et al.*, 2003).

Chlorins, the target of this dissertation, are predominantly considered as type II photosensitizers, which exert their cytotoxic effect through singlet oxygen. This gives us another aspect to take into consideration which is the fact that despite singlet

oxygen's high reactivity, this ROS has a very short lifetime ($\tau\Delta$) and is quite influenced by the external chemical environment (e.g., solvent). There is much controversy regarding its biological half-life and, consequently, the diffusion distance of the transient oxygen species, but what can be concluded after several studies, which have gone from photobleaching to the evaluation of phosphorescence by laser and microscopy, is that its lifespan, (approximately 3 μ s), restricts the radius of action to $\approx 0.02 \mu$ m, a distance considered negligible at the cellular scale (≈ 100 nm) and diffusion coefficient of 2 to 4×10^{-6} cm²/s (Hatz *et al.*, 2008; O'Connor *et al.*, 2009; Agostinis *et al.*, 2011; Anand *et al.*, 2012; da Silva *et al.*, 2012). Therefore, determination of its exact location is crucial for the evaluation of the cytotoxic effect, once the oxidative response occurs predominantly in the vicinity of the photosensitizer. Due to these characteristics, PDT becomes a selective therapy for the local effects it produces. On the other hand, the photosensitizing molecule must be located close to its target at the time of irradiation. The subcellular location of the photosensitizers is critical in mediating the cytotoxic response to PDT and is determined by the chemical properties of the molecule, formulation, concentration, microenvironment of the lesion and also by the target cell phenotype (Hopper, 2000; Triesscheijn *et al.*, 2006; Robertson *et al.*, 2009; Agostinis *et al.*, 2011; Huang *et al.*, 2008).

ROS produced during PDT are responsible for a complex cascade of oxidative reactions that target many biomolecules such as DNA, lipids or proteins, which participate in various cellular structures. The plasma membrane, intracellular membranes, and organelles such as the endoplasmic reticulum, Golgi complex, lysosomes, mitochondria and even nucleus were identified as subcellular targets of many photosensitizing substances. From all ROS, singlet oxygen is, in most cases, the most important in this process, owing its importance to its chemical characteristics, namely, the ability to oxygenate or oxidize numerous organic functional groups (Jiménez-Banzo *et al.*, 2008; da Silva *et al.*, 2012). Cell antioxidants, such as glutathione (GSH), play an important role in the defence system against oxidative stress. The GSH system represents the first line of defence against intracellular free radicals, reducing free radicals through the action of glutathione peroxidase (GPx), being oxidized to glutathione disulfide (GSSG), which is then reduced back to GSH by glutathione reductase (GR), using NADPH as an electron donor. Superoxide dismutase (SOD), catalase and lipoamide

dehydrogenase are other examples of ROS-eluting enzymes, thus helping to reduce cell sensitivity to PDT. Although these types of mechanisms are part of an intrinsic resistance to the oxidative stress present in most cells, their levels are not the same in all cell types, which explains their distinct antioxidant capabilities.

1.3.3. PS

Lastly, the most important component of PDT is arguably the photosensitizer, responsible, as described before, by the absorption of energy of a specific wavelength and transforming it into useful energy. The therapeutic result is considered to be largely centred on the photosensitizer's chemical structure which is usually based on a tetrapyrrole structure, similar to that of protoporphyrin contained in haemoglobin. The presence of a π electron system guarantees a high absorptive power, which makes them attractive for medical applications furthermore, this kind of structures possess an intrinsic ability to accumulate selectively in tumors, which has been demonstrated in several studies (O'Connor *et al.*, 2009). It is still poorly understood the mechanisms behind this selectivity, however, several authors have developed some hypotheses such as their preference to bind to low-density lipoprotein (LDL) receptors, which are often overexpressed in tumor cells. Another possible hypothesis is a consequence of tumors having surrounding vessels with morphological alterations, typical of the neovascularization process occurring in tumour angiogenesis, which lead them to be quite leaky and tortuous. This occurrence together with the absence of lymphatic drainage in tumours are collectively known as the "enhanced permeability and retention (EPR) effect" (Brown *et al.*, 2004).

It is possible to divide, according to the literature, the photosensitizers of the tetracyclic macrocycles into three different generations. Photofrin® marked the first step in the use of tetrapyrrole macrocycles in PDT, in 1995 (Allison, 2014; Senge, 2012).

Photofrin® and the Hematoporphyrin Derivative (HpD) are known as first generation photosensitizers mainly because they exist as complex mixtures of monomeric, dimeric, and oligomeric structures. These first-generation photosensitizers have

already been extensively studied and approved for commercialization. However, in spite of its success, Photofrin®, in particular, has many drawbacks, namely low intensity of light absorption at the maximum wavelength of Photofrin® (ϵ_{max} at 630 nm \sim 3000 M⁻¹cm⁻¹) which means it absorbs light weakly at 630 nm; low molar extinction coefficient, implying the administration of large amounts of compound to obtain an efficient phototherapeutic response; and low speed of elimination, which causes prolonged photosensitivity of the skin, after treatment (Huang *et al.*, 2008; Byrne *et al.*, 2009; Anand *et al.*, 2012; Senge, 2012).

The so-called second-generation photosensitizers, which include various derivatives of porphyrins, phthalocyanines, naphthalocyanines, chlorins, and bacteriochlorins, was developed from the necessity to overcome such drawbacks (Ormond *et al.*, 2013). Chlorins, in specific, have a strong absorption band in the region of 650 nm, which makes these tetracyclic macrocycles good candidates for second generation photosensitizers for PDT, since they absorb in a region where the light penetration depth is maximum and the damages caused to tissues are minimal (Pereira *et al.*, 2010). As a result, in 2001, temoporfin (Foscan®), from the chlorin family, was approved in Europe with the advantage of being able to reduce the skin post-treatment photosensitivity period to about 2 to 4 weeks, which is a considerable improvement from the 4 to 12 weeks with porfimer sodium. In addition, due to its increased light absorption at a longer wavelength (652 nm), it requires light doses ten times smaller compared to porphyrins. Although representing a significant progress when compared to sodium porfimer, there was still a wide margin of improvement to be done regarding pharmacokinetic profiles and higher phototherapeutic indices, which can be defined as the relationship between its phototoxicity and its toxicity in the dark. Furthermore, there were still some limitations concerning the lipophilicity of these compounds. In fact, in order to achieve the most effective PSs, some characteristics must be present, relatively hydrophobicity being one of them. Enough hydrophobic compounds tend to rapidly, and passively, diffuse into tumour cells and localize in intracellular membrane structures such as mitochondria and endoplasmic reticulum (ER), while more polar compounds tend to be taken up by the active process of endocytosis, necessitating a longer DLI. This gave rise to development of a third generation of photosensitizers that have amphiphilic properties suitable for diffusion through the lipid barrier and endocellular localization. In addition to this, they must also be

activated by long wavelength light, minimize or eliminate the occurrence of skin photosensitivity reactions and demonstrate greater selectivity for tumor tissue (Huang et al., 2008; Byrne et al., 2009; Anand et al., 2012; Senge, 2012), usually by the conjugation of targeting molecules (such as antibody conjugation) or encapsulation into carriers (such as liposomes, micelles, and nanoparticles) to enhance accumulation at the desired site.

We can by this conclude that, over the years, photosensitizers of second and third generation, with their generally high selectivity for neoplastic tissue, absorption radiation in the 650-750 nm region, suitable solubility in physiological media, and no toxicity in the absence of light, have come to shine a light on the negative aspects of first-generation photosensitizers and bring back hope to the promise of PDT.

1.3.3.1. PS ideal characteristics

In addition to the already mentioned characteristics, such as strong light absorption ($\epsilon > 10^5 \text{ M}^{-1} \cdot \text{cm}^{-1}$) at the longest wavelengths of the phototherapeutic window (700 nm $< \lambda_{\text{max}} < 800$ nm) and high quantum yields of ROS (ROS > 0.5) in order to maximize tissue penetration depth and treatment effectiveness, the ideal photosensitizer for PDT cancer should also be a pure compound with adequate life and low production cost. Besides, it should be non-toxic in the absence of light and its physicochemical characteristics should allow for administration in biocompatible formulations. Its solubility is also a factor of relevant importance in the distribution and localization within the tumor cells. While aqueous solubility is critical for the bioavailability of the sensitizer, lipophilicity is important for diffusion through the lipid barrier and endocellular localization. The pharmacokinetic profile should favour selective accumulation in the target tissue and rapid clearance of healthy tissues in order to minimize the occurrence of side effects. Furthermore, it must demonstrate adequate photodecomposition resistance in order to perform its role before being destroyed by the ROS produced (Triesscheijn *et al.*, 2006; Ortel *et al.*, 2009; Agostinis *et al.*, 2011; Allison, 2014).

It is, then, easy to understand that the final outcome of PDT is crucially dependent of a photosensitizer's proper design, which is why current progress in the development of photosensitizers relies on the identification of specific design parameters. On one hand, it is being increasingly better understood the need to integrate molecular design insights emerging from studies of PS-target interactions, cellular signaling processes, and increased resistance. On the other hand, photophysical and photochemical properties of the PS are also highly important, since they can be related with its behaviour in biological systems, namely with aggregation, tumor type-specific PS uptake mechanisms, binding to plasma proteins or change in hydrophilicity/lipophilicity in given physiological environments (Pucelik *et al.*, 2010).

Of all known and studied photosensitizers, modified tetrapyrrolic-based photosensitizers are highly attractive phototherapeutic agents for PDT of cancer, once they possess several of the key features required for an ideal PS. Therefore, they were taken as the molecular subject of this dissertation and will be further explained in the next chapter, along with the logic behind the choice of the final structures that ended up being studied.

CHAPTER 2 – The Chemistry

1. Tetrapyrrolic Macrocycles

Tetrapyrrolic macrocycles are a class of aromatic compounds quite abundant in nature which, as their name suggests, are cyclic conjugated molecules containing four pyrrole-type units, linked together directly or through different sorts of atoms and bonds. This class of molecules has an undeniable biological importance, of which porphyrins are some of the best and simplest examples (Abrahamse *et al.*, 2016).

Porphyrins, from the Greek word *porphura* used to describe the characteristic purple color of several porphyrins, are planar macrocycles, consisting of four pyrrole rings joined by four methine bridges, and if one or two double bonds of their pyrrole rings is reduced two new compound families, designated chlorins and bacteriochlorins, respectively, are obtained (**Figure 2.1**).

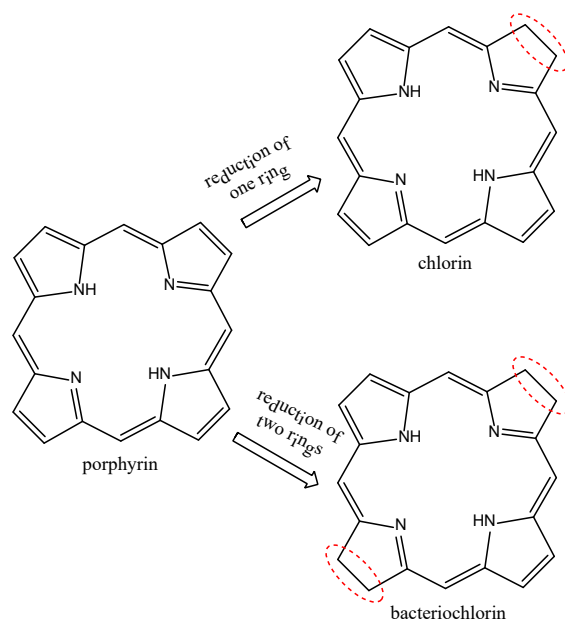


Figure 2. 1 – Central nucleus of a porphyrin and its reduced derivatives: chlorin and bacteriochlorin.

Besides this, their structure has a suitable space to accommodate a metal ion, conjugating with the four nitrogen atoms present in the center. A facility of design and structural versatility, allied to their physical and chemical properties, make porphyrins a desirable target for several applications, maintaining and stimulating the interest of studying the “pigments of Life”. Knowing these structures were indispensable for a variety of natural processes triggered an increasing interest within the scientific community, from the better comprehension of those functions to the investigation of potential applications based on the very same natural phenomena.

1.1. Natural Derivatives

Among the naturally-occurring derivatives, one of the most relevant is the heme group, an iron (II) complex of protoporphyrin IX. It can be found as the prosthetic group of haemoglobin, responsible for the transport and storage of oxygen in many living beings, and it's also a constituent of enzymes such as peroxidases or catalases, as well as cytochromes, which act primarily as electron carriers in various biological processes, such as respiration (Pinto *et al.*, 2016). Chlorophylls and bacteriochlorophylls contain the reduced tetracyclic macrocycles chlorin and bacteriochlorin, respectively. These molecules play a crucial role in transforming solar energy into chemical energy in photosynthetic beings by catalyzing the photosynthesis of carbohydrates from CO₂ and H₂O (Pinto *et al.*, 2016). The structures for the heme group and chlorophyll can be found in **Figure 2.2**.

There are also other compounds of high importance as tetracyclic macrocycles responsible for electron transport, steroid biosynthesis and detoxification in several living organisms (Cavaleiro and Smith, 1989), and metal complexes which have been investigated for a few decades on the account of their catalytic properties on a wide range of oxidation reactions: from hydroxylation and epoxidation of alkenes to drug oxidation and DNA cleavage. More recently, porphyrins have attracted even more attention from researchers in various fields, such as PDT, due to their phototherapeutic properties, more specifically their inherent capabilities as photosensitizers in the activation of reactive oxygen species (ROS) (Maestrin *et al.*, 2004).

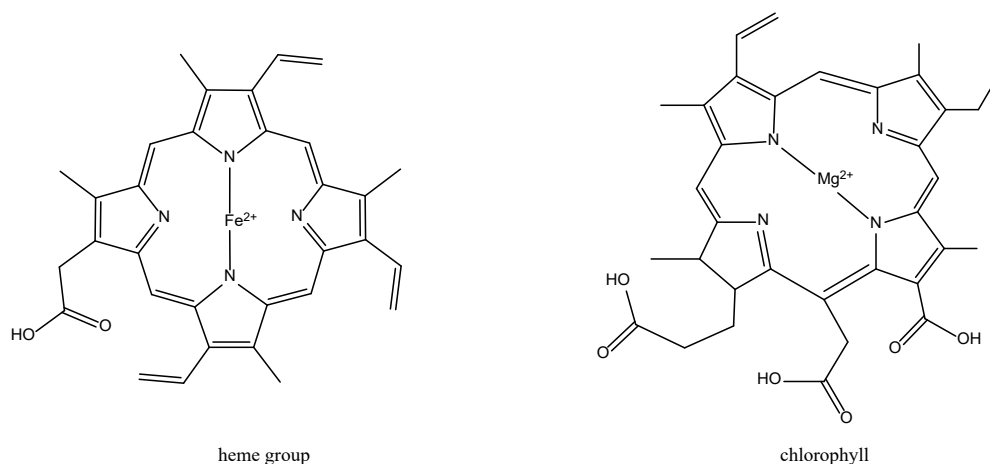


Figure 2. 2 – Structures for the heme group and chlorophyll

This great diversity of biological functions performed by this kind of compounds is due to the very interesting characteristic that small changes in their base structure reflect in quite different biological uses.

1.2. Structure and Nomenclature

In 1912, Küster proposed for the first time the structure of porphyrins, however, it was not very well accepted by the scientific community since they considered that such a large ring should be unstable. Fischer, also known as the "father of the modern chemistry of porphyrins", who was also initially in the group of sceptics, came to confirm this same structure in 1929 when synthesizing the heme group.

Although being planar macrocycles in their simpler form (without substituents), porphyrins may acquire more or less twisted shapes depending on the number and type of substituent groups introduced at the periphery, or with the saturation of one or two β -pyrrole positions.

Porphyrins have all the carbon atoms of the rings with sp^2 hybridization, whereas 2,3-dihydroporphyrins (chlorins) have two sp^3 carbons, due to the reduced β -pyrrole bond; and 7,8,17,18-tetrahydroporphyrins (bacteriochlorins), which undergo a further saturation, wherein the saturated carbons are in two diametrically opposite pyrrole

units along with their isomers (isobacteriochlorins), have four sp^3 carbons. Furthermore, porphyrins have a total of 22 π electrons, of which only 18 of these π electrons contribute to the aromatic character of the macrocycle, thus respecting Hückel's law.

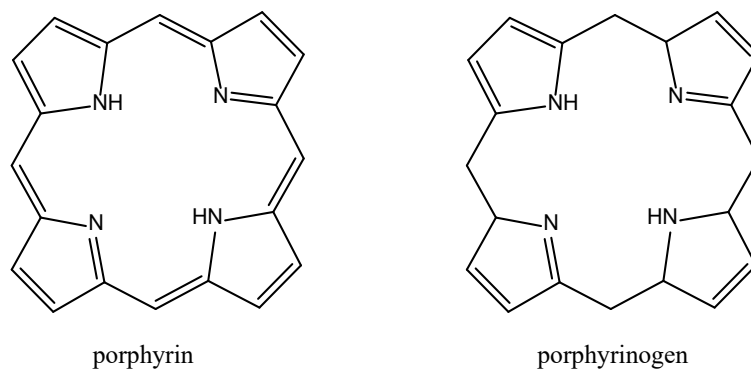


Figure 2.3 – Representation of porphyrin and porphyrinogen

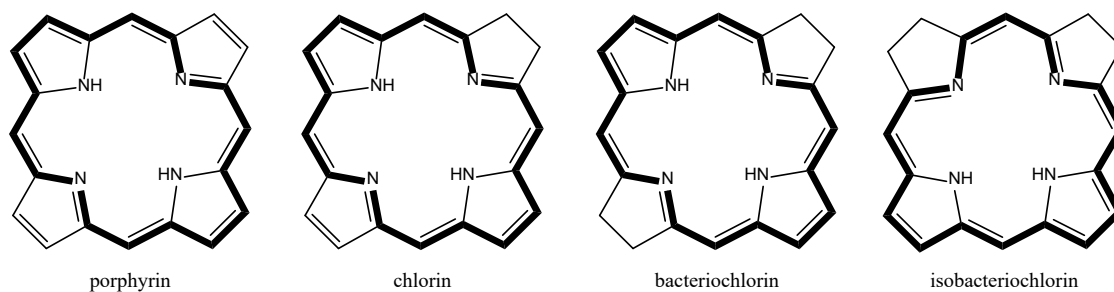


Figure 2.4 – Representation of the aromatic distribution on chlorin, bacteriochlorin, and isobacteriochlorin

As a result of this extensive conjugation, porphyrins are coloured compounds that exhibit strong absorption in the visible region around 400 nm, the so-called Soret band, and other bands of lesser intensity between 450-700 nm, referred to as Q-bands. In

the case of chlorins and bacteriochlorin, the aromatic character is maintained since they have 20 and 18 π electrons, respectively. The structural differences, among these porphyrin compounds, cause them to differ in certain photophysical properties. Hydroporphyrins exhibit higher absorption in the red and near-infrared regions compared to porphyrins. Chlorines have typical absorption bands around 650 nm and bacteriochlorins around 730-750 nm. When speaking of porphyrins, two nomenclature systems stand out: the nomenclature proposed by Fischer and the IUPAC nomenclature. An illustrative example of both systems can be found in **Figure 2.5**.

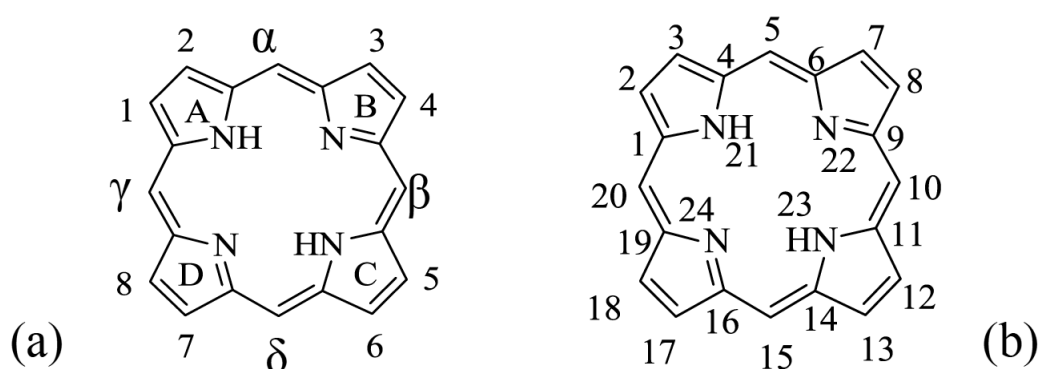


Figure 2.5 – Numeration of tetrapyrrolic macrocycles according to the Fischer Nomenclature (a) and IUPAC (b)

The first nomenclature system is based primarily on the use of trivial names combined with a numbering system. According to this author, the conjugated tetrapyrrole macrocycle is called porphyrin, the pyrrole rings are designated by A, B, C and D, the peripheral carbons of the pyrrole rings by β -positions and the methyl bridges by *meso* positions. The β -pyrrole positions are numbered from 1 to 8 and the *meso* positions are designated by the Greek letters α , β , δ , and γ . The pyrrole carbons adjacent to the nitrogens are designated α -pyrrole positions. The same author also adopted trivial names to a wide number of compounds of this family, regarding their natural occurrence or function. This system quickly became insufficient due to the great growth of the chemistry of porphyrins leading to the appearance of a new system of systematic nomenclature. The IUPAC recommendations have proposed a numbering

system for tetrapyrrole macrocycles where the carbons are sequentially numbered from 1 to 20, the nitrogens from 21 to 24 and the outer carbon atoms are designated with indices.

In this dissertation, Fischer's nomenclature was mainly used, where the atoms of the tetrapyrrole macrocycle can be referenced according to their position, namely β -pyrrole or *meso* position.

1.3. Properties

As all molecules, most of the porphyrins' properties are due to their structure, and so it's of capital importance to understand how these two are related, in order to know how a modification of the structure influences the properties and to take advantage of this knowledge. These macrocycles are, for example, characterized by hydrophobicity and their solubility in organic solvents varies according to the substituents at the periphery of the macrocycle. Furthermore, the high number of conjugated double allows the absorption of radiation in the visible zone of the electromagnetic spectrum, evidenced visually by the color display, an important characteristic in this type of tetrapyrrole compounds.

The absorption spectrum of porphyrins presents a band of strong intensity in the region of 400 nm, called the Soret band, which results from the delocalization of the eighteen π -conjugated ions of the macrocycle, and that only disappears when the ring is opened, or the conjugation is interrupted for any other reason, thus remaining in macrocycles of the chlorin, bacteriochlorin and isobacteriochlorin type. These structures are also characterized by a number of bands, usually four, of lesser intensity (compared to Soret) in the 500-650 nm region, designated by Q bands (**Figure 2.6**).

The relative intensity of these bands varies depending on the number and relative position of the substituent groups found in the periphery of the macrocycle and are responsible for conferring the different colours to the compounds. These bands result from transitions prohibited by symmetry and are designated IV, III, II, I, or Q_y (1,0), Q_y (0,0), Q_x (1,0), Q_x (0,0) respectively (Abrahamse *et al.*, 2016).

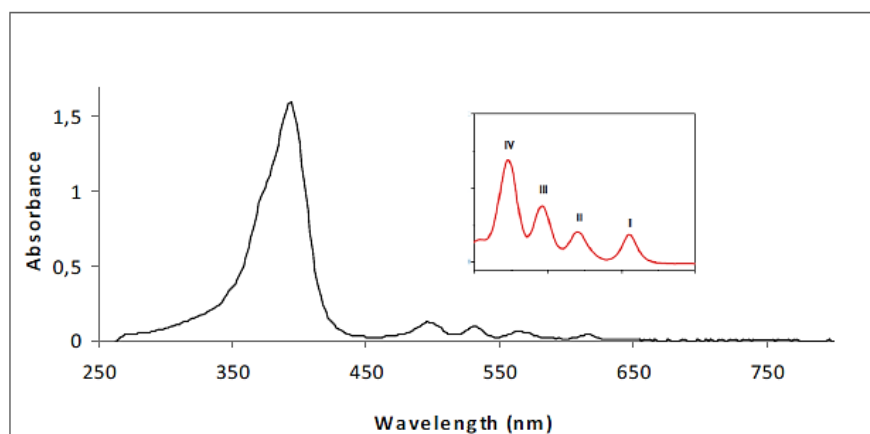


Figure 2.6 – UV-vis spectrum of a porphyrin with an expansion of Q region between 480-720 nm.

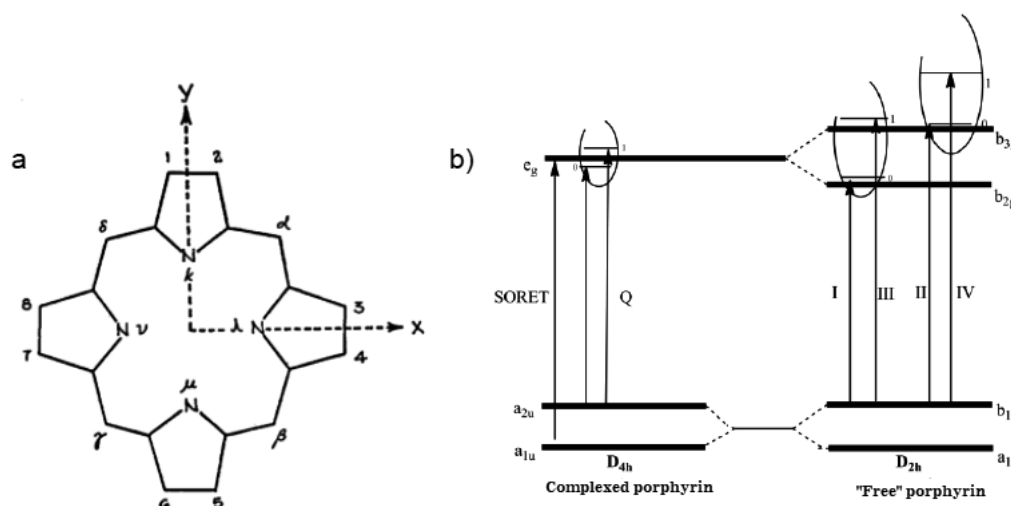


Figure 2.7 – a) Axes system on the porphyrinic “backbone”; b) Representation of the orbitals and electronic transitions between the fundamental state and the excited state of complexed and “free” porphyrins according to the model proposed by Gouterman.

The electron spectrum of porphyrin absorption is explained by Gouterman's theory of the four frontier orbitals (**Figure 2.7 (b)**), in which the bands are the result of $\pi\text{-}\pi^*$ transitions between two HOMO orbitals (Highest Occupied Molecular Orbital) and two LUMO orbitals (Lowest Unoccupied Molecular Orbital). These transitions are polarized along the x and y-axes of the porphyrin ring, being two x-polarized, and two y-polarized, (**Figure 2.7 (a)**).

If we analyze the UV-Vis spectra of the reduced porphyrins we can find significant differences, in particular with respect to the Q bands, when compared to porphyrins, which are mainly due to their different transitions between the HOMO and LUMO orbitals (**Figure 2.8**).

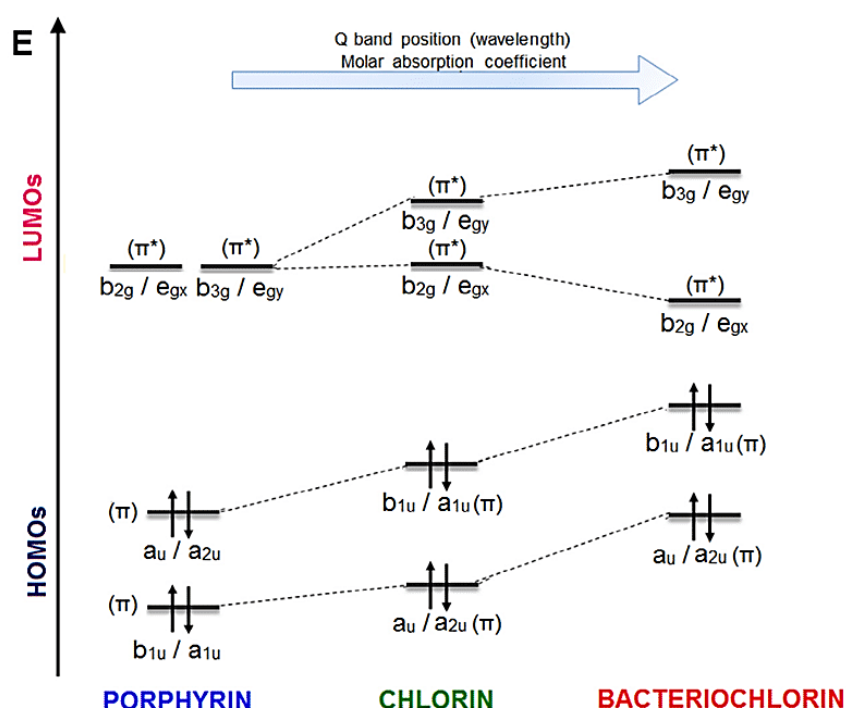


Figure 2.8 – HOMO and LUMO energies.

The Q band in the 650 nm region of the absorption spectrum of chlorins, for example, is much more intense than in porphyrins, since as the double bonds are successively reduced, the Q-band is substantially red-shifted and the height of the band also increases. This is also observed in the spectrum of bacteriochlorins, which have a strong absorption band in the region of 700-750 nm (**Figure 2.9**). These differences are also seen in the color of these compounds since chlorins generally form dark solids which when dissolved give rise to green solutions and usually bacteriochlorins form clear green solutions. Isobacteriochlorins generally form pink/violet solutions and have a set of three Q bands of decreasing intensity between 500 and 600 nm and a

peak of low intensity in the 650 nm region. In this way, UV-Visible spectroscopy is usually used to identify these compounds, allowing a clear distinction between porphyrins, chlorins, bacteriochlorins, and isobacteriochlorins.

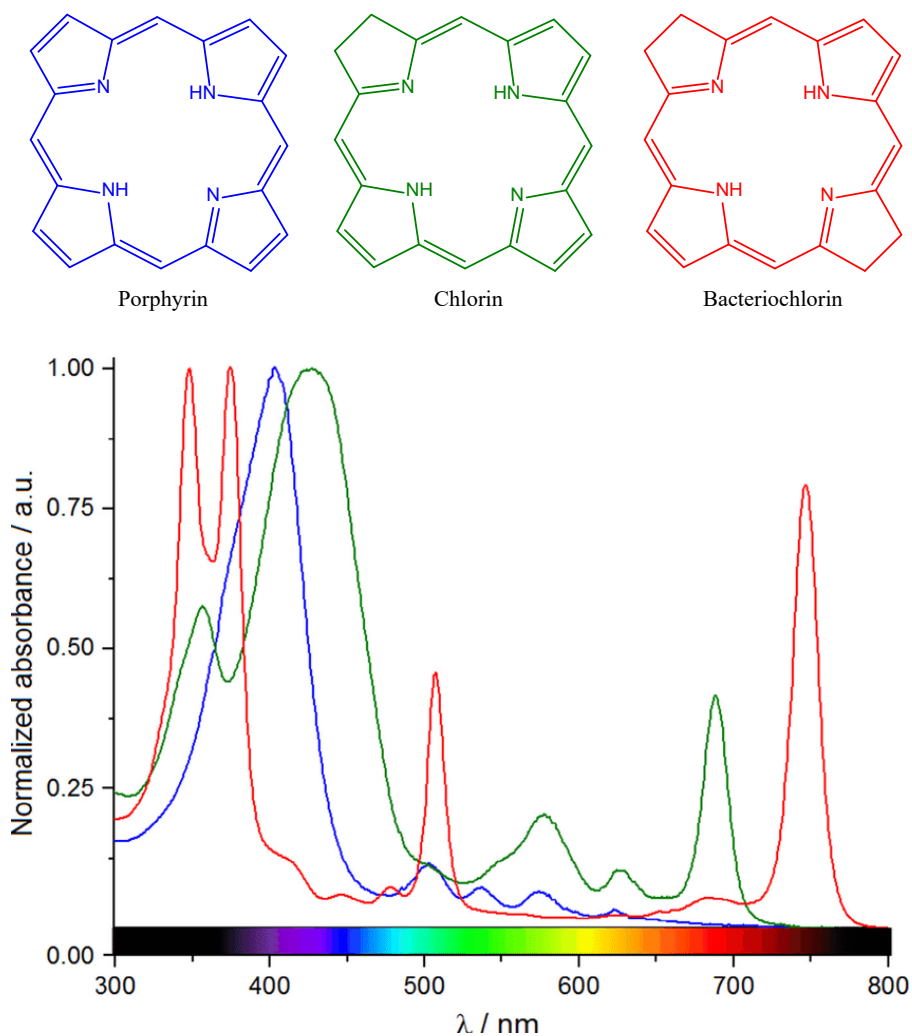


Figure 2.9 – Standard electronic absorption spectra for porphyrin, chlorin, and bacteriochlorin.

^1H NMR spectra of porphyrins are very characteristic. Uncomplexed porphyrins are characterized by a singlet with a value of δ (-2 to -3 ppm) lower than that of the tetramethylsilane (TMS) protons, due to the strong shielding that these protons suffer. Unlike the central N-H protons, the peripheral β -pyrrolic protons are unprotected due to the same electronic current that revolves around the ring, shifting their resonances to lower fields (δ between 7 and 9).

The reduction of one or two β -pyrrole positions leads to a decrease in the flow of the electronic current causing an increase in the value of the chemical shift of the internal protons (δ between -1 and -2 ppm) and sometimes a slight decrease in the value of the chemical shift of the peripheral protons.

1.4. Reactivity

When it comes to the porphyrin macrocycle, the cavity and the periphery of the ring are the two main reaction-prone regions. The internal reactions are usually involved in acid-base reactions promoted by the nitrogen atoms of the pyrrole units. In an alkaline medium, they act as Brønsted-Lowry acids (donating a proton) forming mono- or dianionic species, and in acid medium they function as Brønsted-Lowry bases (accepting a proton) forming mono- and dicationic species. They also have the ability to use the same nitrogens to coordinate with metal ions, thus forming very stable chelates or complexes, metalloporphyrins (Smith, 1975; Lascelles, 1964). The two hydrogens of the porphyrinic nucleus are dissociable, and so, through ionic bonds, divalent metal ions can coordinate within the same plane, with the four nitrogen atoms (Phillips, 1960) to form stable complexes, however when the metals are monovalent (Na^+ , K^+ , L^+ , Ag^+), the thermodynamic stability of the metalloporphyrins decreases (Smith, 1975). The incorporation of a metal atom in the centre of the porphyrin nucleus alters the absorption, fluorescence and solubility properties of porphyrins and their metal complexes (Milgrom, 1997).

Due to their aromaticity, porphyrins can also undergo typical reactions of electrophilic aromatic substitution in two possible positions, the β -pyrrole positions and the *meso* positions. Some possible reactions would be nitration, halogenation, sulfonation, alkylation and acylation (Milgrom, 1997) and the activation of one position over the other is achieved by modeling the macro-electronegativity. For example, in general, the porphyrin nuclei in the free form are electronically more reactive in the *meso* positions, which Woodward suggested might be explained by the tendency of the pyrrole subunits to be in an electronic sextet state in order to become independent of the macrocycle conjugation (Woodward *et al.*, 1969). Thus, the porphyrins and chlorins

present an electronic distribution in which the *meso* positions are poorer in electrons (**Figure 2.10**).

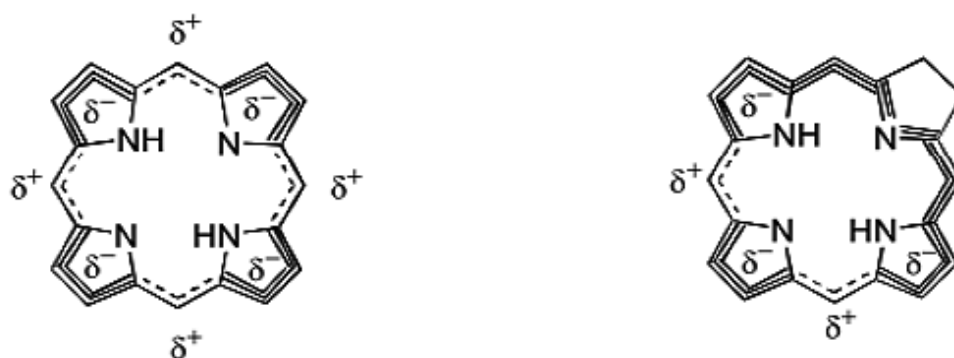


Figure 2.10 – Schematic representation of the electronic distribution on porphyrins and chlorins, according to Woodward

Another example would be the complexation of the macrocycle which highly influences the π -electronic system, interfering with the reactivity of the *meso* and β -pyrrole positions to the point that the use of metals of low electronegativity ($\text{Mg} < \text{Zn} < \text{Cu} < \text{Ni} < \text{Pd}$) in an electrophilic substitution causes the activation of the *meso* positions, while using the complexed porphyrin with more electronegative ions ends up activating the β -pyrrole positions.

To conclude, and because in the context of this work they cannot be left out, it should be noticed that there are other types of reactions such as oxidation, reduction, nucleophilic substitution or cycloaddition reactions, especially in the peripheral groups of porphyrins, which can also take place and produce significant structural alterations. These types of reactions can be very useful as a way of altering and optimizing the properties of the tetrapyrrolic macrocycle, and that was exactly what the intention of this work. The present dissertation focused, thereby, on the development of pentafluorophenyl chlorins fused with a 4,5,6,7-tetrahydropyrazolo[1,5-*a*]pyridine ring-functionalized with ester groups. These were obtained selectively by cycloaddition [$8\pi + 2\pi$] between pentafluorophenyl porphyrin and diazafulvenium methides, generated by thermal extrusion of sulfur dioxide from 2,2-dioxo-1*H*,3*H*-pyrazol[1,5-*c*]thiazoles. Furthermore, to increase the hydrophilicity of chlorins and its derivatives and thus the potential application in PDT, two

strategies were thought, one of them based on a nucleophilic reaction another being a reduction of the ester groups to alcohols, both of which will, later, be explained. However, we cannot forget that in order to obtain the desired chlorins, first, it was necessary to synthesize the porphyrinic precursors and the right strategy had to be thought out.

1.5. Synthetic Strategies for *meso*-substituted porphyrins

Porphyrins have a very versatile structure, allowing for the modulation of their physical and chemical properties by the introduction of substituent groups. This versatility has translated, in the last decades, into a rising interest in the manipulation of porphyrins already existing in nature, due to their involvement in biological processes of extreme importance. Consequently, a breakthrough regarding the artificial synthesis of new macrocycles originated from pyrrole and aromatic aldehydes, especially *meso*-substituted ones, has been observed.

Naturally occurring porphyrins are usually substituted at the β -pyrrole positions, however, because of the great difficulty of synthesizing these compounds, the synthetic porphyrins generally have substituents at the *meso* positions, since their synthesis is much simpler. It is possible to find in the literature two main different approaches to the synthesis of *meso*-substituted porphyrins: either by a single reaction process, where the total synthesis of the compounds - condensation, cyclization, and oxidation - occurs in a single reaction process, of which the Rothmund/Adler-Longo's Method is an example; or by a two separate steps reaction procedures, first with the condensation and cyclization and last with the oxidation.

1.5.1. Rothmund/Adler-Longo's Method

It was Rothmund who described, for the first time in 1935, the synthesis of symmetrical porphyrins, in a single process. It consisted of the pyrrole condensation reaction with the appropriate aldehyde, carried out in an inert atmosphere using pyridine as the solvent. Twenty five new porphyrinic compounds with different

substituents at the *meso* positions, all in fairly low yields, were obtained by this method. The only exception observed was when benzaldehyde was used, yielding at 10% for *meso*-tetraphenyl porphyrin (TPP). Calvin *et al.* continued this work and were able to conclude that the contamination with about 10-20% of the corresponding chlorin that was always detected in this kind of reactions was not only dependent on temperature but also on the presence of transition metal salts. Further studies allowed to conclude that when the reaction was carried out in the presence of zinc acetate and, like Rothmund, using pyridine as the solvent, it was able to significantly improve the yield for the preparation of TPP.

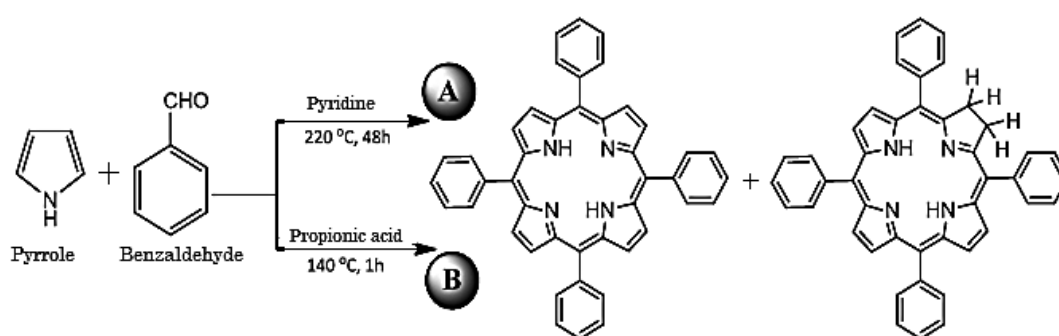


Figure 2.11 – Synthesis of 5,10,15,20-tetrakis(phenyl)porphyrin according to the reactional conditions established by (a) Rothmund's and (b) Adler-Longo's Method.

A few years later, in the 1960s, Adler and Longo modified the protocol developed by Rothmund and synthesized TPP starting from equimolar amounts of pyrrole and benzaldehyde in acid medium (e.g., propionic acid, acetic acid) and oxidizing atmosphere (**Figure 2.11**). The reaction was run under reflux at 140 °C for a period of 0.5-1 h, but, despite the considerable increase in reaction yield ($\approx 20\%$), chlorin contamination persisted, which Adler and Longo discovered was possible to rapidly be solved by converting the chlorin back to the corresponding porphyrin by the action of oxidizing agents such as 2,3-dichloro-5,6-dicyano-1,4-benzoquinone (DDQ).

Although this work was one of the major contributions to the development of a reliable method of obtaining TPP, it was unable to solve all the problems associated with the synthesis of *meso*-tetrasubstituted porphyrins, such as the formation of other by-products that hindered the purification process and the preparation, in acceptable

yields, of *meso*-arylporphyrins with bulky substituents at the *ortho* positions of the phenyl groups, and *meso*-alkylporphyrins in a reproducible manner. This method was also limited by the fact that some aldehydes may contain acid-sensitive functional groups and that in order to obtain pure porphyrins by this method, it was essential to oxidize chlorins using quinones of high oxidative potential (DDQ or chloranil). It is, thereby, easy to understand why this method, while widely used in the condensation process of aldehyde mixtures, does not have great application in the synthesis of *meso*-tetra-alkylporphyrins, and other methods were explored.

1.5.2. Lindsey's Method

In 1987, Jonathan Lindsey proposed a new two-step methodology for the synthesis of *meso*-substituted porphyrins, based on the premise that the reactional conditions adopted in Rothmund and Adler-Longo methodologies negatively influenced reaction yield (**Figure 2.12**). It starts with the condensation reaction of the pyrrole with an aldehyde in equimolar concentrations (10^{-2} M), carried out under an inert atmosphere at room temperature for 1 h in the absence of light. The solvent used has to be chlorinated and the presence of an acid catalyst (Boron trifluoride or Trifluoroacetic acid 10^{-3} M) is needed, resulting in the formation of a reduced intermediate, the porphyrinogen. In the next step, the oxidation of this intermediate, by the action of quinones of high oxidative potential (DDQ), results in obtaining the porphyrin of interest (Abrahamse *et al.*, 2017).

The mild reactive conditions and the high dilution of the reactants allowed to reduce the formation of undesired side products, which facilitates the purification process and contributes to the increase of reaction yield (35-40%). In contrast, quinones used in the oxidation of porphyrinogen imply a greater environmental and economic impact (Abrahamse *et al.*, 2017).

Since this approach has two key steps, there is room for the optimization on both of them, either on the preferential condensation and cyclization of the pyrrole with the aldehydes to give the porphyrinogen; or the oxidation of the porphyrinogen to the corresponding porphyrin. It has been demonstrated that regarding the condensation

of pyrrole with benzaldehyde, the process is very sensitive to the concentration of the reactants, the nature of the acid used in catalytic amounts and the co-catalysts used, such as ethanol or salts. Modulating these parameters, it was possible to produce TPP in yields between 5% and 58%, the best results being obtained with $\text{BF}_3\text{-Et}_2\text{O}$ (1 mM), NaCl (25 mM), in a solution of pyrrole (10 mM) and benzaldehyde (10 mM) using CH_2Cl_2 as the solvent. However, it should be emphasized that these conditions cannot be generalized since there is a strong dependence on aldehydes and catalysts used (Abrahamse *et al.*, 2017).

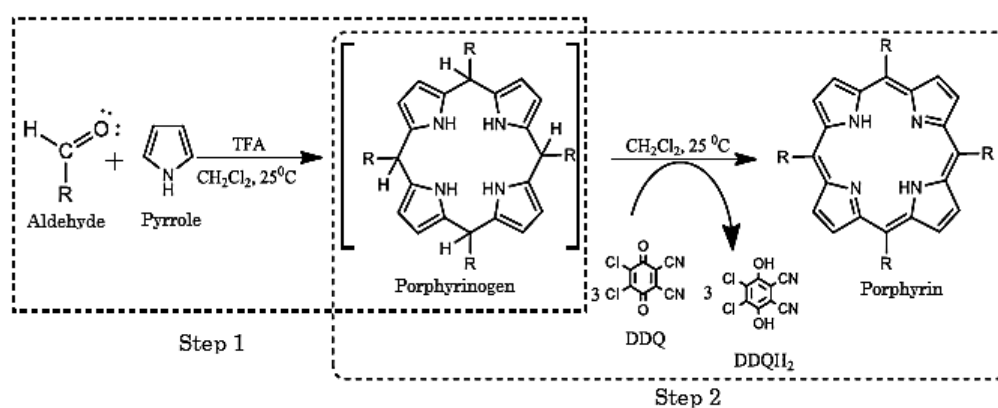


Figure 2.12 – Two-step method proposed by Lindsey in 1987 for the synthesis of *meso*-substituted porphyrins.

Due to the improved yields and also because the final products do not show any contamination with the corresponding chlorin, the Lindsey method is currently considered a landmark in the synthesis of *meso*-substituted porphyrins. For this reason, this method has been used in the synthesis of a wide range of symmetrical and asymmetric *meso*-substituted porphyrins. Despite the good results achieved by this method, it still has some disadvantages for large-scale application, namely the use of quinones as oxidizing agents, the need for large dilutions in the first step and the use of expensive and costly purification processes. Alternatives have emerged centred on the use of hydrogen peroxide as the oxidizing agent of porphyrinogen, in an attempt to quench the use of quinones in the oxidation process, which have proved to be a good alternative to the use of DDQ but are yet still to be widely used in the synthesis of *meso*-substituted porphyrins.

Despite all the advances done, it is important to note that the optimization of *meso*-tetraarylporphyrins synthesis is still a challenge and a matter of great interest to chemists since synthetic porphyrins have numerous applications.

1.5.3. The Nitrobenzene Method

The Nitrobenzene Method consists of a single reaction of pyrrole with different aldehydes at a temperature of 130 °C for about 1 h using a mixture of acetic acid/nitrobenzene (7: 3). This novel *meso*-porphyrin synthesis replaces propionic acid with a mixture of acetic acid and nitrobenzene, as the name suggests, and was developed in Coimbra in order to overcome the limitations of the previous method. The nitrobenzene is a good choice because it has a high boiling point and doesn't allow any alternative reactions, therefore being used as a solvent, especially for electrophilic reagents.

Some of the advantages of this method consist on the direct crystallization of the porphyrin into the reaction medium, after addition of methanol, with a high degree of purity and with little or no contamination with the respective chlorin; and the capacity of the nitrobenzene/air mixture at temperatures above 120 °C to not only promote the oxidation of the porphyrinogen to the corresponding porphyrin but also oxidize other intermediates to the respective porphyrins, avoiding contaminations of the final product. Like the Adler method, the nitrobenzene method has been used to synthesize numerous *meso*-substituted porphyrins, with the added advantage of allowing them to have voluminous substituents at the *ortho* positions of the phenyl groups of the *meso* positions, in a reproducible manner and with reasonable yields, which was not possible under Adler's conditions.

As mentioned before, there is yet another synthetic approach, initially developed by Gonsalves and Pereira for the synthesis of *meso*-tetraalkylporphyrins, which consists in the separation of the reaction/condensation/cyclization processes from the oxidation of the porphyrinogen. This strategy resulted in obtaining the porphyrinogen in high yields and the improvements introduced consisted of the use of catalytic amounts of

trifluoroacetic acid (TFA), acetals to the detriment of the respective alkyl aldehydes and carbon tetrachloride as a solvent.

Three different oxidation strategies have been developed in order to promote the transformation of porphyrinogen into its porphyrin. The first uses high-potency quinones as oxidizing agents, the second consists of photo-oxidation in the presence of acetic acid and the third uses air as an oxidant in the presence of zinc (II) acetate. Of the three methods used, the first approach, in which 2,6-dichloro-3,5-dicyano-1,4-benzoquinone (DDQ) is used as the oxidizing agent, was the one that led to better yields.

1.6. Synthesis of *meso*-substituted chlorins

Having understood the different methods from which we could choose to synthesize our porphyrinic backbone, the next step was to decide the best route to transform such porphyrins into the desirable chlorins. In recent years, mainly due to the potential use of such compounds in several scientific areas, with a special emphasis in medicine, a great effort has been put forth towards the development and improvement of new methods to convert porphyrins into dihydroporphyrins (chlorins) and tetrahydroporphyrins (isobacteriochlorins and bacteriochlorins) (Silva *et al.*, 2005).

While reductions or annulation transformations at the porphyrin core are the most common strategy to furnish chlorins, the requirement of multi-step synthesis and the lack of stability of simple chlorins, namely by the ease of back oxidation to the porphyrin state and photobleaching, make cycloaddition reactions a much more interesting and powerful tool for obtaining these derivatives, since they allow the formation of new carbon-carbon bonds and inhibit re-oxidation reactions leading back to the porphyrin core (Pereira *et al.*, 2015; Pereira *et al.*, 2018).

Several research groups have shown that Diels-Alder reactions and 1,3-dipolar cycloadditions can be excellent tools for preparing novel derivatives containing such macrocyclic features (Pereira *et al.*, 2010; Silva *et al.*, 2005). In addition, the high versatility and the region/stereoselectivity found in those reactions can be used to

prepare new porphyrinic compounds with well-defined stereochemistry. It was also shown that the stability of chlorins can be dramatically enhanced by the introduction of a fused ring. If required, they can even be further derivatized into more promising PDT agents, namely, by converting them into cationic derivatives by simple alkylation procedures (Silva *et al.*, 2005). At the same time, Cavaleiro's laboratory has explored the reactivity of *meso*-tetrakis(pentafluorophenyl)porphyrin (TPFPP) to act as a dipolarophile with azomethine ylides, reporting the synthesis of chlorin and isobacteriochlorin derivatives under such methodology (Souza *et al.*, 2014).

Recently, Pinho e Melo and co-workers reported a synthetic methodology which allowed the preparation of a new type of stable 4,5,6,7-tetrahydropyrazolo[1,5-*a*]pyridine-fused chlorins and bacteriochlorins, through a new and unprecedented $[8\pi + 2\pi]$ cycloaddition of diazafulvenium methides with porphyrins and chlorins. The reaction of *meso*-tetraarylporphyrins with diazafulvenium methide, generated by thermal extrusion of SO₂ from 2,2-dioxo-1*H*,3*H*-pyrazolo[1,5-*c*][1,3]thiazole, afforded new 4,5,6,7-tetrahydropyrazolo[1,5-*a*]pyridine-fused chlorin derivatives in a selective fashion with preliminary studies of photophysical characteristics that showed an intense absorption band at 650 nm, thus having one of the appropriate features for their possible use in therapy (Pereira *et al.*, 2011). Furthermore, the first results regarding the *in vitro* study of some of these chlorins showed that they are promising photosensitizers to be used in PDT against melanoma cancer cells, which is why this methodology was the chosen one for the synthesis of all described chlorins in this thesis.

1.6.1. Some strategies for the synthesis of chlorins

The synthesis of particular chlorins and derivatives was the ultimate goal of the first part of the experimental work for this dissertation. It has already been discussed the different paths possible for the synthesis of porphyrins and the strategy behind the synthesis of 5,10,15,20-tetrakis(pentafluorophenyl)porphyrin. However, to better understand the choice of methodology regarding the synthesis of the ring-fused 5,10,15,20-tetrakis(pentafluorophenyl)chlorin, first, we must understand the most used strategies in general.

1.6.1.1. Reduction

There is a variety of ways of transforming porphyrins into chlorins. Whitlock, for example, was able to carry out the reaction of 5,10,15,20-tetraphenylporphyrin with *p*-toluenesulfonylhydrazide, utilizing pyridine as the solvent, at reflux, and potassium carbonate as the base, forming a mixture of chlorin and bacteriochlorin, with the added advantage of being able to oxidize the bacteriochlorin to chlorin by the use of *o*-chloranil, the yield of this reaction being 72%. However, if the desired product was to be the bacteriochlorin instead, then an excess of the diimide precursor was to be administered, giving 50% yield (Whitlock *et al.*, 1969). This was, actually, the same method applied to synthesize the *meso*-tetrahydroxyphenylchlorin, the active principle of Foscan, in 37% yield. (Bonnet *et al.*, 1989).

In 2010, Pereira *et al.*, aware of the environmental disadvantages inherent to this method, such as the use of a large amount of solvent and base, adapted the method described above. By doing so, they ended up describing the synthesis of bacteriochlorins, through the reduction of porphyrins with diimide, in the absence of solvent and base (Pereira *et al.*, 2010). Another research group, in the same year, described the synthesis of hydroporphyrins under microwave irradiation, based on the Whitlock method (Nascimento *et al.*, 2010)

1.6.1.2. Dihydroxylation

Another strategy for the synthesis of hydroporphyrins is through dihydroxylation. It was described in 1995 that by using OsO₄ as, for example, it is possible to oxidize *meso*-substituted porphyrins and obtain hydroporphyrins. Brückner *et al.*, added a stoichiometric amount of OsO₄ to TPP to form diols at the β-pyrrole position and, thereby, 2,3-cis-dihydroxy-*meso*-tetraphenylchlorin, in a yield of 50% (Brückner *et al.*, 1995). However, some drawback like the long reaction time (7 days) and the need to use expensive reagents and hazardous substances, such as OsO₄, have contributed to the replacement of this method by others (Calvete *et al.*, 2009).

1.6.1.3. Cycloaddition

Reduction and oxidation, despite being common strategies to obtain hydroporphyrins, have, amongst others, the main disadvantages of the resulting chlorin is very often unstable being easily oxidized back to the porphyrin and the synthesis route having many steps. Once the interest is the synthesis of stable chlorins, alternative methods, other than these, were necessary. A better alternative can be the chemical modification of simple porphyrins, namely via cycloaddition transformations involving the pyrrole units of the porphyrins. For instance, if a porphyrin macrocycle is substituted with a vinyl group, then the latter and a peripheral double bond of the macrocycle can act as a diene system. In such way, the macrocycle can react with dienophiles to yield Diels-Alder adducts. Besides that, *meso*-tetraarylsubstituted porphyrins can also participate as dienophiles or as dipolarophiles, increasing the possibilities of using these compounds in other types of cycloadditions.

1.6.1.4. Diels-Alder

Ever since it was discovered, in 1996, that porphyrins substituted with vinyl groups at the β -pyrrole positions can act as dienes in Diels-Alder reaction, through the reaction of a nickel-complexed substituted *meso*-porphyrin with tetracyanoethylene (TCNE) dienophiles and acetylene dicarboxylate (DMAD), intensive work has been done in the study of cycloaddition reactions with porphyrins as a simple and easy strategy to produce chlorins and other reduced porphyrins.

Shortly after, in 1997, Cavaleiro and his investigators described the participation of porphyrins as dienophiles in Diels-Alder reaction as they made *meso*-tetra-arylporphyrins react with the reactive diene, benzoquinodimethane, at reflux, of 1,2,4-trichlorobenzene, forming the corresponding chlorins via cycloaddition $[4\pi + 2\pi]$, and in some cases obtaining bacteriochlorins and/or porphyrins (resulting from the oxidation of chlorins) as by-products, which were very difficult to separate by chromatography (Tome *et al.*, 1997; Cavaleiro *et al.*, 2000).

✓ 1,3-dipolar cycloaddition reactions

As mentioned previously, porphyrins may also act as dipolarophiles in 1,3-dipolar cycloaddition reactions and can react with several 1,3-dipoles, such as azinete, diethyl nitriles, diazoalkanes and carbonyl imines, resulting in chlorins. In 1999, Cavaleiro and his investigators published the first study of the reactivity of *meso*-substituted porphyrins and showed that porphyrins containing aryl groups with electron-attracting substituents, showed higher reactivity as dipolarophiles, obtaining the respective chlorins with better yields (Silva *et al.*, 1999). These kinds of reactions, well-known to be applied for the formation of five-membered heterocyclic rings, have been successfully applied for the synthesis of ring-fused hydroporphyrins, one example being the reaction of porphyrins with diazomethane, which subsequently undergoes through an extrusion of nitrogen to give the chlorin fused to a cyclopropane ring (Silva *et al.*, 2002; Desjardins *et al.*, 2002).

✓ 1,7- dipolar cycloaddition reactions

In order to minimize some of the problems present in other synthetic strategies, Pinho e Melo *et al.* have developed a new and innovative synthetic process which produces fairly stable hydroporphyrins through an $[8\pi + 2\pi]$ reaction of diazafulvenium methides with porphyrins. The reaction of *meso*-tetraarylporphyrins with this dipole, generated by thermal extrusion of SO_2 from 2,2-dioxo-6,7-dimethyl-1*H*,3*H*-pyrazolo[1,5-*c*][1,3]thiazole-6,7-dicarboxylate, affords 4,5,6,7-tetrahydropyrazolo[1,5-*a*]pyridine-fused chlorins (Pereira *et al.*, 2010). With this strategy, stable chlorins (and bacteriochlorins if an excess of the dipole is used) can be formed, in reasonable yields, in a selective way, with heterocyclic rings having electron attracting groups near the reduced rings. Furthermore, in this synthetic process, better yields were achieved when the reaction was carried out using the microwave technology (250 °C and for 20 minutes) instead of conventional heating (Pereira *et al.*, 2011; Nascimento *et al.*, 2013).

1.7. Fluoride, more than a Hydrogen bioisostere

It takes years of cumulative research to develop a clinically useful drug. A lead compound with a desired pharmacological activity, either a cure for a particular disease or symptomatic relief from a physiological disorder, usually has undesirable side effects associated with it. In medicinal chemistry, bioisosteres are chemical substituents or groups with similar physical or chemical properties that produce biological properties broadly similar to other chemical compounds. Bioisosterism, thereby, represents one approach used by the medicinal chemist for the rational modification of the structural features of the lead compounds and, consequently, enhance their desired biological characteristics, such as bioavailability, metabolism, and excretion from the body, into safer and more clinically effective agents (Patani *et al.*, 1996). The ring-fused (pentafluorophenyl)chlorins which are the subject of this dissertation have, as the name suggests, pentafluorophenyl groups on the *meso* positions of the chlorin structure, which were thought to be included based on some of the conclusions that have come to the surface along the years.

Bioisosteres can be classified as either classical or nonclassical. Classical bioisosteres have been traditionally divided into several distinct categories: (A) monovalent atoms or groups; (B) divalent atoms or groups; (C) trivalent atoms or groups; (D) tetrasubstituted atoms; and (E) ring equivalents. Similarities in certain physicochemical properties have enabled investigators to successfully exploit several monovalent bioisosteres such as fluorine vs hydrogen replacements; fluorine, hydroxyl, amino, and methyl group interchanges (Grimm's Hydride Displacement Law); or chloro, bromo, thiol, and hydroxyl group interchanges (Erlenmeyer's Broadened Classification of Grimm's Displacement Law) (Patani *et al.*, 1996). Nonclassical isosteres do not obey the steric and electronic definition of classical isosteres and do not have the same number of atoms as the substituent or moiety for which they are used as a replacement, despite this they are able to be divided into two groups: (A) rings *vs.* noncyclic structures; and (B) exchangeable groups (Zhu *et al.*, 2015).

It is well-known that porphyrins containing fluorine have attracted increasing attention in PDT especially since investigation on fluorine analogs showed that some fluorine porphyrins selectively bind to specific tumor tissue (Gao *et al.*, 2015). An example of the advantage of using fluorine as a bioisostere of hydrogen would be the *meso*-tetrakis(pentafluorophenyl)porphyrin, that with a total of 20 strongly electron-withdrawing fluorine atoms has a significant inductive effect on the chromophore and is considered to be oxidatively more robust than its phenyl analogue. Moreover, its solubility is significantly better in common organic solvents than that of *meso*-tetrakisphenylporphyrin or many of its simple phenyl derivatives (such as 4-methyl-, 4-methoxy-, or 4- carboxyphenyl derivatives) (Hyland *et al.*, 2012).

The substitution of hydrogen by fluorine is one of the most commonly employed monovalent isosteric replacements. The basis for the major differences in the pharmacological properties of agents where fluorine has been substituted for hydrogen is mostly due to the difference in the electronic effects (fluorine being the most electronegative element in the periodic table), since the steric parameters for hydrogen and fluorine are similar, their van der Waal's radio being 1.2 and 1.35 Å, respectively. Due to its electronegativity, fluorine exerts strong field and inductive effects on the adjacent carbon atom and a diminished electron-withdrawing effect at distal sites. However, fluorine can donate a lone pair of electrons by resonance, commonly referred to as its mesomeric effect. The pharmacological differences can be attributed to the influence of the electron-withdrawing effect that the fluorine substitution causes on interaction with either a biological receptor or enzyme, as well as its effect on the metabolic fate of the drug.

A classical example of how fluorine substitution of a normal enzyme substrate can result in a derivative which can alter select enzymatic processes is the antineoplastic agent 5-fluorouracil (5-FU). *In vivo*, it is biochemically transformed into 5-fluoro-2 ϕ -deoxyuridylic acid, that because of its close similarity to uracil allows this fluoro derivative to be a successful mimetic. This biochemically altered form of 5-FU, due to the inductive effect of fluorine which results in its covalent binding to thymidylate synthase, has an increase in its activity and can, then, inhibit the thymidylate synthase, an enzyme involved in the conversion of uridylic acid to thymidylic acid and critical for DNA synthesis.

Substitution of one or more hydrogens for fluorine has also been used to modulate metabolism or off-target activity because the C-F bond is particularly strong and therefore resistant to metabolic cleavage. Since fluorine is also highly electronegative, it helps reducing the potential for oxidative metabolism and the drug candidate may have a longer half-life. However, it must be remembered that any advantage can be compensated by the resulting increase in LogD.

Combining the potentialities of the tetracyclic macrocycles in medicine with the advantages of the presence of fluorine atoms in organic molecules, the main objective of this work is the synthesis of fluorinated chlorin derivatives as potential photosensitizers. Tetrapyrrolic derivatives remain the most promising PDT photosensitizers in terms of strong absorption in the visible and excellent photosensitizing ability due to their long-lived triplet states, which allow the formation of reactive oxygen species (ROS), the major cytotoxic agents during the photodynamic action. It is well known that the incorporation of metal ions or halogen atoms, like chlorine and fluorine, in the macrocycle changes the balance between fluorescence and intersystem crossing and can influence many photophysical parameters. This is assigned to the “heavy atom effect” resulting from the increased spin-orbit coupling in the presence of atoms with higher atomic number and, consequently, higher spin-orbit coupling constants that enable efficient intersystem crossing, large triplet quantum yields and the generation of ROS with high yields.

It is important to understand that one molecule of “excited” photosensitizer only interacts with one molecule of oxygen at a time, and that the addition of fluoride atoms in the structure does not change that “stoichiometry”. The way that this addition works for the generation of ROS with high yields is that it makes the overall structure of the photosensitizer more stable / less photodegradable (lower decomposition quantum yield), allowing it to be “recycled” and therefore excited a higher number of times (higher turnover and higher fluorescence quantum yield, respectively) in comparison to its phenyl analogue, which translates into more interactions with O₂ and, consequently, more ROS generated.

Lastly, as mentioned before, one of the main goals is also to increase the hydrophilicity of chlorins and thus to potential application in PDT. A strategy applied in drug design to achieve compounds with the ideal properties to be used in biological media and to

improve cell permeability is the incorporation of polyethylene glycol (PEGs) moieties. Therefore, we decided to prepare a new type of PEGylated ring-fused (pentafluorophenyl)chlorins by exploring nucleophilic aromatic substitution reactions on the *para* position of the pentafluorophenyl group on the *meso* position of the chlorin. Previously, 5,10,15,20-tetrakis(pentafluorophenyl)porphyrin, TPFPP, has revealed to be a surprisingly versatile template to new porphyrin derivatives. In fact, the reaction of TPFPP with nucleophiles provided a simple and general access to functionalized *meso*-tetraarylporphyrins containing electron-donating substituents in the *para*-position of their *meso*-aryl groups. The pentafluorophenyl group is not chemically inert and has been shown to undergo several nucleophilic aromatic substitution reaction (S_NAr) with a range of nucleophiles (Samaroo *et al.*, 2007). Besides, the nucleophilic aromatic substitution of the *para*-F atoms is highly selective and frequently occurs with high yield (Costa *et al.*, 2011). This is yet another advantage of using fluorine since the fluoride ion is widely used as a nucleophile and a leaving group in organic nucleophilic reactions, in particular in arene chemistry (Vlasov, 1993). The key point to understanding why it is such a good leaving group in the nucleophilic aromatic substitution is knowing the rate determining step of the reaction mechanism (**Figure 2.13**). The mechanism is the shown in the following picture (Nu = Nucleophile, X = leaving group).

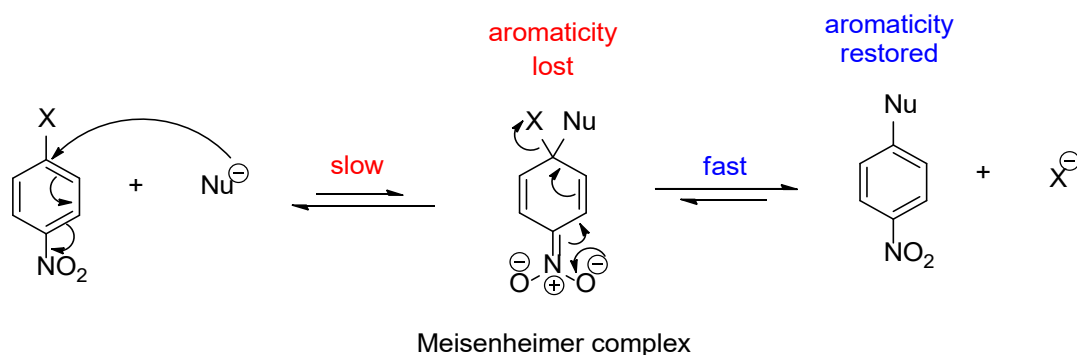


Figure 2.13 – Schematic representation of the mechanism of an aromatic nucleophilic substitution reaction.

Once aromaticity is lost in the first step, the energy barrier becomes higher, making the first step (addition) very slow. On the other hand, since the second step

(elimination of the leaving group) involves the aromaticity being restored, it is quite fast, making the actual quality of the leaving group not very important, because even if you use a very good leaving group (e.g. iodine), which speeds up the elimination step, the overall reaction rate will not increase as the additional step is the bottleneck of the reaction.

Fluorine is not a good leaving group, but, as stated, that doesn't matter. What makes the reaction go faster than with, say, bromine or chlorine, it's its high inductive effect, due to its large electronegativity, which helps to stabilize the negative charge in the Meisenheimer complex and thus lowers the activation barrier of the (slow) addition step. Since this step is the bottleneck of the overall reaction, a speedup here speeds up the whole reaction. As listed before, there is a set of characteristics provided by the bioisosterism that made impossible not to use the substitution of hydrogen by fluorine in the design of our target molecules, but this isn't the only strategy used, and so, to finish this chapter, and the Introduction itself, a brief resume of the rationality behind the design should be given, in order to better understand the choice of these structures over any others.

1.8. The rationality behind the design

The question that imposes itself right now is why these compounds? What was the logic for choosing them? What are the advantages they possess over any others?

We are taught that the rational design of a compound, nowadays, starts by trying to understand a target disease, more specifically its mechanisms of action, and to go from there. Many compounds are, for example, designed bearing in mind a certain protein/receptor that has an active site for which the compound must bind, in most cases selectively. In this case, the disease of concern was cancer, in particular oesophageal cancer and melanoma, since they are not only two of the most concerning cancers regarding therapy, it has been stated before how in the case of melanoma there's currently an issue surrounding resistance to conventional therapies, for example, but also because of their easy accessibility to a light source for PDT treatment. After having done some research involving photodynamic therapy and how it interacts with cancer, the goal was to understand how to take advantage of the

knowledge of its characteristics in order to further modulate of our molecules. After understanding the main points that we could focus on, such as light, oxygen and the photosensitizer itself, it was time to try and find the best structure/activity relationship.

Tetrapyrrolic macrocycles were undeniable the family of compounds that showed most promises and so that was the starting point. After that, chlorins due to their chemical and physical properties, and based on recent studies where they had been applied as photosensitizers and showed promising results, stuck out as the possible main backbone for our compounds, especially pentafluorophenyl chlorins not only because halogen atoms (-F, -Cl) in the *ortho* positions of the phenyl rings in the *meso* position of macrocycle are known to improve the photophysical properties by promoting intersystem crossing and increase singlet oxygen quantum yields, but also due to all the other characteristics previously referred (Piñeiro *et al.*, 2001). In addition, the chlorins proposed for the study did not result from a simple reduction of the porphyrin, but from a $[8\pi + 2\pi]$ cycloaddition of diazafulvenium methides with 5,10,15,20-tetrakis(pentafluorophenyl) porphyrins, which allowed to obtain ring-fused chlorins, proven to be much more stable on the matters of back oxidation and photobleaching and also able to be further functionalized at its ester moieties.

5,10,15,20-tetrakis(pentafluorophenyl) chlorin reveals itself to be a surprisingly versatile template to new chlorin derivatives as well, since the pentafluorophenyl substituent is also easily functionalizable. Their reaction with nucleophiles provides a simple and general access to functionalized *meso*-tetraarylchlorins containing electron-donating substituents in the *para*-position of their *meso*-aryl groups. Besides, the nucleophilic aromatic substitution (S_NAr) of the *para*-F atoms is highly selective and frequently occurs with high yield. Furthermore, the fact that it was used dimethyl-4,6-dihydropyrazolo[1,5-*c*]thiazole-2,3-dicarboxylate-5,5-dioxide to do the cycloaddition, enables it to be further functionalized in its di-ester groups, which leads us to the last part of the design. At this moment, the pentafluorophenyl ring-fused chlorins have advantages on the light aspect, absorbing at longer wavelengths and, thereby, solving competition problems with endogenous chromophores; also at the oxygen level, since the addition of the fluorine moieties has as a consequence the increase in yield of reactive oxygen species as explained before; but there is still room

for alteration at the photosensitizer level itself. One of the main drawbacks of this kind of compounds is their low lipophilicity and solubility in biocompatible media. It is widely recognized that the hydrophobic nature of the majority of unmodified porphyrins and chlorins is a limiting factor for their biomedical applications, furthermore, it was demonstrated that the hydrophilicity of these compounds is crucial to ensure high cytotoxicity against cancer cells. Thus, hydrophilic substituents are frequently inserted into the macrocycle in order to develop clinically relevant photosensitizers. Various hydrophilic substituents have been introduced in the phenyl rings of tetraphenylporphyrin (TPP) and their effects on the photodynamic behavior of the compounds have been examined. The number of polar groups and pattern of the substitutions significantly affect the photocytotoxicity of porphyrin derivatives and phthalocyanines (Pucelik *et al.*, 2017).

Bearing this in mind, the molecular design thought of in order to solve this issue found itself divided into two different approaches. The first one involves peripheral substituents to obtain polarity-tunable compounds. Since a well-known strategy applied in drug design to achieve compounds with the ideal properties to be used in biological media and to improve cell permeability is the incorporation of polyethylene glycol (PEGs) moieties, it was decided to prepare a new type of PEGylated ring-fused pentafluorophenyl chlorins by exploring nucleophilic aromatic substitution reactions. The other strategy focuses on the reduction of the fused ring ester groups to hydroxymethyls in order to increase the hydrophilicity of these chlorins and, consequently, their efficiency as photosensitizers.

1.9. So, what are the goals?

The aim of this dissertation was, then, the synthesis and *in vitro* studies of novel ring-fused pentafluorophenylchlorin derivatives on two different cell lines, the OE19 and the A375 which are, respectively, oesophageal cancer and melanoma; the main goal being the disclosure of the synthetic details, structural characterization and cytotoxicity evaluation of these very promising PDT agents as well as the understanding of the influence of the introduction of both the pentafluorophenyl groups and PEG-moieties into the structure on the overall activity of these molecules, especially regarding cell permeability.

CHAPTER 3 – Experimental Section

REAGENTS

All reagents were supplied by Aldrich, Merck or Fluka and used directly, without any further purification.

SOLVENTS

The solvents used, except 1,2,4-trichlorobenzene which was used directly as purchased, were purified following the methods reported in the literature (Amarego *et al.*, 1997).

- **Ethyl Acetate** – refluxed during 3 hours in the presence of potassium carbonate and then distilled.
- **Dichloromethane** – refluxed during 3 hours in the presence of calcium chloride, distilled and then stored on 4 Å molecular sieves.
- **Ethanol and methanol** – refluxed for 2 hours with magnesium (5 g/L) in the presence of iodine (0.5 g/l), followed by distillation from sodium alkoxide and then stored on 3 Å molecular sieves.
- **Diethyl ether and hexane** – refluxed in the presence of sodium strands, using benzophenone as indicator, distilled and stored on 4 Å molecular sieves.

EQUIPMENT USED

○ Nuclear magnetic resonance spectroscopy

Nuclear magnetic resonance spectra (RMN 1H e RMN 13C) were obtained on Bruker Avance III spectrometers, operating at 400 MHz (1H) and 100 MHz (13C). Solvent used was deuterated chloroform (CDCl₃), except on indicated cases. Chemical shifts were presented in ppm relatively to the intern standard tetramethylsilane (TMS) and coupling constant values (J) were expressed in Hz.

○ Mass spectrometry

Mass spectra were obtained on a Bruker FTMS APEXIII mass spectrometer, with ionization by electrospray (ESI) or HP 6890 Plus, with ionization through electronic impact (EI).

○ Microwave

Reactions with microwave irradiation were conducted on a Discover S-Class equipment from CEM Focused Synthesis System.

○ Chromatography

On reactions which evolution was accompanied through thin layer chromatography, it was used 60 F254 silica plates on aluminium support, provided by Merck. Most compounds were isolated by silica column chromatography, using silica gel 60 (0.040-0.063 mm) provided either by Merck, Macherey-Nagel or Fluka.

○ Ultraviolet-Visible Absorption Spectroscopy

Some reactions were controlled through absorption spectroscopy in the region of UV-Vis, using a Hitachi U-2001 spectrophotometer.

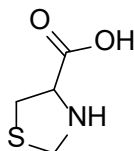
1. Experimental Section Part I – Synthesis and Characterization

In this section, it will be presented the procedures used for the synthesis of the desired chlorins and their precursors. Characterization details of these compounds will also be described.

1.1. SYNTHESIS OF DIAZAFULVENIUM METHIDE 3.0 PRECURSORS

The synthesis of dimethyl 4,6-dihydropyrazolo[1,5-*c*]thiazole-2,3-dicarboxylate (3.0) was performed according to an adapted literature (Pereira *et al.*, 2011) procedure, and it involves 4 steps, starting with the preparation of 1,3-thiazolidine-4-carboxylic acid (3.0).

✓ Synthesis of 1,3-thiazolidine-4-carboxylic acid (3.0a)

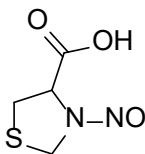


To a solution of L-cysteine (0.2 mol; 14.40 g) in water (120 mL) a solution of formaldehyde (0.16 mol; 12 mL) in ethanol (90 mL) was added and the reaction mixture was left stirring at room temperature for 24 h (Sutcliffe *et al.*, 2000).

A white solid precipitated from the mixture which was then filtered and washed with diethyl ether. The product was dried under vacuum and obtained in 97% yield (15.5 g; 0.116 mol).

^1H NMR (400 MHz, CDCl_3): δ = 4.38 (d, J = 9.6, 1H), 4.22 (d, J = 9.6, 1H), 3.72-3.75 (m, 1H), 2.99-3.02 (m, 2H) ppm.

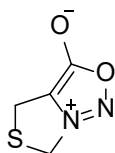
✓ **Synthesis of 3-nitrosothiazolidine-4-carboxylic-acid (3.0b)**



Concentrated HCl was slowly added to a suspension of the previously obtained 1,3-thiazolidine-4-carboxylic acid (0.12 mol; 15.5 g) in water (70 mL) until their complete dissolution. Then, an aqueous solution (70 mL) of sodium nitrite (0.18 mol; 12.19 g) was added dropwise and the reaction mixture left to react for 24 h at room temperature (Sutcliffe *et al.*, 2000). A few drops of concentrated HCl were added to the mixture and the product was extracted with ethyl acetate (3 x 100 mL). The organic layer was dried with anhydrous sodium sulphate and the solvent evaporated. The product was obtained as a yellow solid in 65% yield (12.33 g; 76 mmol).

^1H NMR (400 MHz, CDCl_3): δ = 4.95 (t, J = 7.1 Hz, 1H), 4.88 (d, J = 11.7 Hz, 1H), 4.49 (d, J = 11.7 Hz, 1H), 3.48-3.30 (m, 2H) ppm.

✓ **Synthesis of 4,6-dihydrothiazolo[3,4-c][1,2,3]oxadiazol-7-ium-3-olate (3.0c)**

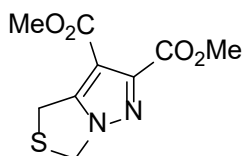


Trifluoroacetic anhydride (77.76 mol; 10.9 mL) was added dropwise to a suspension of 3-nitrosothiazolidine-4-carboxylic-acid (**3.0b**) (12.37 g) in diethyl ether (750 mL),

previously cooled in an ice bath, and the reaction mixture was left stirring at 0 °C for 6 h. After that time, the mixture was kept stirring at room temperature for an additional 24 h (Sutcliffe *et al.*, 2000). The solvent was evaporated, the crude mixture dissolved in ethyl acetate (300 mL) and then washed with water (200 mL) and with a solution of NaHCO₃ (200 mL). The organic layer was dried with anhydrous Na₂SO₄ and the solvent evaporated. Compound **3.0c** was obtained by precipitation in cool diethyl ether as a yellow solid in 28% yield (3 g; 20.8 mmol).

¹H NMR (400 MHz, CDCl₃): δ = 5.42 (t, *J* = 1.8, 2H), 4.04 (t, *J* = 1.7, 2H) ppm.

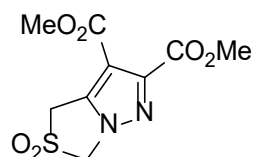
✓ **Synthesis of dimethyl 4,6-dihydropyrazolo[1,5-*c*]thiazole-2,3-dicarboxylate (3.0d)**



Dimethyl acetylenedicarboxylate (33.27 mmol; 4.16 mL) and dimethyl 4,6-dihydropyrazolo[1,5-*c*]thiazole-2,3-dicarboxylate (3.0c) (20,82 mmol; 3 g) in xylene (30 mL) were heated to reflux (T=140 °C) and the reaction mixture was left stirring for 3 h (Sutcliffe *et al.*, 2000). The solvent was then evaporated under reduced pressure and the product, purified by recrystallization from methanol, was obtained as a white solid in 67% yield (3.4 g; 14 mmol).

¹H NMR (400 MHz, CDCl₃): δ = 5.25 (t, *J* = 2.0, 2H), 4.31 (t, *J* = 2.0, 2H), 3.96 (s, 3H), 3.86 (s, 3H) ppm.

✓ **Synthesis of dimethyl 4,6-dihydropyrazolo[1,5-c]thiazole-2,3-dicarboxylate 5,5-dioxide (3.0)**



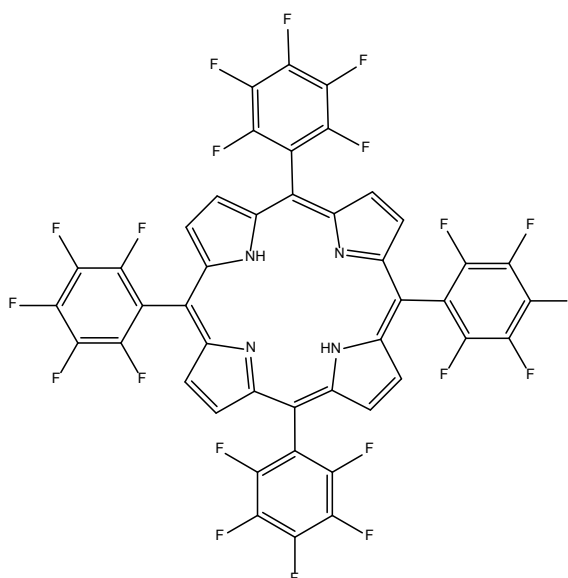
To a stirred solution of **3.0d** (3.39 g; 14 mmol) in dry dichloromethane (125 mL), at 0 °C, 3-chloroperoxybenzoic acid (77%; 9.47 g; 41.88 mmol) was added, in small portions. After the addition was finished, the reaction mixture was allowed to warm to room temperature and left stirring (Sutcliffe *et al.*, 2000). After 12 h the oxidation was controlled by TLC and deemed complete. The reaction mixture was washed with a 10% aqueous sodium bisulfite solution (2 x 100 mL) followed by a saturated solution of NaHCO₃ (200 mL). The organic layer was dried with anhydrous Na₂SO₄ and the solvent evaporated. Dimethyl 4,6-dihydropyrazolo[1,5-*c*]thiazole-2,3-dicarboxylate 5,5-dioxide (**3.0**) was purified by recrystallization in diethyl ether and obtained as a white solid in 79% yield (3.04 g; 11.08 mmol).

¹H NMR (400 MHz, CDCl₃): δ = 5.25 (t, *J* = 2.0, 2H), 4.31 (t, *J* = 2.0, 2H), 3.96 (s, 3H), 3.86 (s, 3H) ppm.

1.2. SYNTHESIS OF PORPHYRINS

The second precursor needed for the synthesis of the desired chlorins through an $[8\pi + 2\pi]$ cycloaddition reaction is the dipolarophile, which in this case is the porphyrin since diazafulvenium methide, generated by thermal extrusion of SO_2 from sulfone **3.0**, acts as the dipole (Pereira *et al.*, 2010, 2011)

1.2.1. Synthesis of 5,10,15,20-tetrakis(pentafluorophenyl)porphyrin (3.1a)



The synthesis of porphyrin **3.1a** was performed based on Lindsey's method (Lindsey *et al.*, 1986; 1987; 1989). To a solution of pentafluorobenzaldehyde (1.96 g; 1×10^{-2} mol) in dichloromethane (900 mL) was added pyrrole (0.68 mL; 1×10^{-2} mol) and the reaction mixture was left stirring, in the dark, at room temperature for 2 min under inert atmosphere (N_2). After that period, trifluoroacetic acid was added (0.77 mL; 10 mmol) and the stirring continued for 4 h. Then, DDQ was added (1.7 g; 7.5 mmol), along with a few drops of trimethylamine, and the reaction mixture was stirred for another 1 h. The porphyrin formation was followed by UV-Vis (Soret band at ~ 410 nm).

The solvent was evaporated under reduced pressure and the product purified by silica-gel column chromatography, using as eluent a mixture of hexane:dichloromethane (1:1). The obtained purple solid was then recrystallized with methanol, filtered and dried under vacuum. The porphyrin was achieved in ~7% yield (0.68 g; 69.8 mmol).

1.2.1.1. Alternative method

Porphyrin **3.1a** was also synthesized based on another method described in the literature. To a solution of benzaldehyde (4.62 g; 23.6 mmol) in acetic acid (70 mL) was added pyrrole (1.6 mL; 23.6 mmol). The reaction was carried out for 2 h at 120°C and then the mixture was allowed to cool to room temperature. The solvent was evaporated and the product was purified by flash chromatography, using dichloromethane as eluent. The isolated porphyrin was obtained as a purple solid in 4% yield (0.38 g; 3.9 mmol).

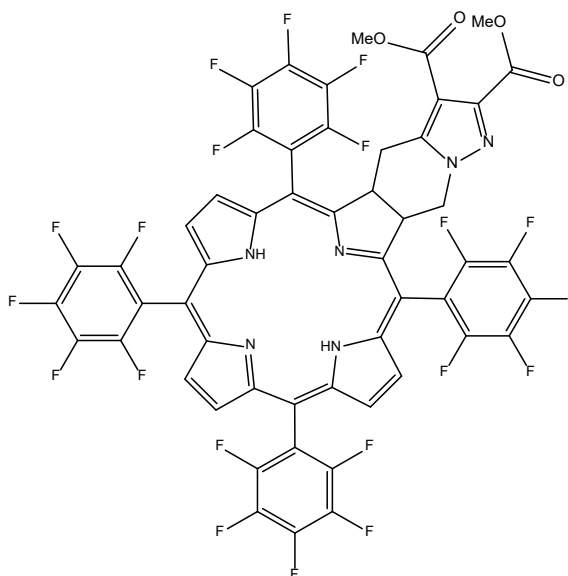
^1H NMR (400 MHz, CDCl_3): δ = 8.92-8.96 (m, 8H, H- β pyrrolic), -2.93 (s, 2H, NH) ppm.

^{13}C RMN (100 MHz; CDCl_3): δ = 130.1-132.4 (C- β), 104.2 (C-5,10,15,20), 103.6 ppm.

UV-Vis λ_{max} (CH_2Cl_2): 409, 506, 536, 582, 636 nm.

1.3. SYNTHESIS OF THE DESIRED CHLORINS

1.3.1. Synthesis of the diester ring-fused 5,10,15,20-tetrakis(pentafluorophenyl)chlorin (**3.2**)



The fluorinated ring-fused chlorin **3.2** was prepared according to a procedure described by our group for the synthesis of other chlorin derivatives of this type (Pereira *et al.*, 2010, 2011). A solution of dimethyl 4,6-dihydropyrazolo[1,5-*c*]thiazole-2,3-dicarboxylate (**3.0**) (0,18 mmol; 50 mg) and 5,10,15,20-tetrakis(pentafluorophenyl)porphyrin (**3.1a**) (2 equivalents; 0.365 mmol; 356 mg) in 1,2,4-trichlorobenzene (3 mL) was bubbled with nitrogen for about 5 minutes. The reaction is carried out under microwave irradiation at 250 °C for 20 minutes. After cooling the reaction mixture to room temperature, a few drops of triethylamine were added and the residue was purified by flash chromatography, first with dichloromethane to recover the unreacted porphyrin (42%; 150 mg; 0.15 mol) and then with (dichloromethane:ethyl acetate, 95:5) to isolate the chlorin. Chlorin **3.2** was obtained as a dark green solid in 24% yield (50.8 mg; 4.3 mmol).

1.2.1.1 Alternative method

Synthesis of chlorin **3.2** was also carried out following a conventional heating procedure adapted from the literature (Pereira *et al.*, 2010, 2011). A solution of sulfone **3.0** (50 mg; 0.18 mmol) and porphyrin **3.1a** (2 equiv.; 356 mg; 0.365 mmol) in 1,2,4-trichlorobenzene (3 mL) was bubbled with nitrogen for about 5 minutes. The reaction was then performed at reflux at 250 °C, for 3 h under an inert atmosphere of N₂. After cooling the reaction mixture, compounds were isolated as in the previous method. Chlorin **3.2** was obtained in 28% yield (60.2 mg; 5 mmol) and 70% of the starting porphyrin is recovered (250 mg; 25.6 mmol).

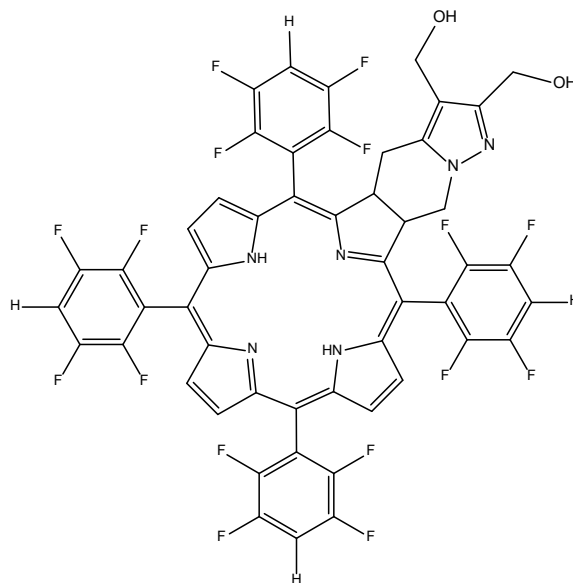
¹H NMR (400 MHz, CDCl₃): δ = 8.77 (d, *J* = 5.0 Hz, 1H, β-H pyrrolic), 8.74 (d, *J* = 5.0 Hz, 1H, β-H pyrrolic), 8.51 (s, 2H, β-H pyrrolic), 8.48 (d, *J* = 4.8 Hz, 1H, β-H pyrrolic), 8.38 (d, *J* = 4.5 Hz, 1H, β-H pyrrolic), 5.69-5.56 (m, 1H, reduced β-H pyrrolic), 5.20-5.13 (m, 1H, reduced β-H pyrrolic), 4.67 (dd, *J* = 13.3, 8.1 Hz, 1H), CH₂ from fused ring), 4.24 (dd, *J* = 13.3, 10.2 Hz, 1H, CH₂ from fused ring), 3.96 (s, 3H, CO₂Me), 3.95-3.89 (m, 1H, CH₂ from fused ring) 3.88 (s, 3H, CO₂Me), 2.82 (dd, *J* = 15.6, 11.0 Hz, 1H, CH₂ from fused ring), -1.67 (s, 2H, NH) ppm.

¹³C NMR (100 MHz, CDCl₃): δ = 166.1, 163.8, 162.2, 162.1, 153.4, 153.1, 143.3, 143.2, 140.6, 140.3, 135.8, 135.3, 132.9, 132.6, 131.1, 130.3, 128.4, 128.3, 124.6, 124.2, 111.1, 107.2, 106.8, 96.8, 96.4, 52.8, 51.7, 48.6, 48.5, 46.8, 29.7, 25.5 ppm.

HMRS (ESI): *m/z* = 1185.1302 (found), 1185.1299 calcd for [C₅₃H₂₀F₂₀N₆O₄ (M + H)⁺].

UV-Vis λ_{max} (CH₂Cl₂): 403, 503, 600, 652 nm.

1.3.2. Synthesis of the dihydroxymethyl ring-fused 5,10,15,20-tetrakis(tetrafluorophenyl)chlorin (**3.3**)

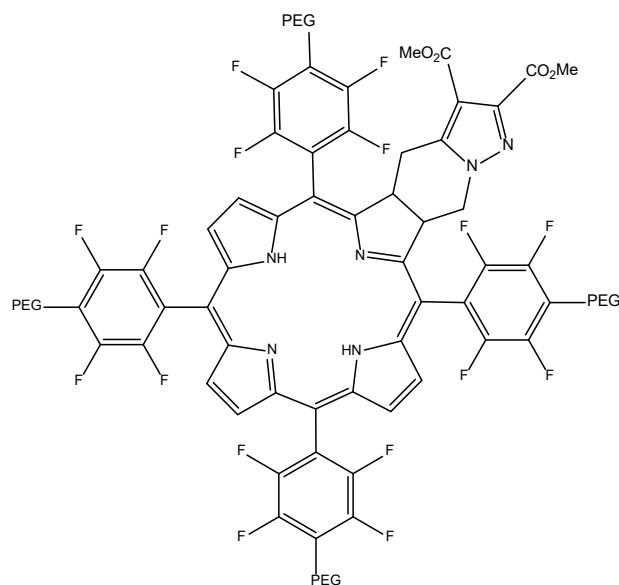


The reduction of the ester groups of the ring-fused 5,10,15,20-tetrakis(pentafluorophenyl)chlorin **3.2** to alcohols was performed based on a procedure described in the literature (Pereira *et al.*, 2018). To a suspension of LiAlH_4 (12 equiv.; 0.019 g; 50 mmol) in dry tetrahydrofuran (1.5 mL) at 0 °C was added, dropwise, a solution of chlorin **3.2** (0,04 mmol; 47 mg) in THF (1.5 mL). After the addition, the reaction mixture was allowed to warm to room temperature and left stirring, under N_2 . TLC was used to monitor the reaction progress and after 24 h indicated the disappearance of the starting chlorin. Then, the reaction mixture was cooled with an ice bath and quenched by the addition of ethyl acetate (0.5 mL) followed by water (0.5 mL) and aqueous 5% HCl (0.5 mL). The solution was vigorously stirred for 1 h and the solvents evaporated under reduced pressure. The residue was dissolved in a small volume of THF, two drops of triethylamine were added, and the product was purified by flash column chromatography [1st: dichloromethane/ethyl acetate (95:5); 2nd: ethyl acetate/methanol (90:10)]. Chlorin **3.3** is obtained as a green solid in 38% yield (16 mg; 0.015 mmol).

^1H NMR (400 MHz, CDCl_3): δ = 8.72 (overlapped d, J = 4.9 Hz, 1H, β -H pyrrolic), 8.71 (overlapped d, J = 4.9 Hz, 1H, β -H pyrrolic), 8.49-8.47 (m, 2H, β -H pyrrolic), 8.43-8.42 (m, 1H, β -H pyrrolic), 8.39-8.38 (m, 1H, β -H pyrrolic), 7.61-7.53 (m, 4H, Ar), 5.60-5.53 (m, 1H, reduced β -H pyrrolic), 5.24-5.17 (m, 1H, reduced β -H pyrrolic), 4.59 (s, 2H, CH_2OH), 4.49-4.46 (dd, J = 13.3, 7.6 Hz, 1H, CH_2 from fused ring), 4.37 (s, 2H, CH_2OH), 4.46 (dd, J = 13.3, 7.6 Hz, 1H, CH_2 from fused ring), 3.23 (dd, J = 15.2, 6.7 Hz, 1H, CH_2 from fused ring), 2.82 (dd, J = 15.2, 9.8 Hz, 1H, CH_2 from fused ring), -1.66 – -1.81 (m, 2H, NH tautomerism) ppm.

HMRS (ESI): m/z = 1057.1782 (found), 1057.1778 calcd for $[\text{C}_{51}\text{H}_{25}\text{F}_{16}\text{N}_6\text{O}_4 (\text{M} + \text{H})^+]$.

1.3.3. Synthesis of the PEGylated ring-fused 5,10,15,20-tetrakis(pentafluorophenyl)chlorin (3.4)



Two different strategies were carried out in order to obtain the PEGylated derivatives of the fluorinated chlorins. One focused on the PEGylation of the chlorin **3.2**, while the second starts with the PEGylation of the porphyrin **3.1a** which then undergoes a cycloaddition to form the PEGylated ring-fused chlorin **3.4**.

Strategy A

A mixture of the previously synthesized diester ring-fused 5,10,15,20-tetrakis(pentafluorophenyl)chlorin **3.2** (50 mg; 0.042 mmol) and the amine-PEG, 2-(2-aminoethoxy)ethanol, (10 equiv., 44 mg, 0.42 mmol) in 1,4-dioxan (1 mL) was left stirring at 50 °C for two weeks. The extent of the reaction was followed by TLC. The solvent was evaporated and the product was purified first by column chromatography (eluent: starting with ethyl acetate and then with a mixture of ethyl acetate/methanol, increasing the amount of methanol 2-10%) followed by preparative TLC [eluent: ethyl acetate/methanol (95:5)]. The isolated compound was crystallized from diethyl ether. Tetra-PEGylated chlorin **3.4** was obtained as a brown solid in 12% yield (7.61 mg; 0.005 mmol).

^1H NMR (400 MHz, CDCl_3): δ = 8.76 (overlapped d, J = 5.4 Hz, 1H, β -H pyrrolic), 8.74 (overlapped d, J = 5.4 Hz, 1H, β -H pyrrolic), 8.55 (s, 2H, β -H pyrrolic), 8.46 (d, J = 4.9 Hz, β -H pyrrolic), 8.39 (d, J = 4.9 Hz, 1H, β -H pyrrolic), 5.69-5.62 (m, 1H, reduced β -H pyrrolic), 5.14-5.07 (m, 1H, reduced β -H pyrrolic), 4.78-4.68 (m, 5H, NH from PEG and CH_2 from fused ring), 4.19 (dd, J = 13.2, 10.4 Hz, 1H, CH_2 from fused ring), 4.37 (s, 2H, CH_2OH), 4.46 (dd, J = 13.3, 7.6 Hz, 1H, CH_2 from fused ring), 3.95 (s, 3H, CO_2Me), 3.91-3.88 (m, 25H, CH_2 from PEG and CH_2 from fused ring) 3.77-3.72 (m, 12H, CH_2 from PEG and OH), 2.69 (dd, J = 15.8, 11.4 Hz, 1H, CH_2 from fused ring), -1.67 (s, 2H, NH) ppm.

HMRS (ESI): m/z = 1525.4164 (found), 1525.4209 calcd for $[\text{C}_{69}\text{H}_{61}\text{F}_{16}\text{N}_{10}\text{O}_{12} (\text{M} + \text{H})^+]$.

UV-Vis λ_{max} (CH_2Cl_2): 412, 506, 534, 602, 652 nm.

Strategy B

The second strategy starts with the PEGylation of the 5,10,15,20-tetrakis(pentafluorophenyl)porphyrin (**3.1a**). A solution of porphyrin **3.1a** (25 mg, 0.0257 mmol) and 2-(2-aminoethoxy)ethanol (10 equiv.; 27 mg; 0.257 mmol) in *N*-methyl-pyrrolidone was irradiated in a microwave reactor with the temperature set to 100 °C for 10 min. The reaction mixture was dissolved in dichloromethane and washed with saturated NaHCO_3 (added some NaCl), in order to remove the excess of amine-PEG. The organic phase was dried with anhydrous sodium sulphate and the solvent evaporated. The obtained residue was purified by flash chromatography, using a mixture of dichloromethane/ethyl acetate/methanol (1st: 50:45:5, 2nd: 40:50:10) as eluent. The solvent is then evaporated and the tetra-PEGylated porphyrin **3.1b** obtained as a brown solid in 77% yield (29.8 mg; 0.02 mmol).

^1H NMR (400 MHz, CDCl_3): δ = 8.95 (s, 8H, β -H pyrrolic), 8.74 (overlapped d, J = 5.4 Hz, 1H, β -H pyrrolic), 4.78 (s, 4H, NH from PEG), 3.87-3.82 (m, 24H, CH_2 from PEG), 3.74-3.72 (m, 12H, CH_2 from PEG and OH), -2.87 (s, 2H, NH) ppm.

The second step of this strategy was the cycloaddition reaction of the previous PEGylated porphyrin with diazafulvenium methide **3.1b**, generated in situ from sulfone **3.0**. A solution of porphyrin **3.1b** (2 equiv.; 150 mg; 0.11 mmol) and sulfone **3.0** (16 mg; 0.058 mmol) in trichlorobenzene (1 mL) was flushed with nitrogen for about 5 minutes and then subjected to microwave irradiation for 20 minutes at 250 °C. After cooling the reaction mixture, a few drops of triethylamine were added, and the products purified by column chromatography [ethyl acetate/methanol (90: 10)]. The chlorin **3.4** was obtained as a dark green solid in 14% yield (12.36 mg; 8.12x10⁻⁶ mol) and 71% (105 mg; 0.08 mol) of the starting porphyrin was recovered. However, it should be noted that usually the formation of the oxidized product was observed and, in this case, all attempts of isolating pure **3.4** were not successful, which is why, overall, the chosen strategy applied for the rest of this dissertation was the first one.

2. Experimental Section Part II – In Vitro Studies

After the synthesis and characterization of the previous compounds, it was intended to evaluate their cytotoxicity and potential therapeutic effect as photosensitizers for photodynamic therapy in the treatment of cancer. In order to do so, three *in vitro* studies were carried out: metabolic activity assay, cell viability assay and subcellular uptake, each one focusing, as their name indicates, on a different parameter.

2.1. Cell Cultures

Cell culture is a set of techniques originated in the early twentieth century that allows for cells outside the organism of origin to be cultivated and kept isolated. This methodology is an essential tool that, by providing models of excellence for the evaluation of physiological and biochemical behaviour (e.g., metabolic studies) and for the study of the effect of drugs or toxic compounds on mutagenesis or carcinogenesis processes, has made it possible to reduce the use of animal models and, consequently, the costs associated with research. However, it is essential to ensure the asepsis of the culture and its growth in a sterile and strictly controlled environment at 37 °C in a humidified atmosphere with 5% (v/v) CO₂, in order to minimize the occurrence of contaminations, by bacteria, fungi, mycoplasmas or other cell lines (Freshney *et al.*, 2005; Sinha *et al.*, 2008).

2.2. Cell Lines

Since this work aimed at the synthesis and characterization of chlorins and evaluation of its potential as a photosensitizer agent in PDT, the choice of a carcinogenic cell line is obvious. In addition, since melanoma and oesophageal cancer are the focus of this study for reasons already explained, to which should be reinforced the easy accessibility for PDT treatment, it would be of particular interest to evaluate the influence of these compounds and PDT, in cell lines derived from these types of cancer (Fan *et al.*, 2011).

In this work two human cell lines from different tumor tissues were used, one from oesophagus cancer obtained from the European Collection of Cell Cultures (ECCC, JROECL19) designated OE19; and another from melanoma, designated A375 and obtained from the American Type Culture Collection (ATCC, CRL-1619).

Both cell lines were maintained according to the suppliers' recommendations at 37 °C in a humidified atmosphere with 95% air and 5% CO₂ in a HeraCell 150 incubator. Dulbecco's Modified Eagle's culture Medium (DMEM, Sigma D-5648) supplemented with 10% fetal bovine serum (Sigma F7524), 250 µM sodium pyruvate (Gibco 11360), and 1% antibiotic (100 U/ml penicillin and 10 µg/ml streptomycin; Sigma A5955) was used for the A375 cell line, while for the OE19 cell line Roswell Park Memorial Institute 1640 Medium (RPMI, Sigma R6504) culture medium supplemented with 10% fetal bovine serum, 1mM sodium pyruvate and 1% antibiotic was used.

Since these cell lines grow adherent to the solid support (flasks and plates suitable for culturing cells), forming a monolayer, it is required to prepare cell suspensions when transferring them to other suitable substrates, often multi-compartment plates, in order to carry out the *in vitro* studies. To prepare these suspensions, first the cell cultures are washed with a phosphate buffer saline solution (PBS) and then incubated at 37 °C with 2 mL of trypsin-EDTA solution 0.25% (Sigma, T4049) until the cells start to release from the vial. After, at least 4 ml of culture medium needs to be added in order to inactivate the enzyme solution, the cell suspension is then homogenized and the cell concentration determined. To determine concentration, an aliquot is stained with Trypan blue and cells are counted in a Neubauer chamber in an inverted optical microscope (Nikon Eclipse TS 100). After counting, the volume of the cell suspensions is adjusted with culture medium in order to obtain the desired cell concentration for each study.

2.3. Cell storage: cryopreservation

In order to minimize the occurrence of genetic changes (e.g., genomic instability, senescence, among others) and contamination by microorganisms, while providing for the creation of a reserve of cells with a reduced number of passages, for later use, a storage strategy is used named cryopreservation. To carry out this process, it is

required the use of a cryoprotective agent (e.g., DMSO or glycerol) which minimizes the formation of ice crystals and the consequent dehydration, protein denaturation and membrane fragmentation responsible for cell death. DMSO, the more usual cryoprotector, effectively permeabilises cell membranes and promotes the reduction of water content and the formation of ice crystals. However, DMSO is cytotoxic and therefore its concentration should be as low as possible (Freshney *et al.*, 2005; Aschner *et al.*, 2011; Masters *et al.*, 2000; Pappas *et al.*, 2010).

2.4. Cryopreservation of cells

A375 and OE19 cells were resuspended, after trypsinized (see Culture Maintenance), in culture medium and centrifuged for 5 minutes at 1500 rpm. After removal of the supernatant, the cell pellet was resuspended in a solution consisting of culture medium and 10% DMSO. After addition of 1 ml of suspension to each cryotube, final density in each cryotube being 10×10^6 cells per mL of suspension, these were placed in a freezing vessel with isopropanol, a solvent which allows gradual cooling at a rate of 1 °C/min) to -80 °C. This procedure minimizes the formation of ice crystals that could damage the cell and cause it to die. The tubes were kept for a minimum of 5h at -80 °C and were then transferred to a liquid nitrogen container at -196 °C.

2.5. Initiation of culture

An aliquot of cryopreserved cells (10×10^6 cells) was thawed and the contents were transferred to a 75 cm² flask with 14 mL culture medium. Cells were incubated at 37 °C in a humidified atmosphere and 5% (v/v) CO₂. After 24 h, the culture medium was replaced to remove dead cells and DMSO used as a cryo-protectant.

2.6. Maintenance of culture

The protocol used consisted of removal of the old culture medium, washing of the growth surface with 1x PBS (5-8 mL), and the addition of the trypsin solution (1-2 mL). Trypsin is a protease that enables the individualization of adjacent cells by promoting the digestion of the intercellular proteins and the proteins that bind the

cells to the bottom of the flask. However, it is important to note that prolonged exposure to this protease results in disruption of structural integrity and cell death. Thus, a few minutes after addition, culture medium was added (2x the amount of trypsin, 2-4 mL) to neutralize the action of trypsin. The cells were then resuspended, a small volume of the suspension was collected to count the cells under an optical microscope and the volume of suspension and culture medium required to prepare a new culture.

2.7. Trypan blue exclusion method

Trypan blue (**Figure 3.1**) is a dye that has a negatively charged di-azo acid chromophore in its structure (Tran *et al.*, 2013) and is usually used to count cells in culture, since it allows one to determine if the cells are alive or dead based on the integrity of the membranes and the interaction it establishes with them. Thus, while the dye is rapidly absorbed by non-viable cells whose membranes are damaged (blue), on the other hand, it is excluded by viable cells whose membranes are intact (colorless) (Langdon *et al.*, 2004; Louis *et al.*, 2011).

Although widely used, this method is subject not only to the subjectivity of the operator but also to some ambiguities. Thus, while some researchers argue that this method underestimates the number of dead cells, especially as the culture ages (Altman *et al.*, 1993); others argue that since there are other factors, such as increased membrane permeability or the presence of pores in the membrane, that also allow the diffusion of trypan blue, it overestimates the number of dead cells (Tran *et al.*, 2013).

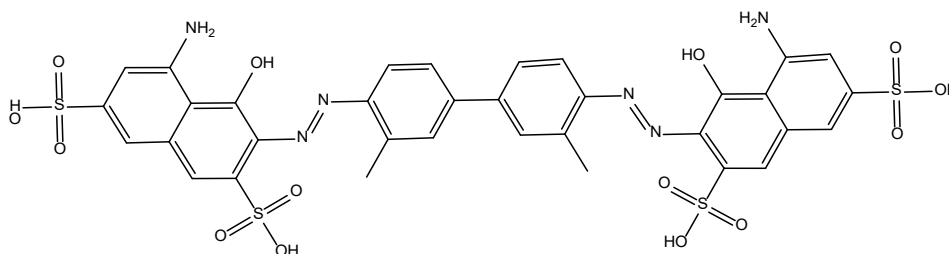


Figure 3. 1 – Chemical Structure of Trypan Blue

In this dissertation, cell counts were performed for the preparation of new cultures, a process that requires the determination of the number of cells per milliliter of suspension (Louis *et al.*, 2011).

$$\text{Cells}/_{mL} = \frac{\text{Average of the number of cells} \times \text{dillution factor}}{10^{-4}}$$

The cell count was performed after trypsinization and resuspension of the cells in fresh culture medium. Samples for counting were prepared by adding 20 μ l of the suspension to an equal volume of 0.4% (m / v) trypan blue solution. The solution was transferred to a haemocytometer (Neubauer chamber) and counted using an optical microscope. There were two independent counts, considering the average of both, and if these differed by more than 10%, a further count was carried out.

2.8. Photodynamic Treatment

For each experiment, cells were plated and kept in the incubator overnight, to allow the attachment of the cells. The formulation of the sensitizers consisted of a 1 mg/mL solution in DMSO (Fisher Chemical, 200-664-3) and the desired concentrations being achieved by successive dilutions (from 10 nM to 10 mM). Controls were included on every plate, including untreated cell cultures and cultures treated only with the vehicle of administration of the sensitizers, i.e., DMSO.

The cell cultures submitted to the photodynamic treatment were incubated always for 24 h at the desired photosensitizer concentrations. After this time, they underwent a wash with phosphate buffered saline (PBS) which ensured that the whole photosensitizer not internalized by the cells was removed, and placed in fresh culture medium. In all studies, the cultures were irradiated with a photon flux of 7.5 mW/cm² to a total of 10J. Irradiation for photodynamic treatment was performed using a fluorescent light source equipped with a red filter ($\lambda_{\text{cut off}} < 560 \text{ nm}$).

2.9. Cytotoxicity studies

In order to prove their potential therapeutic effect and to test the sensitivity of the cell lines to the sensitizers, it was intended to evaluate the cytotoxicity of the synthesized photosensitizers in human tumor cells (A375 and OE19) through a MTT (3-(4,5-dimethylthiazol-2-yl)-2,5-diphenyltetrazolium bromide) colorimetric assay (Mosman *et al.*, 1983). This spectrophotometric method allows a cheap, simple, rapid and accurate evaluation of proliferation rate and cell viability, based on the functional state of the cells.

2.9.1. Metabolic Activity

For the performance of this study, cell suspensions of the OE19 and A375 cells were prepared. The cell concentration of each suspension was adjusted to 8×10^5 cells/ml with respective culture medium from each cell line. The suspensions were distributed into 48-well plates, each well containing a final volume of 500 μ L. After being submitted to the procedure described in the previous section, cell culture medium was aspirated and the plates washed with PBS. Subsequently, 100 μ L of a solution of MTT (0.5 mg/ml; Sigma M2128) in PBS, pH 7.4, was placed in each well, and each plate was left to incubate with a solution of 3-(4,5-dimethylthiazol-2-yl)-2,5-diphenyltetrazolium bromide (0.5 mg/mL, Sigma M5655) in PBS, pH 7.4, in the dark at 37° C for at least 3h.

MTT is a water-soluble, yellow-colored monotetrazolic salt (Liu *et al.*, 2002; Stockert *et al.*, 2012). This compound is reduced by metabolically active cells due to the action of dehydrogenase enzymes, mainly through the action of complex II of the mitochondrial respiratory chain, succinate dehydrogenase or succinate-coenzyme Q reductase. The dehydrogenases have the ability to cleave the MTT tetrazolium rings and form violet formazan crystals (**Figure 3.2**) which can be subsequently solubilized by 200 μ L of a 0.04 M solution of hydrochloric acid.

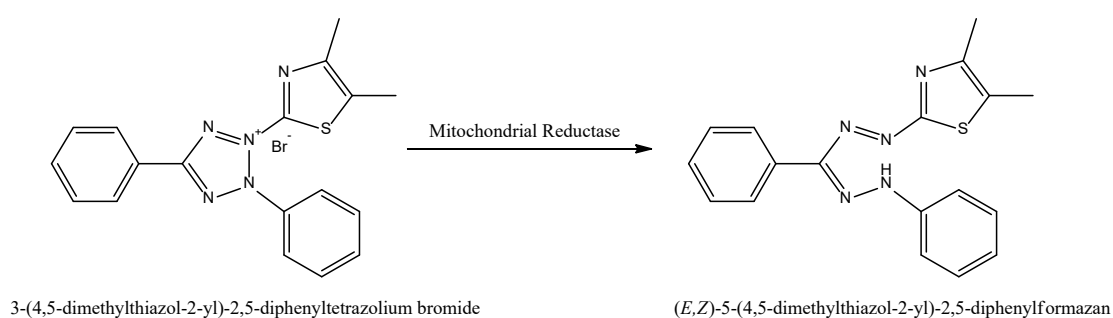


Figure 3.2 – Opening of the MTT's tetrazolium rings by mitochondrial reductase to form violet formazan crystals

After stirring for 30 minutes, and once all crystals are solubilized, the contents of each well were then homogenized and transferred to a 96-well plate (Sarstedt 83.1835), and the absorbance was quantified at 570 nm with a 620 nm reference filter using the Biotek® Synergy HT spectrophotometer (Mosman *et al.*, 1983; Hamid *et al.*, 2004; Cole *et al.*, 1986; Freimoser *et al.*, 1999; Carmichael *et al.*, 1987; Dias *et al.*, 1999; Liu *et al.*, 2009; Denizot *et al.*, 1986). This method is, thus, an indirect way of evaluating mitochondrial cell function (Lodish *et al.*, 2008) and the number of formazan crystals obtained is directly proportional to the metabolic activity of the cell.

The results were expressed as a percentage of the metabolic activity of the cultures submitted to the photodynamic treatment in relation to the cultures treated with the sensitizer administration vehicle alone. This procedure allowed to establish dose-response curves and to determine the concentration of the sensitizers that inhibits the metabolic activity of the cultures in 50% (IC₅₀). The obtained results were analysed and processed in the program OriginPro 9.0, expressed in percentage of metabolic treated cells in relation to non-treated according to the equation below, where Abs refers to absorbance.

$$\text{Metabolic Activity} = \frac{\text{Treated Cells (Abs 570 - Abs 620)}}{\text{Non - treated Cells (Abs 570 - Abs 620)}} \times 100\%$$

As one of the requirements for the use of an organic compound in PDT is the safety of PS in the absence of light (Milgrom *et al.*, 1997), determination of the effect of porphyrin *per se* is critical. Dark cytotoxicity studies were, therefore, performed as described above but omitting the irradiation step and using the highest concentrations of 1, 5 and 10 mM. Each experiment was performed in duplicate and repeated in three sets of tests.

2.10. Cell viability

The Sulforhodamine B (SRB, **Figure 3.3**) assay was used in order to assess cell viability. SRB assay is the preferred high-throughput assay of the National Cancer Institute (NCI) in the USA and is the assay used in the NCI's lead compound screening program (van Tonder *et al.*, 2015). The advantages of this test as compared to others include cell enumeration dependent on protein content and high reproducibility. The assay also has better linearity, higher sensitivity, a stable endpoint that does not require time-sensitive measurement, and lower cost. The disadvantages include the low sensitivity with non-adherent cells, as well as the need for the addition of acetic acid to fix the cells (van Tonder *et al.*, 2015). This step is critical because, if not added gently, acetic acid could dislodge cells before they become fixed, generating possible artifacts that will affect the results. Sulforhodamine B is a purplish, anionic dye with affinity for amino acids, binding electrostatically and pH dependently; this way it can be said that this assay works through correlation with total protein content (Papazisis *et al.*, 1997; Voigt, 2005; Vichai & Kirtikara, 2006).

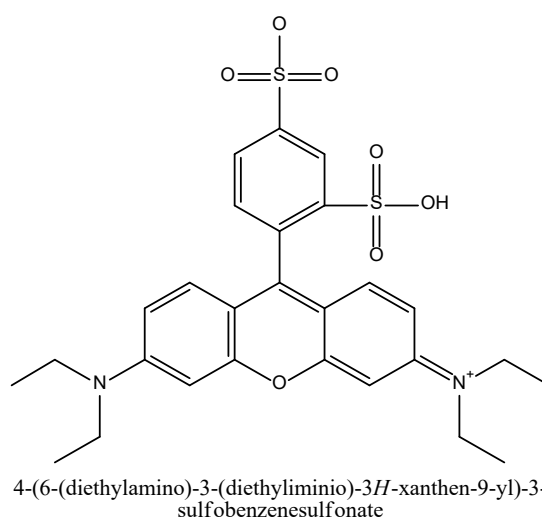


Figure 3.3 – Chemical Structure of Sulforhodamine B

Cell suspensions of the A375 and OE19 cell lines were prepared with 250.000 cells/mL, which were distributed through 24-well plates and incubated overnight to allow adhesion of the cells to the substrate. 24 h later, sensitizers were administered at

concentrations of 50 nM, 250 nM, 500 nM and 1000 nM and photodynamic treatment was performed as described above. In each study two controls were performed, one with untreated cells and the other with the sensitizer administration vehicle. SRB assay was performed 24 h after irradiation.

For the purpose of this assay, the culture medium was discarded, washed with PBS and allowed to dry. 200 µl of 1% acetic acid in methanol was added to fix the cells and incubated for 1 h at 4°C. After this time the methanol was removed and allowed to dry at room temperature. 200 µl of a 0.4% solution of sulforhodamine B (Sigma S9012) in 1% acetic acid was added and incubated for 1 h in the dark. After this time, the plate was washed to remove excess SRB and, after drying the plate, 200 µl of TRIS-NaOH (pH = 10) was added. Absorbance reading was done on a Biotek® Synergy HT spectrophotometer at wavelength 540 nm, with a reference filter of 690 nm. The results are expressed as a percentage of the protein content of the cultures submitted to the photodynamic treatment in relation to the protein content of the cultures treated only with the sensitizer delivery vehicle.

2.11. Cellular uptake

Cellular uptake studies were carried out, as to characterize the intracellular action of the photosensitizers, by taking into account the photochemical properties of the sensitizers and then evaluating the concentration of the compound by quantifying the emission of fluorescence. This spectrofluorometric quantification methodology used for the *in vitro* studies is possible due to the linearity observed between the emission of fluorescence and the concentration of the photosensitizers. The linear fit between the concentration of the photosensitizer and the peak height of the 645 nm of several dilutions of the compounds in study in methanol allowed to define the following calibration curves:

- $F = 35,96039x + 1078,0446$ (for the PEGylated chlorin)
- $F = 101,20236x + 951,2398$ (for the reduced chlorin)

Where F corresponds to the fluorescence intensity and x corresponds to the concentration in µg/ml.

Having determined the standard curves, uptake studies were performed with the purpose of knowing the concentration of photosensitizer that is effectively internalized by the cells. To this end, 6 well plates were prepared with 1×10^6 cells per well, which were incubated with the photosensitizers in the concentrations of 250 nM, 500 nM and 1 mM for 24 h and washed with cold PBS in order to remove any photosensitizer present on the outside of the cells. Contrary to the other *in vitro* studies, in this one, the cell cultures do not undergo photodynamic therapy since the goal is not to treat cells but only to assess the uptake of the sensitizers by them. After washing them with ice-cold PBS (4 °C), the cells were lysed, in order to release their contents, with a solvent suitable for maximum solubilisation of the photosensitizer, methanol (3 ml). The contents of each well were collected into properly identified tubes, which were centrifuged at 1000 G, the supernatants collected and kept in the dark at 4 °C until reading.

The fluorescence intensity of the supernatant was determined by fluorescence spectroscopy with a Perkin Elmer LS45 spectrophotometer using ~650 nm excitation wavelength, and the intracellular concentration was determined using the previously obtained calibration curves for each sensitizer. The spectra and fluorescence emission obtained can be found in the Discussion of Results section.

CHAPTER 4 – Discussion of Results

1. Discussion of Results Part I – *Synthesis*

As previously explained, the photosensitizer is one of the three essential components for successful photodynamic therapy. By modulating its characteristics, it is possible to influence the other two components or to make the most of them. Chlorins, among other porphyrin derivatives, are widely used in PDT for reasons already mentioned, however, the synthesis of these compounds presents some limitations, among them the formation of undesired side products or the low yield.

Pinho e Melo's research group developed a synthetic methodology that allowed the production of chlorins (and bacteriochlorins) in a selective manner, minimizing the formation of unwanted products. These authors studied the synthesis of several tetraarylchlorins (and bacteriochlorins) with different groups in the *meso* positions (Pereira *et al.*, 2010; Pereira *et al.*, 2011). With promising results, not only at the level of synthesis but also at the level of *in vitro* studies, it is only logical to extend this strategy to other families of compounds, which will be addressed in this work.

Thus, the fused chlorins with the ester-functionalized 4,5,6,7-tetrahydropyrazolo [1,5-*a*] pyridine ring were synthesized from the reaction of the diazafulvenium methide **3.0b** with pentafluorophenyl porphyrin **3.1a** since some studies have shown that halogen-containing porphyrins in the phenyl rings exhibit a significant increase in quantum singlet oxygen yield as a consequence of increased cross-system intersection due to the effect of the heavy atom (Piñeiro *et al.*, 2001), and thus, there may be an increase in the efficiency of photosensitizers in PDT. Lastly, after the synthesis of this new chlorin, two more structure modifications were carried out in order to increase cell permeability and consequently improve this compounds' biological activity: reduction of the ester groups of the 4,5,6,7-tetrahydropyrazolo [1,5-*a*] pyridine ring, and PEGylation on the *para* position of the pentafluorophenyl groups in the *mesa* positions of the chlorin (**Figure 4.1**.)

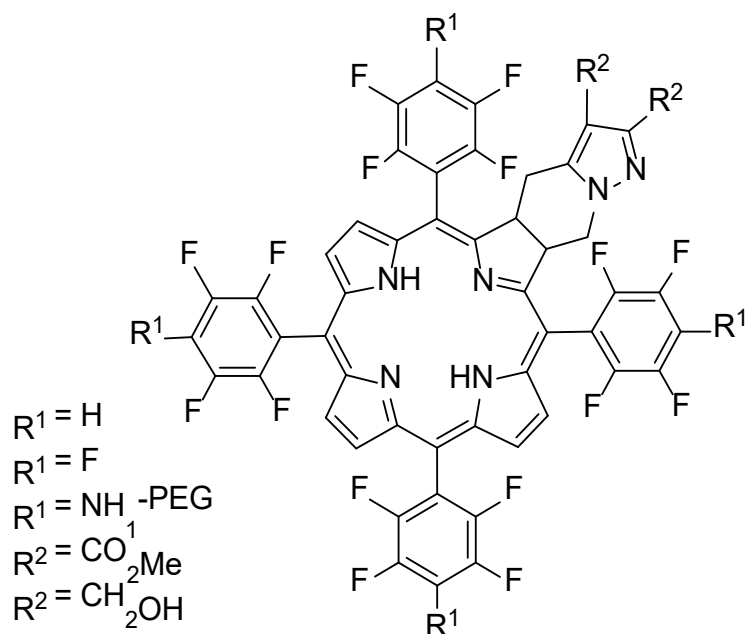
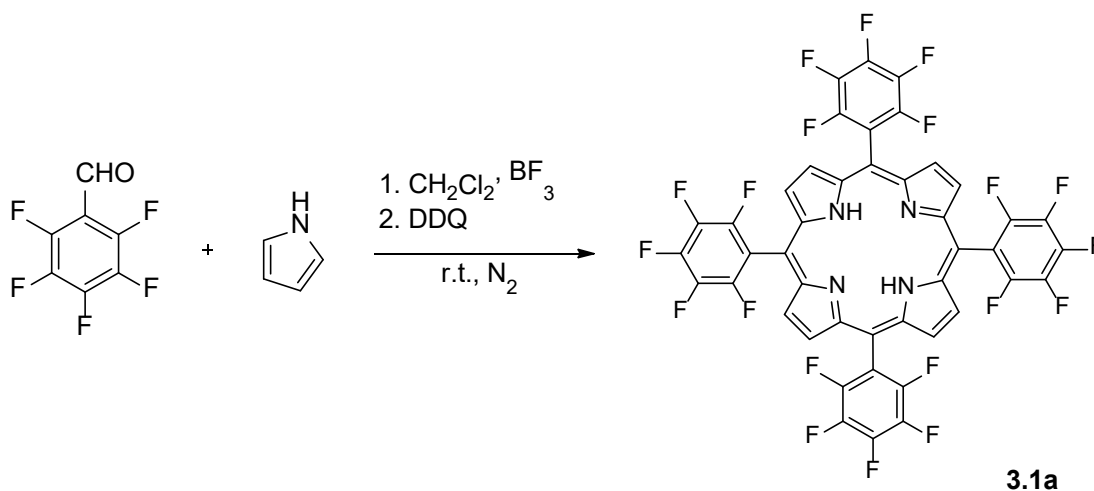


Figure 4.1 – Overview of synthesized photosensitizers

1.1. Synthesis of the precursors

With the objective of obtaining new pentafluorophenyl chlorins via $[8\pi + 2\pi]$ cycloaddition reaction of diazafulvenium methide with pentafluorophenyl porphyrin, the synthetic part of the experimental work started with the synthesis of the two required precursors. Pentafluorophenyl porphyrin **3.1a** was prepared through Lindsey's method (Lindsey *et al.*, 1986; 1987; 1989), which consists of adding pentafluorobenzaldehyde and dichloromethane on a flask at room temperature in inert atmosphere (N_2), then add the pyrrole and BF_3 etherate, leaving this mixture to react for at least 4 h, after which DDQ is added and the reaction left to be carried out for another 1 h at least (**Scheme 4.1.1**).

Another strategy was tried, which consisted of adding pyrrole to a solution of pentafluorobenzaldehyde in acetic acid. The reaction is then carried out for 2 h at 120 °C.

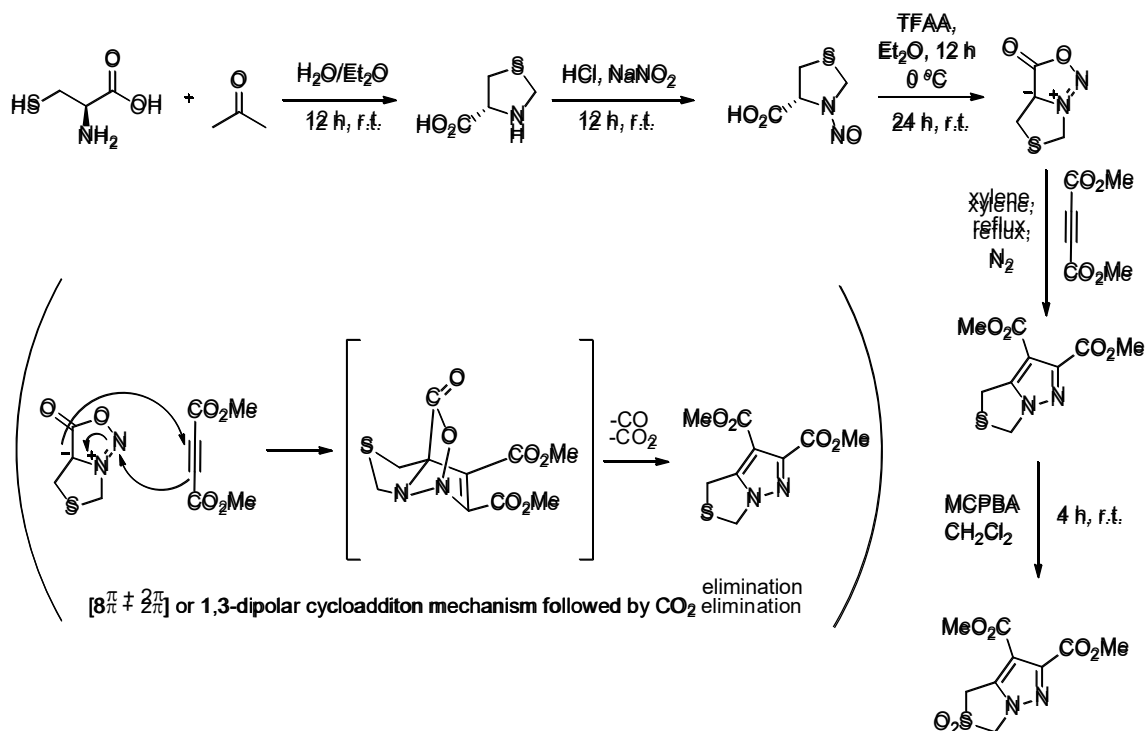


Scheme 4.1.1 – Schematic route for the synthesis of porphyrin **3.1a**

The main difference between choosing to use the first method instead of the last for subsequent needed synthesis of the pentafluorophenyl porphyrin came down to yield, since the first one had an average yield of 9%, while the second was even lower, around 4%. Although, some other factors should have been taken into consideration, such as environmental factors, more specifically the use of high quantities of dichloromethane used, not only for the reaction but also for the isolation procedure. In the end, however, yield prevailed as the most significant and determinant factor for the choice of the first method.

It is interesting to note, however, that the yields achieved for both methods were not similar to those that can be found in the literature (Costa *et al.*, 2011), which revolve around 30 and 15%, respectively. The highest yield achieved in this dissertation was 12% with Lindsey's method, which is still less than half of the one described in the literature. This might be due to eventual small changes of protocol, such as time periods between the beginning of the experiment and the addition of an oxidizing agent, temperature variations or eventual light exposure during the time reaction, which can lead to degradation of the final product.

After the preparation of the intended porphyrin, the synthesis of the diazafulvenium methide precursor, (dimethyl 4,6-dihydropyrazolo[1,5-*c*]thiazole-2,3-dicarboxylate-5,5-dioxide) was carried out. The synthetic strategy involves various steps (**Scheme 4.1.2**), which have been already described in full detail in the previous chapter.

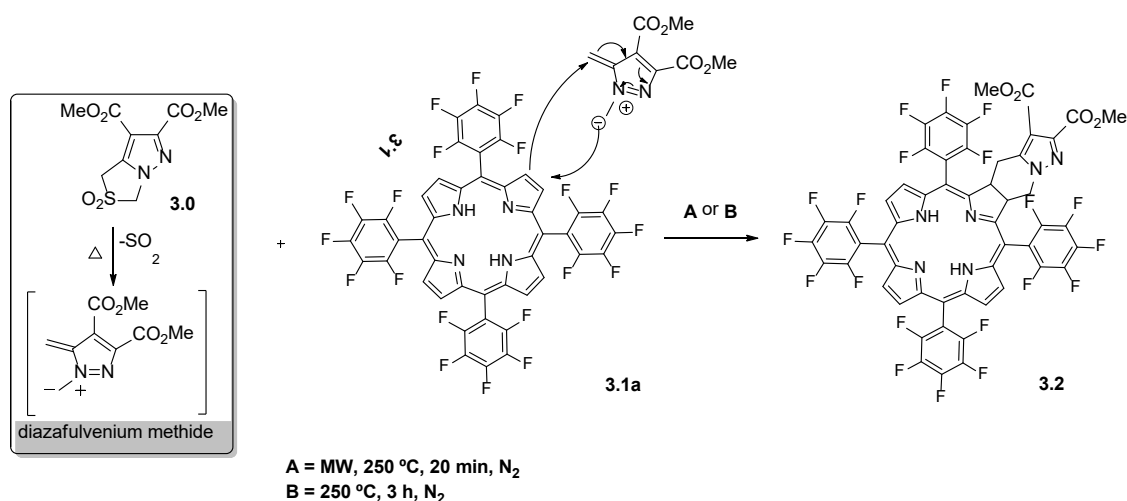


Scheme 4.1.2 – Schematic route for the synthesis of sulfone **3.0**

To start, the 1,3-thiazolidine-4-carboxylic acid was prepared by reaction of L-cysteine with formaldehyde, at room temperature for 12 h. The obtained compound is then nitrosylated with sodium nitrite in the presence of HCl, at room temperature, culminating in the formation of the 3-nitrosothiazolidine-4-carboxylic acid, which then reacts with TFAA, for 6 h at 0°C . The obtained dipole is left to react with DMAD, in reflux at 140°C for 3 h, giving dimethyl 4,6-dihydropyrazolo[1,5-c]thiazole-2,3-dicarboxylate. This reaction consists of a $[4\pi+2\pi]$ or 1,3-dipolar cycloaddition, forming a cycloadduct, which posteriorly loses CO_2 . The final dimethyl 4,6-dihydropyrazolo[1,5-c]thiazole-2,3-dicarboxylate-5,5-dioxide sulfone is achieved through oxidation at room temperature, using MCPBA.

1.2. Synthesis of the desired chlorins

The first approach that was tried comprised of exploring the cycloaddition previously described by Pinho e Melo's research group for the synthesis of other *meso*-tetraarylchlorins (Pereira *et al.*, 2010; Pereira *et al.*, 2011). Therefore, in order to achieve the desired pentafluorophenyl chlorin, a reaction between the already synthesized pentafluorophenyl porphyrin and sulfone (**Scheme 4.1.3**, method A) was carried out. This method consists of microwave irradiation at 250 °C for 20 minutes and for this a stoichiometric relationship of porphyrin to sulfone of 2:1 is needed in order to prevent the formation of secondary product (bacteriochlorin), making sure that there is a preferential formation of chlorin **3.2**. The solvent used was 1,2,4-trichlorobenzene. Besides this, N₂ bubbling of the reactional mixture must be performed so that there is no oxidation of the chlorin.



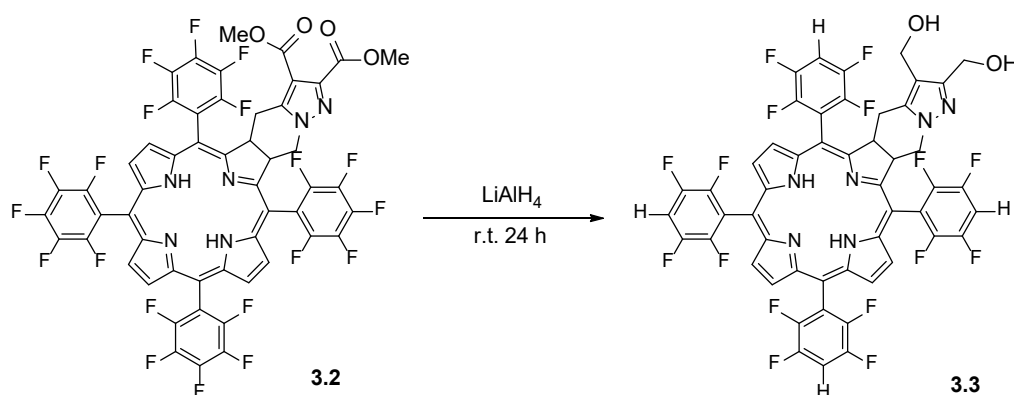
Scheme 4.1.3 – Schematic route for the synthesis of chlorin **3.2**

The non-oxidation can be proved through a UV-Vis spectrum and was indeed observed. A UV-Vis spectrum of a non-oxidized chlorin shows only one Soret band at around 420 nm, while if there were to be any oxidation two wider and smaller bands would be observed and in this case they were not. This synthetic strategy led to the final desired product in a yield of approximately 24% with the recovery of starting porphyrin ca.

42% and ended up being the preferred method of synthesis. However, another strategy was also tried, this one used the same stoichiometric conditions, but instead of microwave irradiation the reaction was carried out under conventional heating, in this particular case, for 3 h and at 250 °C (**Scheme 4.1.3**, method B). With this method, the chlorin is obtained in 28% yield and 70% of the starting porphyrin is recovered. Although having higher yield for both chlorin synthesis and starting porphyrin recovery, the first method was preferred for all subsequent chlorin **3.2** synthesis, simply because time-saving and chlorin quantity were two of the main concerns during experimental work, and for the same time period that is necessary to synthesize chlorin **3.2** through conventional conditions, it was possible to do three microwave-assisted reactions and achieve three times the quantity of chlorin **3.2**.

Another objective of this work was also to obtain the PEGylated (chlorin **3.4**) and reduced (chlorin **3.3**) derivatives of chlorin **3.2**, for reasons that have already been explained, but also to be able to compare the photophysical characteristics and *in vitro* activity between these three compounds, and, therefore, achieve conclusions between the structure-activity relationship. So, after the synthesis of chlorin **3.2**, reduction and PEGylation were carried out.

When it comes to the reduction of the ester groups of the hydroporphyrin **3.2**, a strategy already tested and used in our research group was employed. This strategy consisted of using an excess of LiAlH₄ (12 equivalents), and reduction was carried out in THF, under reflux, at room temperature, for 24 h and under inert atmosphere (N₂), (**Scheme 4.1.4**) which gave the di-alcohol chlorin **3.3** in an overall yield of 38%.



Scheme 4.1.4 – Schematic route for the synthesis of chlorin **3.3**

Non-metalation of chlorin **3.3** with the aluminium preventer of LiAlH_4 was controlled and proved by UV-Vis, since the typical chlorin band at 650 nm did not deviate to values around 620 nm, characteristic of metal-chlorin complexes.

1.2.1. The Nucleophilic Aromatic Substitution

Regarding the PEGylation of chlorin **3.2**, the strategy chosen was to explore the well-known capacity of aryl systems to undergo diverse transformations depending on their substituents, which determine their reactivity to a high extent. Substitution reactions with electrophiles (SEAr) are well-established due to the high electron density of the aryl core, allowing the two-stage *addition-elimination* mechanism through the attack of electron-deficient species by the two-stage addition-elimination mechanism. The efficiency becomes higher and the reaction kinetics faster as the electron donating properties of the substituents, the overall electron density of the aryl system and the electrophilicity of the reaction partner increase.

In contrast to SEAr , nucleophilic substitutions (SNAr) are less common, requiring highly electron-deficient systems which allow the attack of nucleophiles. This electron deficient state can be achieved by functional groups with a negative mesomeric effect (-M), e.g. nitro, cyano or sulfonyl (simplified as R in **Figure 4.1.1**) or a negative inductive effect (-I), e.g. halogen atoms such as fluoride. Most of these substituents exhibit both effects in combination with a preponderance for the M-effect and are an essential requirement for a successful substitution, because they stabilize the additional electrons resulting from the *addition* step.

Typical nucleophiles utilized for SNAr reactions can be cyanide, oxygen or nitrogen centred nucleophiles while good leaving groups are halogen atoms, in particular fluorine. This way, it was decided to take advantage of the properties of the pentafluorophenyl group in the *meta* positions of the chlorin ring, and to explore this type of reaction with different kinds of amine-PEGs.

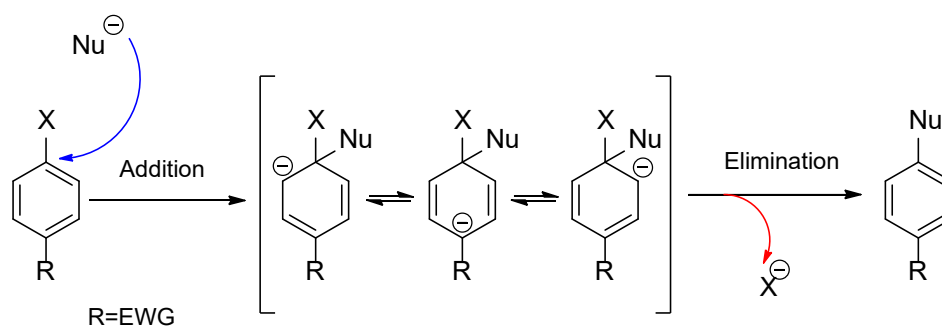


Figure 4.1.1 – The generally established reaction mechanism for a nucleophilic aromatic substitution

Although fluorine itself is a bad leaving group due to the very strong C-F bond, S_NAr reactions involving fluorine generally proceed faster. As it has been explained before, the rate-determining step for the overall reaction is the *addition*, highly accelerated with fluorine due to its strong inductive effect. This acceleration is observed dramatically on aryl systems with several fluorine atoms, in which case the usually necessary anion stabilizing group becomes dispensable.

The pentafluorophenyl group is, therefore, an example of a highly electron-deficient aryl system with a high susceptibility for nucleophilic substitution reactions that stands apart from common electron-rich aromatics. Due to its electron deficiency, it is impossible to carry out conventional electrophilic substitution reactions (Sheppard *et al.*, 1970). The carbon-fluorine bond is characterized by a high polarization due to the strongly diverging electronegativity of the two elements, with a partially negatively charged fluorine and partially positive carbon centre.

Recently, Kvičala *et al.* have done some mechanistic studies based on theoretical calculations (DFT) with pentafluorobiphenyl and monosubstituted PFP-moieties and were able to explain its strong regioselectivity (**Figure 4.1.2**) (Kvičala *et al.*, 2010). Regarding the substituent effects of functional groups attached at the pentafluoroaryl, while electron-withdrawing groups (EWG), such as fluorine, allow a charge stabilization and favour the substitution in *ortho*- and *para*-position with respect to R;

electron-donating groups (EDG), amines per example, facilitate substitution in *meta*-position. The tetrapyrrole backbone of porphyrins and chlorins can be regarded as an electron-stabilizing group what would explain the regioselective *para*-fluorine exchange described by numerous reports with thiols, amines, and alcohols.

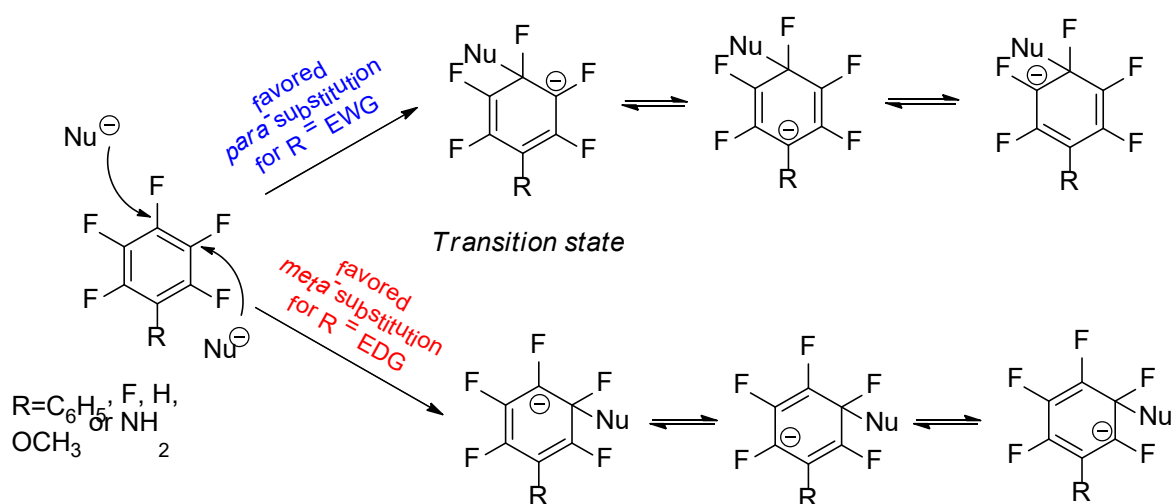
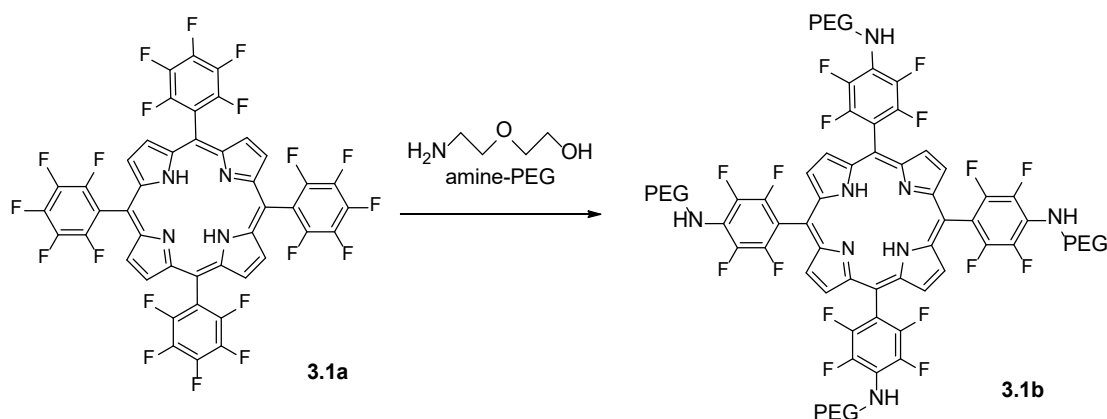


Figure 4.1.2 – Studied regioselectivity of the $\text{S}_{\text{N}}\text{Ar}$ protocol of PFP-substituted systems by Kvičala et al., 2010.

In the particular case of this dissertation, since the PEGylation of chlorins was actually a never tried before strategy, for there had only been a few studies regarding PEGylation on porphyrins (Costa *et al.*, 2011), even less between these kind of ring-fused chlorins and with this amine-PEG ((aminoethoxy)ethanol) in particular, several approaches had to be tested in order to optimize protocol and find the ideal nucleophilic aromatic substitution conditions.

The studies were first carried out using pentafluorophenyl porphyrin and amine-PEG (**Scheme 4.1.5**) based on a procedure previously described in the existing literature (Costa *et al.*, 2011). Thus, porphyrin **3.1a** (1 equivalent) and (aminoethoxy)ethanol (10 equivalents) in N-methylpyrrolidone (NMP) were reacted under microwave irradiation at 200 °C for 2 minutes, which gave **3.1b** in an overall yield of 9%, (**entry 1**,

table 4.1.1) proving that the PEGylation of this porphyrin with this amine-peg was possible. In order to increase the yield, reaction time was increased to 5 minutes (**entry 2, table 4.1.1**). With this small change, the yield went from 9% to 43%. Next, it was tried to increase the number of equivalents of the amine-PEG from 10 to 20, but little to none changes were observed since the yield only went up to 45% (**entry 3, table 4.1.1**).



Scheme 4.1.5 – Overview of the schematic route for the synthesis of porphyrin 3.1b

entry	solvent	reagents (equiv.)		product	reaction conditions	yield
		porphyrin 3.1a	amine-PEG			
1	NMP	1	10	3.1b	MW, 200 °C, 2 min	9%
2	NMP	1	10	3.1b	MW, 200 °C, 5 min	43%
3	NMP	1	20	3.1b	MW, 200 °C, 5 min	45%
4	NMP	1	10	3.1b	MW, 100 °C, 2-10 min	77%
5	NMP	1	10	3.1b	MW, 70 °C, 10-18 min	48%
6	1,4-dioxan	1	10	*a	conv. heating, 50 °C, 48-192 h	n. d.

Table 4.1.1 – Optimization of the reaction conditions for the synthesis of porphyrin 3.1b. (*a = mixture of mono-, di-, tri- and/or tetra-porphyrin-PEG)

The optimized reaction conditions were applied to chlorin **3.2** (**entry 1, table 4.1.2**) instead of porphyrin **3.1a**. However, although the yield of the crude product was 92%, it corresponded to a mixture of what seemed to be chlorin **3.2** itself and its oxidized

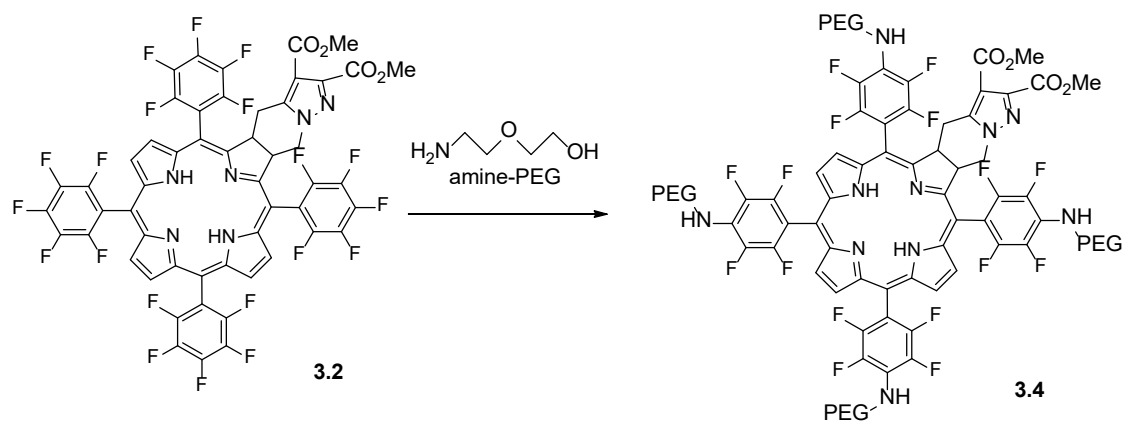
form in a high percentage and a very little percentage of the desired chlorin-PEG (not truly knowing if it was the tetra-PEGylated chlorin or any other of the mono, di- or tri-PEGylated derivatives, since no NMR or mass spectra were performed to confirm this observation). As chlorin **3.2** and its oxidized form are practically impossible to isolate from one another, it was concluded that further studies were required.

Since temperature might be one of the factors influencing oxidization, the logical next step was to decrease it and try to find if it was possible to still PEGylate either porphyrin or chlorin. Bearing this in mind, it was decided to carry out the next experiments at 100 °C and to vary reaction time between 2 and 10 minutes, in intervals of 2 minutes, doing TLCs (thin layer chromatography) and taking UV-Vis spectra in between each time interval, in order to see if porphyrin was being PEGylated without undergoing oxidation, respectively (**entry 4, table 4.1.1**). It was concluded that after 10 minutes porphyrin **3.1b** was obtained in 77% yield with no evidence of oxidization. These new reaction conditions were applied for the PEGylation of the chlorin, (**entry 2, table 4.1.2**) but once again UV-Vis spectra showed that chlorin **3.2** was oxidized at this particular temperature of 100 °C.

To overcome this issue, the temperature was lowered once more to 70 °C and time varied from 10 to 18 minutes (since a longer time period was thought to be necessary), obtaining the highest yield of 48% at 18 minutes (**entry 5, table 4.1.1**) for the PEGylation of porphyrin **3.1a**. Under these conditions, oxidation of chlorin was still observed when PEGylation was tried (**entry 3, table 4.1.2**). A final attempt at the PEGylation of both porphyrin **3.1a** was carried out, this time lowering the temperature to 50 °C and using the conventional heating method instead of microwave irradiation (**entry 6, table 4.1.1**). It was, so, decided to leave the porphyrin and amine-PEG mixture, in 1,4-dioxan, to react at 50 °C on a stabilized paraffin bath for 20 min. However, through TLC analysis, it was possible to conclude that there was still unreacted porphyrin still present, and so this time period was extended all the way to 192 h, following porphyrin oxidization and complete PEGylation through UV-Vis and TLCs, respectively. At the 192 h mark, TLC revealed that there was no porphyrin left to be PEGylated, however the result was a mixture of mono-, di-, tri- and tetra-PEGylated porphyrins, contrary to the mono-product observed (tetra-PEGylated porphyrin **3.1b**) when this reaction was carried out at higher temperatures for shorter periods of time and under microwave irradiation, which is a very interesting

conclusion to be taken. Isolation of porphyrin **3.1b** was not attempted in this case because there was not such interest since the mono-product could be obtained under other reaction conditions (**entry 4, table 4.1.1**) in a much simpler manner.

While this might not be the ideal result, it was not bad enough to not deserve to try these reaction conditions using chlorin **3.2** instead of porphyrin **3.1a** (**Scheme 4.1.6**), especially because the other conditions do not seem to work when chlorin is used instead of porphyrin. What seemed to be, at first sight, not a promising strategy, ended up showing the best results, since, for the first time, no signs of oxidization were observed in the PEGylation of chlorin **3.2**.



Scheme 4.1.6 – Overview of the schematic route for the PEGylation of chlorin **3.2**

On one hand, this allowed to conclude that after approximately 8 days, in these reactional conditions there is not non-PEGylated chlorin left, with evidences that even longer time periods could increase the ratio of tetra-PEGylated chlorin in relation to the other derivatives, resulting in higher yields, i.e. more of the desired compound.

On the other hand, the same result observed for the PEGylation of porphyrin **3.1a** was obtained, which consisted of a mixture of products: mono-, di-, tri-, and tetra-PEGylated chlorin, meaning that further isolation is necessary. After an extensive and lasting isolation procedure, the yield corresponding to the desired tetra-PEGylated

chlorin was 14% (**entry 4, table 4.1.2**), retrieving the starting porphyrin (**3.1b**) in a yield of 71%.

entry	solvent	reagents (equiv.)		product	reaction conditions	yield
		chlorin 3.2	amine-PEG			
1	1,4 - dioxan	1	10	*b	MW, 200 °C, 5 min	n. d.
2	1,4 - dioxan	1	10	*b	MW, 100 °C, 10 min	n. d.
3	1,4 - dioxan	1	10	*b	MW, 70 °C, 18 min	n. d.
4	1,4 - dioxan	1	10	*c	conv. heating, 50 °C, 48-192 h	14 %

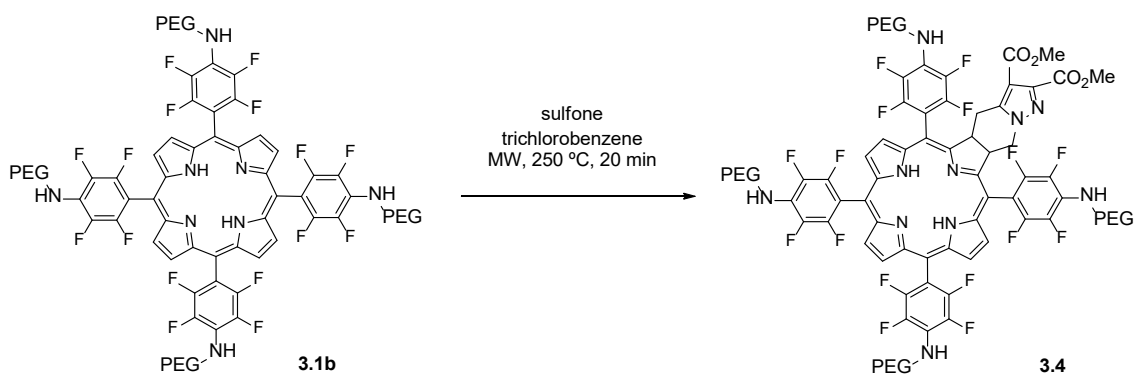
Table 4.1.2 – Optimization of the reaction conditions for the PEGylation of chlorin **3.4**.

(*b = mixture of chlorin **3.2** and its oxidized form

*c = mixture of mono-, di-, tri- and/or tetra-porphyrin-PEG

*d = mixture of chlorin **3.4** and its oxidized form)

As this synthetic route demands a long period of time another strategy was tried: taking the PEGylated porphyrin **3.1a** from the more successful reaction of the PEGylation of porphyrin with amine-PEG at 100 °C for 10 minutes under microwave irradiation, which proved to accomplish not only the mono-product of tetra-PEGylated porphyrin **3.1b** but also to do so with a yield of 77% (**entry 4, table 4.1.1**), and to make it react with sulfone **3.0** in trichlorobenzene (TCB), through the already described cycloaddition reaction, in order to obtain chlorin **3.4** (**Scheme 4.1.7**).



Scheme 4.1.7 – Overview of the schematic route for the synthesis of chlorin **3.4** from the cycloaddition reaction of porphyrin **3.1b** with sulfone **3.0**.

entry	solvent	reagents (equiv.)		product	reaction conditions	yield
		porphyrin 3.1b	sulfone 3.0			
1	TCB	2	1	*d	MW, 250 °C, 20 min	n. d.
2	TCB	2	1	*d	MW, 250 °C, 20 min	n. d.
3	TCB	2	1	3.4	MW, 250 °C, 20 min	47%

Table 4.1.3 – Reaction conditions for the Cycloaddition of porphyrin **3.1b**.
 (*d = mixture of chlorin **3.4** and its oxidized form)

Three individual experiments were carried out all with distinct outcomes not allowing to draw the most concrete conclusions. However, while for two of them (**entries 1 and 2, table 4.1.3**), some oxidization was observed, for the other one the mono-product (chlorin **3.4**) was achieved in a yield of 77% (**entry 3, table 4.1.3**), which is very interesting, since, without the PEG-moieties in its structure, the cycloaddition usually presents a lower yield than this (24%). Due to these incongruences, although this last method is seemingly more successful in terms of yield obtained, the method of PEGylation of chlorin **3.2** under conventional heating was preferred, because ultimately the possibility of oxidizing the chlorin is not worth the risk.

2. Discussion of Results Part II - Aggregation and Photophysical Studies

AGGREGATION

Several factors may contribute to the greater retention of porphyrin derivatives in neoplastic cells such as the low pH of the interstitial fluid in the tumor tissue compared to normal tissue. This can be caused by the increase in production of lactic acid in tumors, due to a change in the respiratory mechanism of the cells. With lower pKa values, due to higher acidity, the ionization of porphyrins also increases turning them more soluble in water and more selectively retained (Lehninger *et al.*, 2000). Another factor would be the high affinity for low-density lipoproteins, (LDL), found in larger amounts in tumor tissues, which allows a localized action of the PDT (Machado *et al.*, 2000). On the other hand, porphyrins with high liposolubility are more prone to auto-aggregation in aqueous solution (Soares *et al.*, 2006), resulting in chromophore changes and decrease in singlet oxygen production.

Aggregation is an intermolecular phenomenon that occurs in solution, involving an association between solute molecules (self-aggregation), or between the solute and the solvent. Although it is still not well understood the process of self-aggregation in porphyrins, it is known that the molecules can be associated in the form of dimers, trimers, and oligomers, as well as in their combinations, and that depending on the extent of aggregation, precipitation may also occur. Hydrogen bonds, electrostatic interactions, including interactions between the π system, Van der Waals forces, and hydrophobic interactions are the most common types of intermolecular forces involved between the aggregate molecules, and the prevalence of one over the other depends on the structure of the compound. The π system interactions are the ones that most contribute to the self-aggregation of porphyrins and other aromatic compounds (Hutener *et al.*, 1990).

The most common self-aggregations of porphyrins are the parallel displaced faces (**Figure 4.2.1**), where the rings are parallel and separated by a distance of 3.4-4.0 Å. This form is associated with the interaction between electron-deficient pyrrole rings, such as endocyclic hydrogens or metal ion in metalloporphyrins (Hutener *et al.*, 1990). Aggregation is a reversible process that is usually in equilibrium, which is affected by

some physical factors, either favoring the formation of the aggregation product or the monomer (Hutener *et al.*, 1990). The lipophilic characteristics of porphyrins are a factor that conditions the self-aggregation process: hydrophobic porphyrins in aqueous media are more prone to form larger dimers or aggregates than the more hydrophilic porphyrins (Kessel *et al.*, 1991). The presence of polar side chains in the porphyrin structures favours the solvation of the molecule by water, reducing self-aggregation as a consequence of the increase in electrostatic repulsion or steric hindrance between the lateral chains (Richelli *et al.*, 1995). Thus, water-soluble porphyrins have lower aggregation.

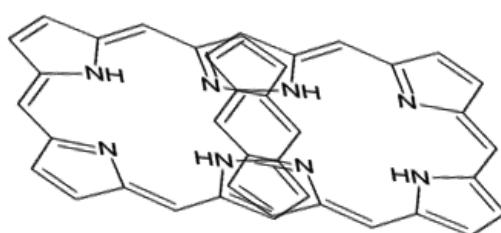


Figure 4.2.1 – Parallel dislocated faces porphyrin self-aggregates

For the aggregation studies, two solutions were prepared, one the of di-alcohol chlorin **3.3** and another of the di-ester chlorin **3.4**. Each one was weighted (0.0151 and 0.022 mg, respectively) on the microbalance, dissolved in DMSO (1 mL each) and kept in different sample flasks. The procedure for both was the same and consisted of several dilutions which were followed by absorbance readings for every concentration.

First, another 1 mL of DMSO was added to the mother solution for one of the compounds (di-alcohol chlorin), obtaining a solution (J1D) with a massic concentration half of the initial, and an absorbance spectrum was taken from an aliquot. From the J1D solution, 1 mL was taken to which another 1 mL of DMSO was added, making the concentration half of the previous one (J2D). To the obtained solution, this time, it was simply added 1 mL of DMSO, which meant that solution J3D had a third of the concentration of the J1D solution. From the J3D 1 mL was taken and 1 mL of DMSO added, in order to reduce its concentration in half (J4D). This step was repeated four more times until J8D, always taking an absorbance spectrum in between dilutions for each concentration (Figure 4.2.2).

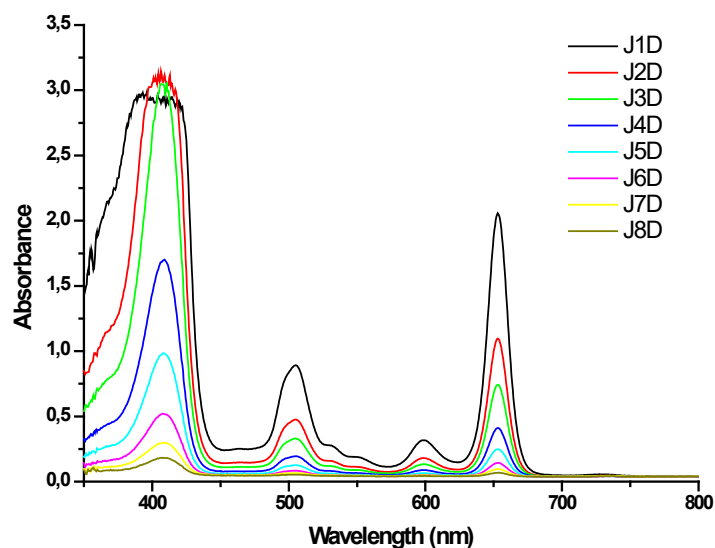


Figure 4.2.2 – Absorbance spectra of the di-alcohol chlorin 3.3 in DMSO at different concentrations

Regarding the J1D solution, for the first part of this study 1 mL had already been taken for the dilutions in DMSO. However, there was still 1 mL left of this solution, which was used to do the following dilutions, this time in water. To this 1 mL of J1D, 1 mL of distilled water was added and an absorbance spectrum was taken (J2A). To the obtained solution, it was simply added 1 mL of distilled water, which meant that solution J3A had a third of the concentration of the J1D solution. From the J3A solution, 1 mL was taken to which another 1 mL of distilled water was added, reducing the concentration in half (J4A). Previously, there had been no evidence of aggregation, however in this concentration there were some signs, more specifically the Soret band was lower and wider when comparing to the J4D, (same concentration in only DMSO). To make sure this was due indeed to aggregation, a surfactant was added (tween) in a quantity which would not influence the concentration (100 μ L) – J4AT. Being a surfactant, it should separate any molecules that might be aggregated, which would translate in a bigger absorption, since it is known that aggregates absorb less. No changes were seen in the absorbance spectrum bands before and after the addition of the surfactant, which meant that there was no aggregation for this concentration. The process was continued, and no significant changes were observed for any of the concentrations tested (**Figure 4.2.3**).

The procedure for the other chlorin (di-ester) was exactly the same, and so were the conclusions: none of the chlorins showed any evidence of aggregation at the studied concentrations.

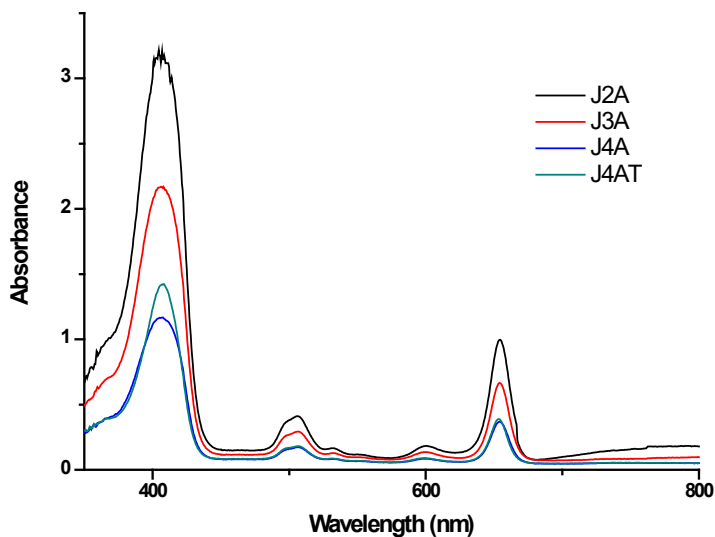


Figure 4.2. 3 – Absorbance spectra of the di-alcohol chlorin 3.3 in water at different concentrations

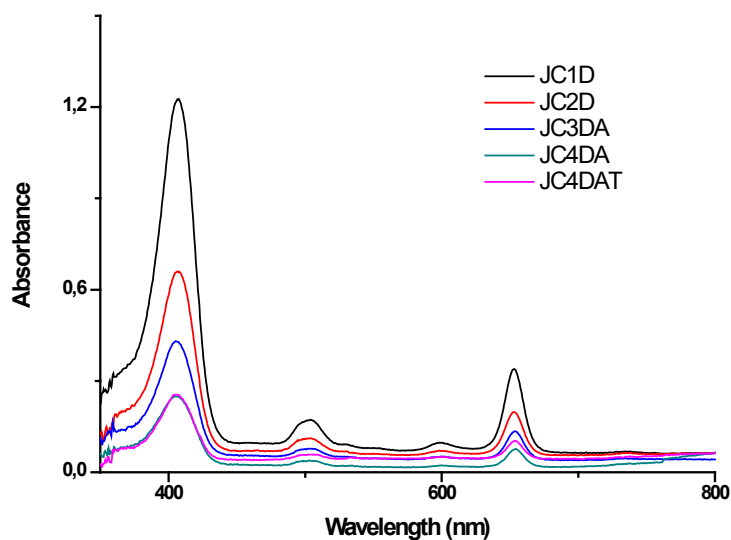


Figure 4.2. 4 – Absorbance spectra of the di-ester chlorin 3.4 in DMSO and water at different concentrations

PHOTOPHYSICAL CHARACTERIZATION

The study of the photophysical properties of chlorins is a key parameter in the characterization of a photosensitizing agent, since these properties can condition the biological activity of the photosensitizers and, therefore, the therapeutic efficacy (Serra *et al.*, 2010).

As already discussed in Chapter 2, free-base porphyrins (non-metallated) exhibit UV-Vis absorption spectra with four bands of low intensity around 500-700 nm, the Q bands, and an intense band in the range of 400-450 nm, referred to as Soret. According to Gouterman's four orbitals model (Gouterman *et al.*, 1961, 1963), these spectra can be explained based on the electronic transitions between two occupied higher energy orbitals (HOMO) and two low energy unoccupied orbitals (LUMO), shown in **Figure 4.2.5**.

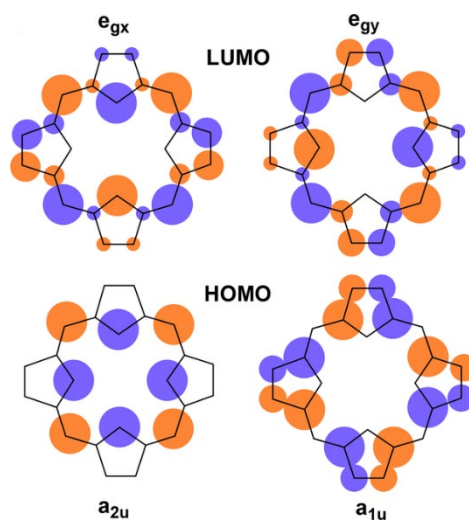


Figure 4.2. 5 – Representation of the orbitals involved in Gouterman four-orbital theory (adapted from Senge *et al.*, 2014)

The two HOMO orbitals are designated b_1 and b_2 and have a_{2u} and a_{1u} symmetry. On the other hand, the LUMO orbitals are denominated c_1 and c_2 , presenting e_g symmetry. The bands observed in the absorption spectrum of the porphyrins can be explained by

arbitrating a system of Cartesian axes x and y on the structure of the tetrapyrrole macrocycle (**Figure 4.2.6**).

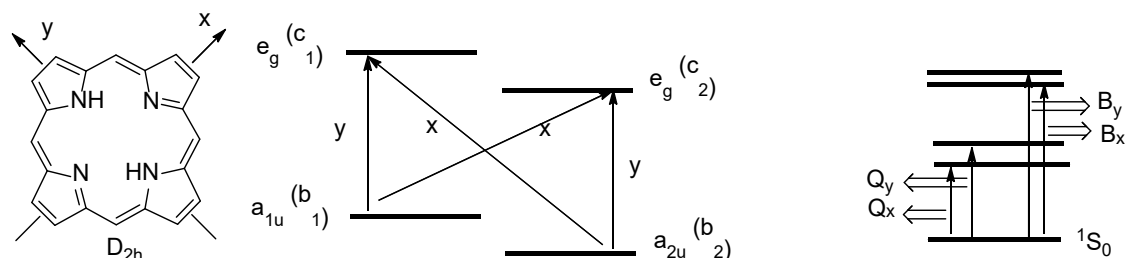


Figure 4.2. 6 – Cartesian axes system for the study of free base porphyrins (D_{2h}) and representation of orbitals and electronic transitions between the ground state and the excited state, according to the Gouterman model (adapted from Nemykin *et al.*, 2010).

As shown in **Figure 4.2.6**, the transitions between the $b_1 \rightarrow c_1$ and $b_1 \rightarrow c_2$ orbitals respectively give rise to the bands Q_y and Q_x , which are characterized by low energy and intensity. On the other hand, the bands B_x and B_y , of greater energy and intensity, correspond to transitions $b_2 \rightarrow c_1$ and $b_2 \rightarrow c_2$. The transitions between the zero vibrational level of the ground state to the zero vibrational level of the excited state give rise to bands that can be represented by $B_x (0,0)$, $B_y (0,0)$, $Q_x (0,0)$ and $Q_y (0, 0)$. The bands $Q_x (1,0)$ and $Q_y (1,0)$, associated with the transitions $Q_x (0,0)$ and $Q_y (0,0)$, are related to electronic transitions to a higher vibrational level. The pair of transitions B_x and B_y , due to the energetic proximity of the c_1 and c_2 orbitals, usually appears as only one band, the Soret.

The reduction of porphyrins to chlorins and bacteriochlorins leads to a distortion of the macrocycle which causes a decrease in symmetry, affecting the HOMO and LUMO orbitals. Considering the electronic densities of the orbitals, the reduction of the pyrrole units preferentially affects $b_2 (a_{2u})$ and $c_1 (e_{gx})$, causing a variation of their energy (Parusel *et al.*, 2001; Bruckner *et al.*, 2003). The decrease in the energy difference between these HOMO and LUMO in chlorins and bacteriochlorins is responsible for the deviation of the long wavelength band (Q_x) – bathochromic shift (Parusel *et al.*, 2001) This small difference strongly influences the photophysical

properties of these compounds. The progressive saturation of the macrocycle leads to an increase in the wavelength and intensity of the last energy band. Thus, hydroporphyrins exhibit greater absorption in the red and NIR regions compared to porphyrins, absorbing around 650 nm (the ϵ of this chlorin band being on average an order of magnitude greater than that of the respective porphyrin) (Arnaut *et al.*, 2011; Muthiah *et al.*, 2007; Nyman *et al.*, 2004; Bonnet *et al.*, 1995).

As mentioned in Chapter 1, after absorption of light the porphyrin compounds are excited to S_n singlet levels. Through non-radioactive relaxation processes the decay of these S_n states to the excited state S_1 occurs. The transition from S_1 to the ground state (S_0), if it is processed through a radioactive process, occurs with emission of fluorescence. This decay can occur at different vibrational levels of the ground state, with the band Q(0,0) in the fluorescence spectrum corresponding to the transition of higher energy (Gouterman *et al.*, 1978).

For the matters of this dissertation, UV-Vis absorption and fluorescence spectra were measured for chlorins **3.2** and **3.4** (**Figure 4.2.5**). The absorption spectra of chlorins **3.2** **3.4** and **3.4** in toluene showed the typical Soret and Q-bands of these compounds. The lowest energy wavelength maximum of these chlorins [Qx(0,0)] was observed at 655 and 649 nm for chlorins **3.2** and **3.4**, respectively. Both compounds were characterized by a maximum fluorescence emission at around 659 nm.

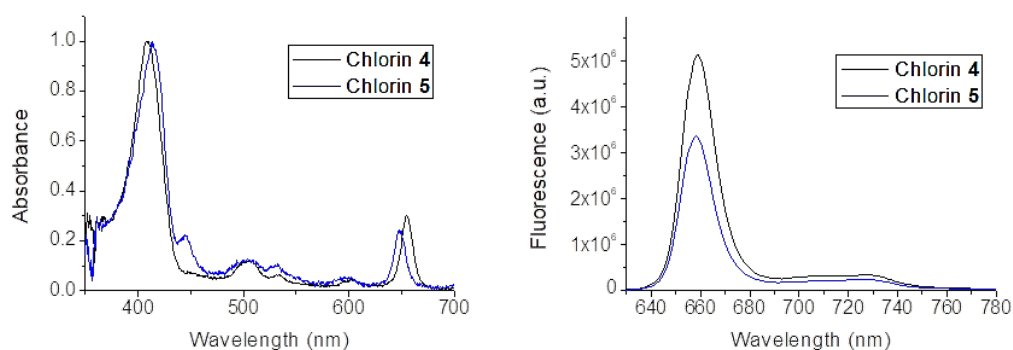


Figure 4.2.7 – Absorption and fluorescence spectra of chlorins **3.2** and **3.4** in toluene.

3. Discussion of Results Part III - *In Vitro* Studies

3.1. Cytotoxicity Studies

After the synthesis and chemical analysis of chlorins **3.2**, **3.3** and **3.4** (Figure 4.3.1), cytotoxicity studies were carried out in order to evaluate their potential as photosensitizer candidates for PDT in two different human cancer cell lines, the OE19 cell line of oesophageal carcinoma and the A375 cell line of melanoma. These chlorins have several characteristics which make the study of their *in vitro* behaviour interesting, such as the fact of being economically synthesized, exhibiting a lower tendency to aggregate, combining strong absorptions in the phototherapeutic window with efficient formation of long-lived triplet states, being chemically stable due to the fact of being ring-fused and bearing electron-withdrawing groups that stabilize the macrocycle against oxidation and provide steric protection.

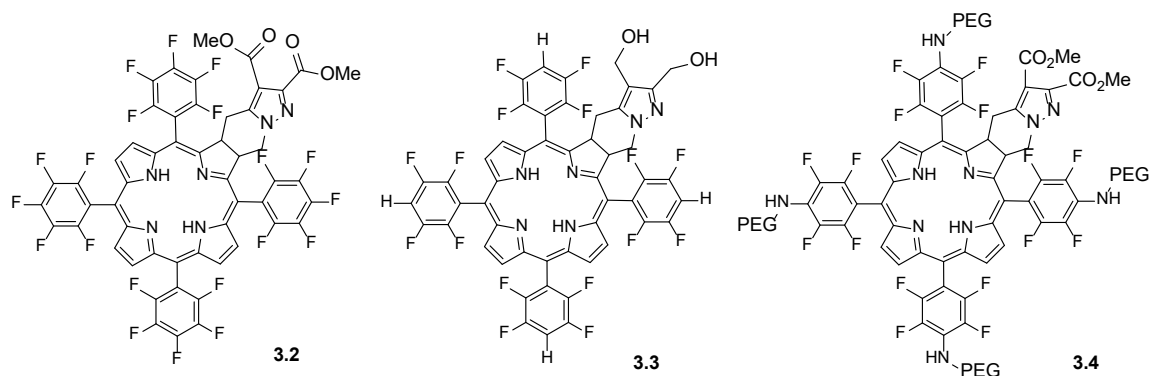


Figure 4.3.1 – Chemical structures of the studied photosensitizers.

During the early phases of PS development, *in vitro* studies are still very important screening tools, since they can provide very useful data that contribute to a better characterization of their photodynamic properties in biological systems, even in the artificially controlled conditions of cell culture experiments. Consequently, they allow to characterize the interaction between PS and cells and to make an early selection of the most promising molecules.

The objective of the *in vitro* studies is, therefore, to describe the biological activity of the synthesized chlorins against cancer cells, starting with the evaluation of their metabolic activity inhibition in the absence of light ($IC_{50\text{dark}}$) and after laser irradiation ($IC_{50\text{PDT}}$). This evaluation is defined by the PS concentration that causes a 50% reduction in cell metabolic activity, determined by the MTT assay. The *in vitro* comparison between the photosensitizers was based on the photodynamic efficiency (PE) index, adapted from J. Berlanda (Berlanda *et al.*, 2010). The photosensitizing efficiency (PE), defined by the ratio between $IC_{50\text{dark}}$ and $IC_{50\text{PDT}}$ for a given PS, was employed to compare the performance of the three photosensitizers in both cancer cell lines. In order to generate comparable data, each PS was tested using the exact same protocol parameters described in the Experimental Section, including concentrations, times of incubation, intervals between administration and irradiation, light dose, fluence, and fluence rate.

$$PE = \frac{IC_{50\text{dark}}}{IC_{50\text{PDT}}} \text{ (equation 4.3.1)}$$

The experimental results, obtained by the MTT assay, were adjusted to the sigmoid dose-response model as represented in **Figures 4.3.2** and **4.3.3**, and from the equation of each curve the mean point corresponding to the IC_{50} value was calculated.

Regarding chlorin **3.2**, the activity against oesophageal carcinoma cell line showed an IC_{50} of 5.3 μM , while the melanoma cell line had an IC_{50} of 6.8 μM . Thus, there are no significant differences between the IC_{50} 's observed for the two cell lines. However, the $IC_{50\text{S}}$ values obtained for chlorin **3.3** and **3.4** are drastically different, which goes as expected since these are the di-hydroxylated and PEGylated derivatives, which were specifically designed to enhance their activity. For these, the $IC_{50\text{S}}$ were respectively 57.5 and 73.2 nM for **3.3**, while for **3.4** the values necessary for the reduction of cell activity in 50% were 160.7 nM and 911,1 nM against OE19 and A375 cell lines.

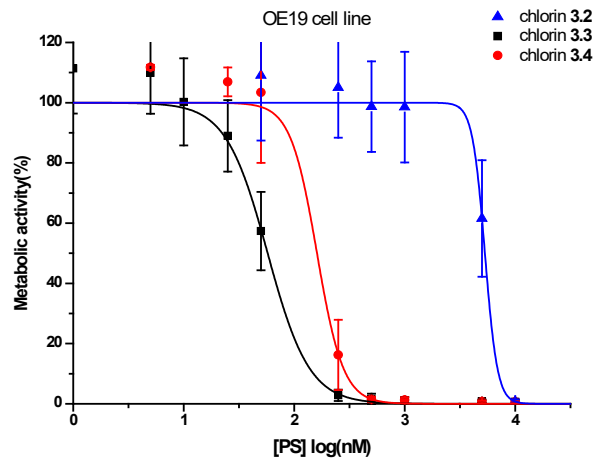


Figure 4.3.2 – Dose-Response curves for the human cell line of oesophagus carcinoma (OE19) 24 h after photodynamic treatment. The experimental values represent the mean and standard deviation of, at least, three experiments.

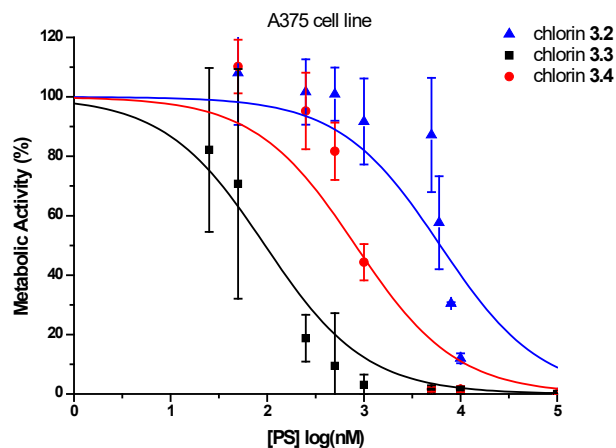


Figure 4.3.3 – Dose-Response curves for the human cell line of skin melanoma (A375) 24 h after photodynamic treatment. The experimental values represent the mean and standard deviation of, at least, three experiments.

It is possible to conclude from these results that there is a great difference in the cytotoxic activity between the diester chlorin and its derivatives on both cell lines, being that the cytotoxicity presented by chlorin 3.3 is the highest of them all and significantly higher than that of chlorin 3.2, being the most promising PS, closely

followed by chlorin **3.4** when it comes to the OE19 cell line. Regarding chlorin **3.4**, however, it's interesting to conclude that it has very different activities between the two cells lines, showing promising results against OE19 cell line, but not so much against melanoma (A375 cell line). The IC₅₀ values and IC₉₅ results are shown in **Table 4.3.1**.

Metabolic Activity						
Cell line	OE19			A375		
Photosensitizer	chlorin 3.2	chlorin 3.3	chlorin 3.4	chlorin 3.2	chlorin 3.3	chlorin 3.4
IC ₅₀ (nM)	5300	57.5	160.7	6800	73.2	911.1
IC ₉₅ (nM)	7793	206.5	360.7	12188	311.2	2812.8

Table 4.3. 1 – IC₅₀ values of chlorins **3.2**, **3.3** and **3.4** against OE19 and A375 cancer cell lines.

It is also important to note the similar behaviour on both cell lines, which have as the most active PS chlorin **3.3** and the least active chlorin **3.2**.

These studies revealed that the small structural differences between chlorins **3.2**, **3.3** and **3.4** culminated in a considerable difference in cytotoxicity. It has been previously reported that one of the factors contributing to the greater efficiency of PDT is the accumulation of PS in tumor cells (Abrahamse *et al.*, 2016) therefore, this increase in the cytotoxicity of the hydrophilic **3.3** and PEGylated **3.4** derivatives will, theoretically, be related to their increased uptake by the cells, which will be discussed later in this section.

In melanomas heavily pigmented with melanin, PDT treatment has some limitations due to the competition between melanin and photosensitizer (Huang *et al.*, 2013) in the absorption of radiation in the "therapeutic window" (650-850 nm). However, the efficiency of chlorin **3.2**, which absorbs at $\lambda = 651$ nm, was remarkably good in the

melanoma (A375) cancer cell line. Thus, chlorin **3.2** appears as a good candidate for use in PDT for the treatment of melanoma cancer with strong pigmentation.

It was also evaluated the metabolic activity of the **3.3** and **3.4** photosensitizers in the absence of light ($IC_{50\text{dark}}$), in order to establish its photosensitizing efficiency, and because one of the ideal characteristics of a PS, as previously stated, is the absence of toxicity in the dark (**Table 4.3.2**). The choice of these two photosensitizers was based simply on their better IC_{50} values, in comparison to **3.2**, which make them the most promising PS and so the ones worthy of continuing studying. All of the other *in vitro* studies were also made with only these two PS for the same reason.

Metabolic Activity				
Cell line	OE19		A375	
Photosensitizer	chlorin 3.3	chlorin 3.4	chlorin 3.3	chlorin 3.4
IC_{50} dark (μM)	4.9	6.6	6.5	7.4
IC_{50} PDT (nM)	57.5	160.7	73.2	911.1
Photosensitivity Efficiency (PE)	85.3	40.8	88.5	8.1

Table 4.3. 2 – IC_{50} in the absence of light (dark) and after irradiation (PDT) of chlorins **3.3** and **3.4** against OE19 and A375 cancer cell line, and respective PE values.

The results of the IC_{50} in the dark and the consequent calculation of the PE allowed to conclude what was already expected: first, none of the photosensitizers showed any signs of toxicity without previous irradiation in the same concentrations as those of the IC_{50} , i.e., at the therapeutic concentrations, which was desirable; and second, chlorin **3.3** proved to have the highest PE and, therefore, to be the most promising on both lines. Chlorin **3.4** showed the worst results on the A375 cell line, which were mainly due to the fact of having an IC_{50} of almost 1 μM after light irradiation. From this, it can be concluded that **3.4** would not be a good choice of PS for this cell line. However, not excluding the possibility of its use for the OE19 one.

With these results, the next step was to analyse deeper into the biological differences of each one and how the structural modulation could be connected to them. So, in addition to the evaluation of metabolic activity, the cellular viability of both lines was tested 24 h after the photodynamic treatment with photosensitizers **3.3** and **3.4**. These results can be found on **Figure 4.3.4**.

3.2. Viability Studies

The viability of the cell cultures was significantly reduced after the photodynamic treatment with both photosensitizers at concentrations lower, equal, or greater than the IC₅₀ of each compound. In melanoma cells, after 24 h of treatment, a significant reduction in viability was observed at concentrations of 250 nM, 500 nM and 1000 nM for chlorin **3.4**, which is extremely interesting since, as stated before, its IC₅₀ in this particular line surrounds the 1 µM. Although viability and metabolic activity not being, obviously, the same, it is expected for these two to be correlated. A decrease on metabolic activity would imply a decrease in viability, however, this is not so linear. This can be due to the fact that the two assays measure different things: MTT assays measures metabolic activity of cytoplasmic enzymes while SRB measures total protein amounts. Besides that, several authors have described that the SRB assay is a much more sensible technique, (Keepers *et al.*, 1991), which could also explain some of the differences observed.

Something very interesting that is also possible to observe in **Figure 4.3.4** is the fact that in melanoma cells, at higher concentrations, more specifically at 500 nM and 1000 nM, **chlorin 3.4** apparently causes a higher decrease in viability than **chlorin 3.3**, which does not go accordingly to previous results. It is even more interesting if it is taken into account that at 500 nM **chlorin 3.3** is way beyond its IC₅₀, while **chlorin 3.4** is only at, approximately, half the concentration of its IC₅₀ value. These observations added to the ones already discussed surrounding these results only reinforce that further studies are, possibly, necessary in order to understand the discrepancies found between these two assays.

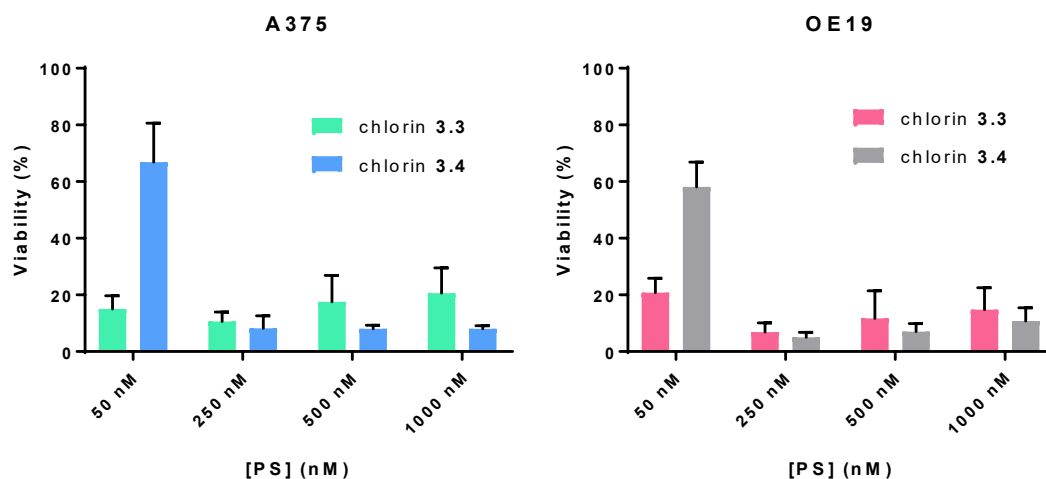


Figure 4.3. 4 – Viability of melanoma cells (A375) and oesophagus carcinoma cells (OE19) 24 h after photodynamic treatment. The results represent the mean and standard deviation of, at least, three experiments

At the same time of evaluation (24 h), oesophageal carcinoma cells, OE19, showed a significant reduction in viability at the same concentrations. However, being that the IC_{50} of chlorin 3.4 for this cell line is 160.7 nM, the results follow the expectations since these cells show a decrease in viability when the concentration goes from 50 nM to 250 nM.

Regarding chlorin 3.3, their profile was very different from chlorin 3.4 showing a reduction on viability right at the concentration of 50 nM, reduction which was maintained almost without significant differences throughout the other concentrations. Since this compound has IC_{50} 's for both cell lines under 100 nM, the results encountered for any concentration higher than that were not surprising. When it comes to the 50 nM, the results can either be explained by the close proximity to the IC_{50} value or maybe to the same hypothesis speculated for chlorin 3.4.

3.3. Uptake Studies

The final *in vitro* study that was chosen to be performed on these photosensitizers took into account the structural differences that were thought and modulated into these two compounds and tried to bring into light the impact these differences might have on the uptake by the cells. The introduction of PEG moieties, in particular, envisions a higher uptake by the cells, since it is a well-known strategy to improve cell permeability. At the same time, the reduction of the ester groups present on **chlorin 3.2** to alcohol groups, originating **chlorin 3.3**, aims to higher hydrophilicity, improving the overall molecular amphiphilicity, which would also translate into a greater uptake by the cells. In order to know the profile of the uptake of these photosensitizers by the cells and to try to understand if the previously characterized and described photochemical properties of the compounds had any influence, uptake studies were carried out. For these studies, the effects of the photosensitizers were, once again, considered for both melanoma and oesophageal carcinoma cell lines. The previous studies showed a clear correlation between photosensitizer concentration and biological activity, and this study shows that there is also a clear correlation between concentration and uptake at any given time, on both cell lines.

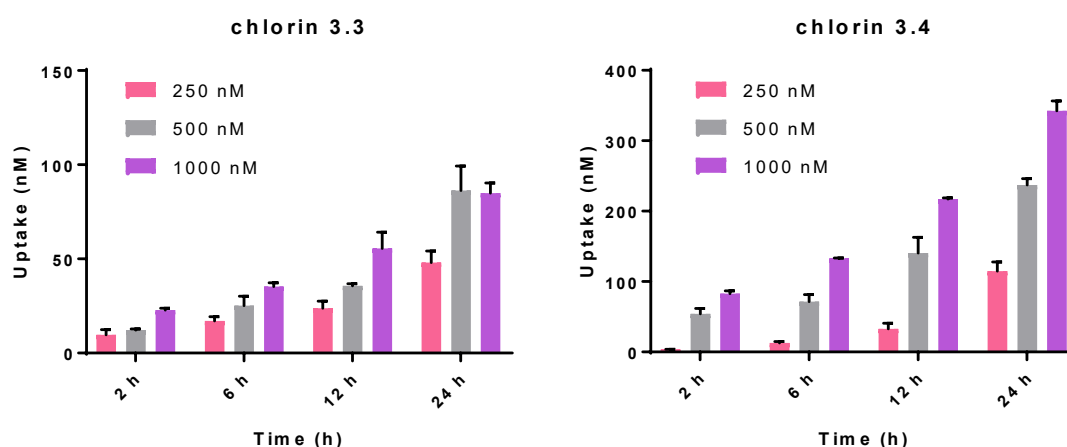


Figure 4.3. 5 – Uptake of the photosensitizers **3.3** (left) and **3.4** (right) at different time points and at different concentrations by cells of oesophageal carcinoma. The results represent the mean and standard deviation of, at least, two experiments.

Through the analysis of the behaviour of these compounds on both cell lines, it is clear that the oesophageal carcinoma line demonstrates a much more linear and expected profile than the melanoma cell line. As it can be seen in **Figure 4.3.5**, uptake of both **chlorin 3.3** and **chlorin 3.4** is enhanced with increasing incubation time in the oesophageal carcinoma cell line, showing best results at 24 h and 1000 nM concentration. These results followed the expectations since an increase in concentration, logically, implies a correspondent increase in uptake.

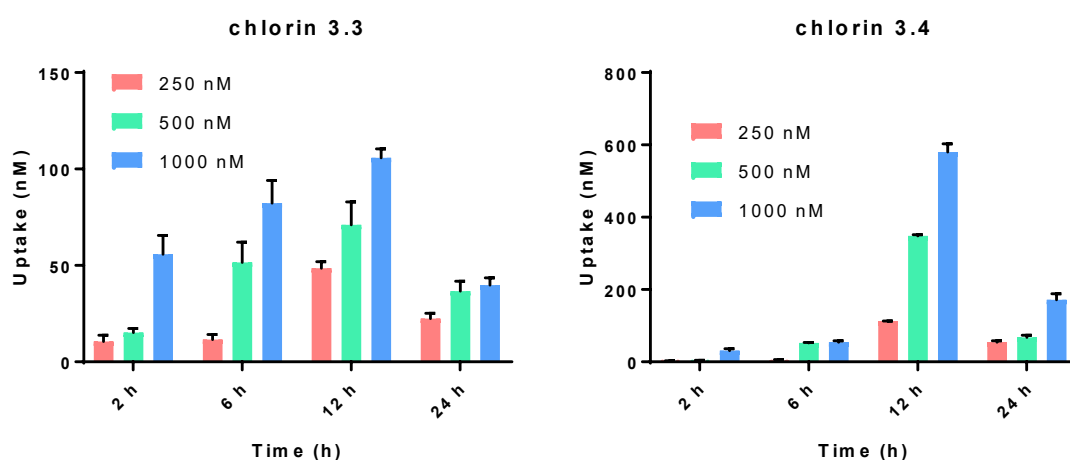


Figure 4.3. 6 – Uptake of the photosensitizers **3.3** (left) and **3.4** (right) at different time points and at different concentrations by cells of skin melanoma. The results represent the mean and standard deviation of, at least, two experiments.

On the other hand, when it comes to the melanoma cell line, this profile is not observed, (**Figure 4.3.6**). It seems that a peak of higher uptake is reached after 12 h and that after that uptake values start to decrease. This can be due to the presence of intrinsic cellular mechanisms responsible for multi-drug resistance, either through drug metabolism or drug expulsion from the intracellular back to the intercellular environment, and might also be the reason for the high IC_{50} values found, more specifically, for **chlorin 3.4** on this line.

In order to understand these results better and to achieve proper conclusions, it would be best to repeat PDT treatment with this compound, and possibly with **chlorin 3.3** also, for this cell line 12 h after PS administration. This study would be of the best interest, in particular for **chlorin 3.4**, since the uptake differences from 6 to 12 and then to 24 h are expressive.

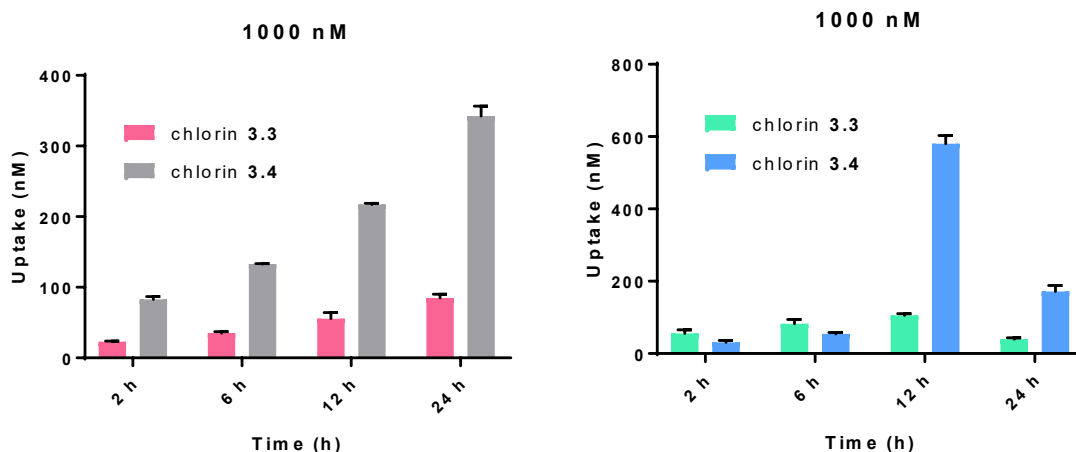


Figure 4.3. 7 – Uptake of the photosensitizers **3.3** and **3.4** at different time points and at 1000 nM by cells of oesophageal carcinoma (left) and skin melanoma (right). The results represent the mean and standard deviation of, at least, two experiments.

Regarding the OE19 cell line (**Figure 4.3.7**), since **chlorins 3.3** and **3.4** have both IC_{50} values under 250 nM for this line and that PDT treatment was done 24 h after PS administration, it is possible to conclude from these results that the uptake of the photosensitizer on a concentration of 48 nM and 115 nM, respectively, is enough to kill 50% of the cells, although, obviously, an higher concentration must be administered in order for these actual concentrations to be uptaken. It is also curious to note that the same administration concentration (250 nM) is uptaken by the cells in different percentages for each compound, more specifically, 19.2% for **chlorin 3.3** and 46% for **chlorin 3.4**, this results being obviously a mean of, at least, two experiments. It is interesting to note that **chlorin 3.3** has shown to always be the most biologically active, but in this case the less uptaken by the cells, which leaves to conclude that maybe **chlorin 3.3** is more intrinsically active than **3.4**, because the different IC_{50} values are, apparently, not related to a higher concentration of one over the other

inside the cells. If this was the case, since **chlorin 3.4** is always in higher concentrations inside the cells, for this cell line (**Figure 4.3.7**), then it would have a lower IC₅₀ value than **chlorin 3.3**.

When it comes to the A375 cell line, the results are not so simple. If the IC₅₀ values are taken into consideration then, at 24 h, the time at which photodynamic treatment was performed, uptake values (mean of at least two experiments) would be of 23 nM (administration concentration of 250 nM, which not being the IC₅₀ for **chlorin 3.3** is still the lowest concentration tested that encompasses it) and 172 nM (administration concentration of 1000 nM), for **chlorins 3.3** and **3.4**, respectively, which can be translated into a 9.2% and 17.2% of uptake by the cells.

However, if the same concentrations are administered but 12 h are considered instead of 24 h, the uptake values would change to 49 nM and 580.5 nM (or 19.6% and 58.1%), respectively. The very different 17.2% to 58.1% change that happens with **chlorin 3.4** by simply changing the time of light irradiation after PS administration from 24 to 12 h, gives enough reason to, in the future, try this approach and see if it translates into a better IC₅₀, which, for this particular chlorin, in this particular cell line, would be of interest since a value of 1 μM is, currently, not good enough. This alteration that is seemingly very simple has apparently drastic outcomes, making it very relevant and worthy of being noticed. The same could be tried for **chlorin 3.3**, however its current IC₅₀ (73.2 nM) does not ask for that much of an optimization.

Moreover, and because it was one of the objectives not only of this study but also of this dissertation, it is possible to conclude that the introduction of PEG moieties is, indeed, a very good strategy to improve cell permeability. It is possible to declare that **chlorin 3.4** most certainly enters the cell, since several washes with PBS are performed before the uptake test is carried out, preventing any compound that is not inside the cell to be considered. It can be argued that this test does not prove that the molecule is indeed taken all the way through the membrane, but after washing with PBS, if the compound is not inside the only other possible options are that it is either contained in the membrane or strongly attached to it, which in itself is already a good enough result. Furthermore, what is sure is that its uptake values, when compared to the non-PEGylated **chlorin 3.3**, are significantly higher, which proves that this strategy was successful and well-thought for an increase in cell permeability.

However, something that may rise some concerns about the PEGylation of these structures is the fact that although, on one hand, it appears to increase their internalization, on the other hand might also change the subcellular localization of these photosensitizers, making them present in organelles or sites of the cell where their action is not as strong or efficient. One of the big advantages of Foscan®, for example, is that it is known to accumulate in organelles such as the mitochondria, which are crucial for the survival of the cell. With PEGylation, that might change, which wouldn't be the best result. Nonetheless, regarding cell line OE19, the IC₅₀ of the PEGylated derivative when compared to the non-PEGylated (chlorin **3.3**), doesn't seem to be significant and when it comes to the A375 cell line, the difference between IC₅₀s, as already mentioned, might be due to inappropriate DLI. This only adds to the conclusion that further studies must be performed in order to rule out any doubts and obtain the most accurate deductions. A good assay for this would be to test irradiation 12 h after chlorin **3.4** administration, while at the same time testing Foscan® in these cell lines so that a fair and true comparison between this commercialized photosensitizer and ours.

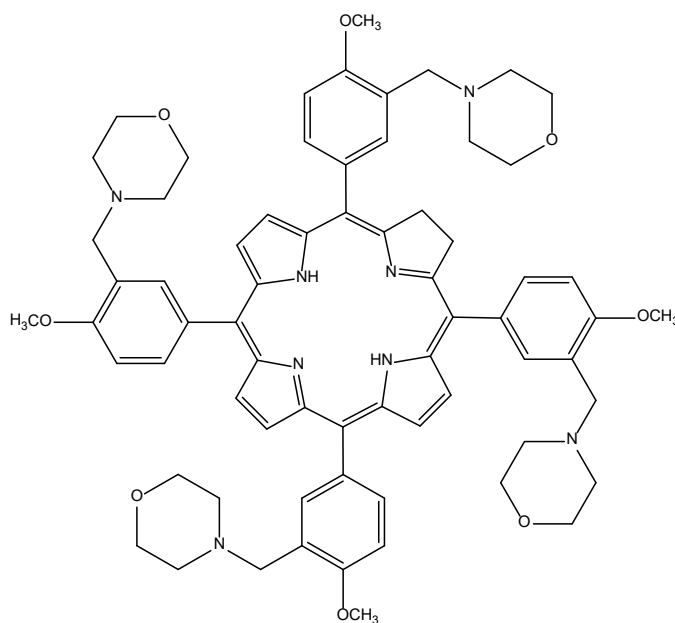
Lastly, in order to prove if the reduction of the ester groups to alcohols also influences cell permeability, it would be necessary to do this same study with **chlorin 3.2**, however it shall not be forgotten that when it comes to IC₅₀ values and metabolic activity, there is, indeed, a significant difference that comes with all these structural alterations.

The results obtained, so far, allowed us to conclude that all compounds revealed dose-dependent anti-proliferative effects and that the increased hydrophilicity of these by either its reduction from di-ester to di-alcohol or the addition PEG moieties, results in a much higher activity against both cancer cell lines.

3.4. Comparison with the literature

The results obtained, although at first sight appear to be very promising, should, however, be considered in comparison with IC₅₀ values of other photosensitizers that, of course, have been evaluated using the same methodology.

Zhang and colleagues, per example, have developed a tetraallyl chlorin (Figure 4.4.1) substituted by methoxyphenyl groups, which has been described as effective and of high potential. The concentrations corresponding to the IC₅₀ of this compound in human oesophageal carcinoma cells submitted to treatment with 12 J/cm² was 1.73 μM (Zhang *et al.*, 2014).



(3-morpholinomethyl-4-methoxyphenyl) chlorin

Figure 4.4 1 – Chemical structure of the chlorin synthesized by Zhang *et al.*

If one compares solely the IC₅₀ values between this compound and all three chlorins in study, it is easily concluded that all of them showed better results (< IC₅₀ values) at the metabolic activity inhibition level of oesophageal carcinoma cells than the photosensitizer proposed by Zhang *et al.*, which allows to be said that these structures are also “effective and of high potential”.

In addition to this, Nishie *et al.* have recently succeeded in the synthesis and isolation of a novel glyco-conjugated compound, hydrophilic O-chlorin having four maltotriose units (Nishie *et al.*, 2016).

In this study, amongst other things, they evaluated its cytotoxicity as a bifunctional photosensitizer for PDT in different cell lines, including two of oesophageal cancer (OE21 and KYSE30).

Previously, the same group had reported that conjugating sugar chains onto photosensitizer compounds increases their cellular uptake and antitumor effect, thus glyco-conjugated chlorin reagents should achieve more effective PDT.

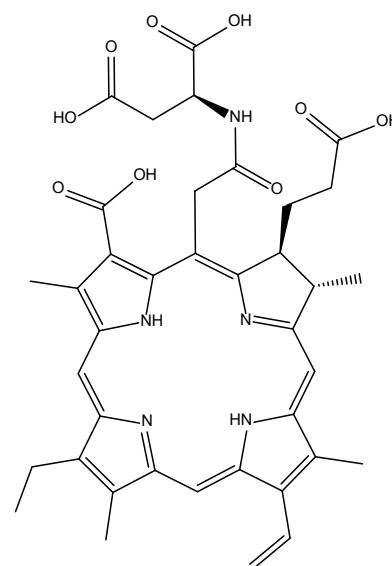


Figure 4.5 - Chemical Structure of TS

While the previously reported glucose-conjugated chlorin (G-chlorin) was a more effective photosensitizer than another widely used photosensitizer, such as Talaporfin Sodium (**Figure 4.5**) it had the disadvantage of being hydrophobic.

The synthesized oligosaccharide-conjugated chlorin (O-chlorin, **Figure 4.4.2**) solved this problem with improved water-solubility and showed higher tumor accumulation than 5-ALA, the longheld 'gold standard' in clinical use worldwide for PDD (photodynamic diagnosis). The higher cellular uptake and accumulation shown by O-chlorin *in vitro* and *in vivo* compared to TS should, therefore, enable lower amounts of photosensitizer to be used clinically for PDT, and, indeed, in this study, the half-maximal inhibitory concentration (IC_{50}) of O-chlorin in cancer cells was, 0.33 μM , against the 17.4 μM of Talaporfin Sodium (TS).

These results are very curious because not only the chlorin backbone is very similar structurally to the ones studied in this dissertation, but also the main objective was the same, to improve cellular uptake and phototoxicity by cells through conjugation of moieties, in this case maltotriose, to do so. Through the comparison of the results

obtained by Nishie *et al.* with this structural modification, it is possible to conclude that PEGylation seems to have a similar result than that of glycosylation, with the added advantage that O-chlorin presents a higher IC₅₀ value than either one of **chlorins 3.3** and **3.4** (58 and 161 nM, respectively). Although this might not be the most faithful comparison since the cell lines used are not the same, it does not invalidate the fact that the chlorins synthesized for this dissertation show promising and interesting results when faced with the ones described in the literature.

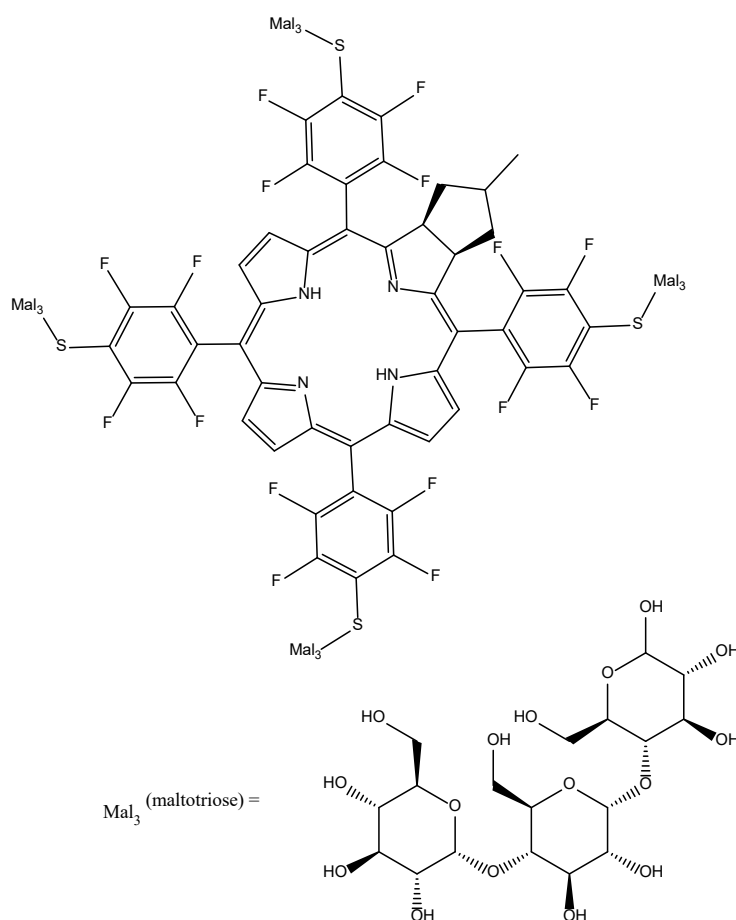


Figure 4.4 2 – Chemical structure of O-chlorin

Still regarding oesophageal carcinoma, Foscan® ((**Figure 4.4.3**) has an IC₅₀ greater than 0.5 μM when tested against the OE21 cancer cell line (Paszko *et al.*, 2013), and, although this is not the same cell line as the one used for the studies conducted in the

experimental part of this dissertation, it can still be considered relevant information, because this cell line has the same origin and Foscan® is an approved and clinically used drug, setting a comparison standard for all subsequently developed photosensitizers. Having this, **chlorins 3.3** and **3.4** have IC₅₀ values lower than that of Foscan®, which suggests they might be more efficient in the matter of cell viability. This is a very attention-grabbing result especially in the case of **chlorin 3.3** since it is a decrease of practically an order of magnitude. When it comes to melanoma, it was not possible to find any data using Foscan® against the A375 cell line. However, in a comparative study of several photosensitizers irradiated with 1.5 J/cm² in A431 squamous cell carcinoma cells, the Foscan® IC₅₀ was the lowest, 30 nM, against 1.94 μM of Photofrin® and 393 μM of the 5-ALA, other two of the most used PS in PDT. Knowing that the most potent of the chlorins studied for this dissertation (**chlorin 3.3**) showed an IC₅₀ of 73 nM, it is undeniable that Foscan® presents itself as more efficient than this one. Still, when compared to the other two photosensitizers, the differences are too significant to not be taken into account.

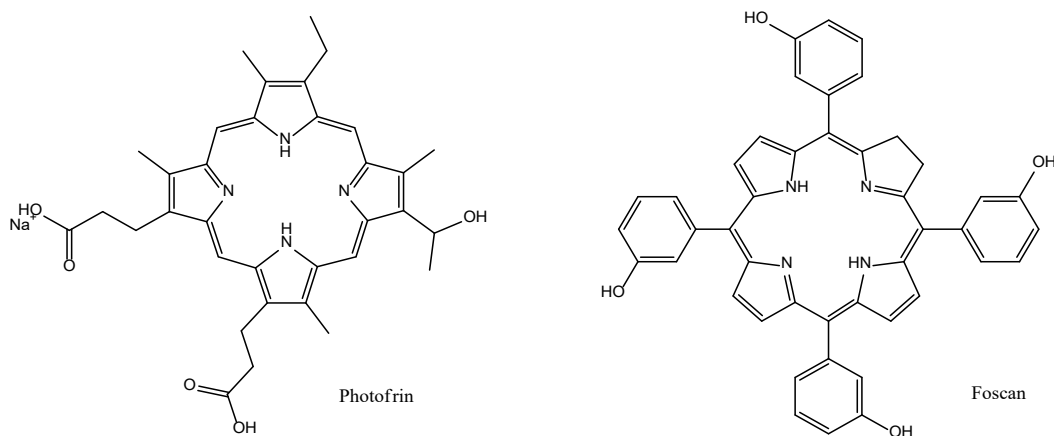


Figure 4.4 3 – Chemical structures of Photofrin® and Foscan®

Lastly, comparing the results obtained with the developed chlorins with the ones from the literature regarding the phenyl derivatives instead of the pentafluorophenyl ones, some conclusions can be taken, which might be of some interest. Preliminary studies on the photodynamic activity of 4,5,6,7-tetrahydropyrazolo[1,5-*a*]pyridine-fused

chlorins (**Figure 4.4.4**) against melanoma cells proved this class of compounds to be very active as photodynamic agents against melanocytic (A375) and amelanotic (C32) cancer cells (Pereira *et al.*, 2015).

Interestingly, dihydroxymethylchlorin **4.2** was particularly active against human melanocytic melanoma cells ($IC_{50} = 31$ nM), just as **chlorin 3.3** proved to be the most active of all the tested photosensitizers (Pereira *et al.*, 2017). Despite **chlorin 4.2** having, seemingly, a lower IC_{50} (31 nM) than **chlorin 3.3** (73 nM), meaning it would be more active, the differences do not seem to be that relevant, and, besides that, **chlorin 3.3** presents other advantages such as the possibility of PEGylation itself, strategy which is, actually, already being explored. Final synthesis has apparently been achieved, following the same protocol of PEGylation of **chlorin 3.2** but for **chlorin 3.3**, and confirmation through mass spectrometry and NMR is currently pendent. If this is confirmed, another promising compound could come from this which studying would be of the best interest.

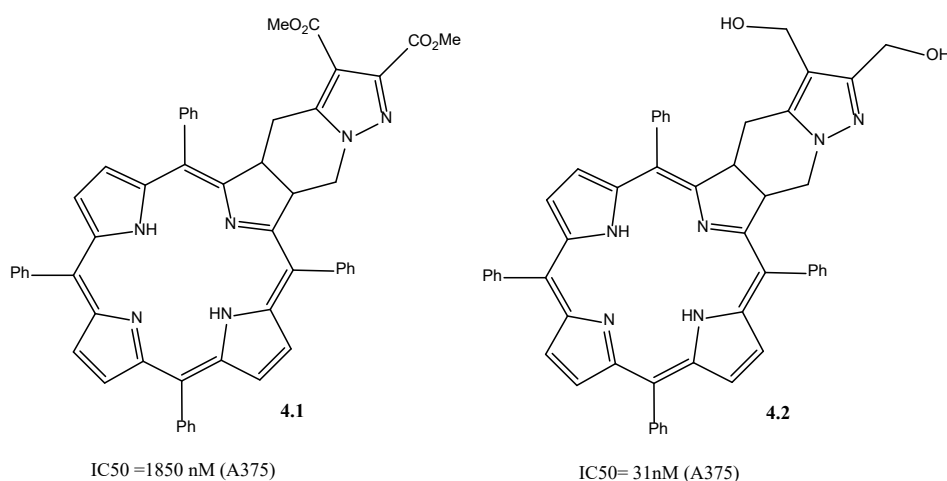


Figure 4.4 4 – Chemical structures of 4,5,6,7-tetrahydropyrazolo[1,5-*a*]pyridine-fused chlorins with photodynamic activity against melanoma cell line (A375).

Conclusions

PDT is a highly multidisciplinary field that involves chemists, physicists, biologists, engineers, and physicians; chemists, of course, are constantly seeking to design, synthesize, purify and characterize new compounds that, in the case of PDT, can be used as PSs.

Throughout this dissertation were presented and discussed the results obtained in the experimental work, which included the synthesis, characterization and *in vitro* evaluation of chlorin derivatives to their application in PDT. From the experimental work, important conclusions were able to be taken and need emphasizes, as well as the prospect of future work. The synthesized and characterized photosensitizers demonstrated photochemical properties suitable for use as a photosensitizer in photodynamic therapy, starting with the fact that seem to have no tendency to aggregate possibly because the steric interaction between the halogen atoms and hydrogen atoms in β positions, increases the angle between the macrocycle and the phenyl ring. In addition, the *in vitro* photodynamic effect of these photosensitizers has shown to be promising for therapeutic application by the finding of IC_{50} values in the nanomolar range in cell lines of various types of cancer, namely oesophageal carcinoma and melanocytic melanoma.

Chlorin 3.3, in particular, has shown not only the lowest IC_{50} for both melanoma and oesophageal carcinoma tumor cells but also good uptake values. **Chlorin 3.4**, however, showed good results for the oesophageal carcinoma cell line regarding all cytotoxicity, cellular viability, and uptake by cells, and promising results for cellular uptake by melanoma cells at 12 h. This opens a line of discussion for further studies involving different time lines of light-irradiation, in order to discover if there is an improvement of IC_{50} values for this cell line. This is of extreme importance because, as explained in the Introduction, high melanin levels in pigmented tumors can lead to optical interference via competition with the photosensitizer for light absorption, which together with the antioxidant effect of melanin can compromise PDT of melanoma. Therefore, it was very pleasant to observe that the new ring-fused chlorins, especially chlorin **3.3** which showed nanomolar activity against A375 melanoma cell lines, are

excellent candidates to be used in PDT of melanoma since they absorb at longer wavelengths than the 500-600 nm interval where melanin is the dominant absorber. Through these studies, it was also possible to conclude that the pentafluorophenyl group at the *meso* position of the chlorin, besides the well-established advantages it brings with the addition of halogens to the molecular structure, is a great substituent to carry out chemical reactions such as nucleophilic aromatic substitution, and, consequently, that PEGylation is an interesting and successful approach in order to increase cellular uptake.

The results obtained demonstrate that these chlorins meet some of the main requirements of an ideal PS and are, thereby, potential photosensitizers for PDT. In the future, it will be necessary to determine other relevant characteristics for their possible use as a photosensitizer in PDT, starting by completing the photophysical studies (calculate quantum yields of fluorescence, triplet state formation, and singlet oxygen), in order not only to characterize them, but also to understand if the addition of the pentafluorophenyl groups at the *meso* position indeed influences their photophysical properties, as it is believed to happen according to the literature.

Another objective at the start of this dissertation, that was not able to be achieved, was the study of the influence of the length of the PEG-moiety on cytotoxicity and cellular uptake. For that, 2-(2-(2-aminoethoxy)ethoxy)ethanol and 2-(2-(2-(2-aminoethoxy)ethoxy)ethoxy)ethoxy)ethanol amine-PEGs would be tested. PEGylation of **chlorin 3.2** with these two amine-PEGs was accomplished in a successful manner, however, isolation was not carried out due to time impediments. The continuation of this study might be of interest and a possible work for the future, especially since the results with **chlorin 3.4** showed such promising effects at the cellular uptake level.

Also, as already stated, it would be of interest to try and study the PEGylated derivative of **chlorin 3.3** and see if the added lipophilicity would lower even further the IC₅₀.

Future Perspectives

The development of this experimental work allowed to acquire knowledge and optimization of procedures, which at a later stage it is ambitious to extend to another study strand. A future objective, given the synthesized structures, might be to develop photosensitizers not only for a therapeutic intent but also molecules with a structural analogy that can be labeled with a radioisotope, making possible the acquisition of molecular images by the application of nuclear medicine techniques. In order to combine these two premises into a single photosensitizer, it would be necessary to continue to develop chemical synthesis associated with radioactive complexation so that in the future, in a single administration, the possibility of diagnosis and personalized treatment would be associated.

The use of photosensitizers complexed with radioisotopes begins a personalized medicine approach in photodynamic therapy, through nuclear medicine, with a possibility of diagnosis, therapy, and follow-up.

In the perspective of the development of a photosensitizer with properties suitable for the diagnostic application, as mentioned in the Introduction, fluorinated molecules are currently the basis for many APIs, due to their biocompatibility conferring, in many cases, greater specificity for their molecular targets and the possibility of labeling with fluoride-18.

Thus, in order to proceed with the radioactive labeling of macrocycles with fluoride-18 and its evaluation for potential application as new contrast agents, using the PET technique, first it would be needed to optimize the laboratory synthesis of the fluorination reaction with a non-radioactive fluorinating agent, maybe taking advantage of the S_NAr reaction that these molecules can undergo at the *para* position of the pentafluorophenyl group at the *meso* position of the macrocycle.

Another possible application of the synthesized compounds for the future would be to explore their properties as photosensitizers not only for PDT but also for photodynamic inactivation (PDI) instead. Photodynamic inactivation (PDI) presents several

advantages over the classic antibacterial and antiviral therapies, from the high selectivity of photosensitizers to the generation of cytotoxic reactive oxygen species near the target. PDI relies on the selective introduction of PSs into targeted cells to undergo apoptosis by singlet oxygen generated through light irradiation. The aim of the project would, therefore, be the development of new tetrahydropyrazolo[1,5- α]pyridine-fused chlorins as a novel class of PDI agents. Their characteristics of not only showing enhanced chemical stability and the required degree of hydrophilicity but also their rich pattern of absorption bands within the phototherapeutic window (600 and 800 nm), which balances deeper penetration of tissues with providing enough energy to excite the oxygen to its singlet state (most effective wavelengths inferior to 800 nm), makes these compounds very active promising PDI agents.

The discovery of the first antibiotics changed dramatically the quality of our life. For the first time, it was possible to effectively control infectious diseases. In addition, the increasing knowledge about the complex mechanisms of viral pathogenesis has greatly contributed to the rapid development of antiviral drugs.

Unfortunately, the use of large quantities of antibiotics and antivirals to control infections in human and animal diseases has created exceptional conditions for mobilization of resistance elements in microorganism populations and their capture by previously antibiotic and antiviral sensitive pathogens.

Consequently, there is an urgent need to find other methods for reducing the antimicrobial and antiviral resistance problem. Fortunately, alternative therapies exist and, at the forefront of research, lay the photodynamic inhibition approach mediated by porphyrin-based photosensitizers.

PDI has recently been considered as a viable alternative method to antibiotic and antiviral chemotherapy of infective diseases. PDI has shown potential to eliminate all currently known classes of microorganism. Moreover, PDI treatment itself is unlikely to cause resistance, as microbial apoptosis by ROS proceeds via a nonspecific inhibition mechanism as compared with antibiotics that inhibit a specific enzyme or feature of the microbial. PDI is a simple and controllable method which requires the combined action of oxygen, light and a photosensitizer (PS), which absorbs and uses the energy from light to produce those ROS. Therefore, the photodynamic effects depend on multiple variables including the structural features of the PS. The majority

of PS used in PDI is derived from tetrapyrrolic macrocycles such as porphyrins, chlorins and bacteriochlorins, which are involved in very important biological functions, such as respiration (heme group) and photosynthesis (chlorophyll and bacteriochlorophyll) (Kyziol *et al.*, 2017).

Why invest in these chlorins?

Recently, Durantini *et al.* demonstrate that 5,10,15,20-tetrakis [4-(3-N,N-dimethylaminopropoxy)phenyl]chlorin (TAPC) was more efficient in photoinactivation of *E. coli*, *S. aureus* and *C. albicans* than its porphyrin analog. This might be because chlorins differ significantly from porphyrins in greater absorption at longer wavelengths ($\lambda_{\max} = 650\text{--}670$ nm) (Kyziol *et al.*, 2017).

Previous work carried out by the research team has already demonstrated that 4,5,6,7-tetrahydropyrazolo[1,5-*a*]pyridine-fused chlorins are excellent photosensitizers for the generation of generation of cytotoxic reactive oxygen species (ROS).

Part of the focus of this dissertation was the synthesis of PEGylated 4,5,6,7-tetrahydropyrazolo[1,5-*a*]pyridine-fused chlorins and their application as PDT agents for cancer therapy. Their found exceptional antitumoral activity is believed to be not only due to their action as photosensitizers but also because of their biocompatibility characteristics given by the incorporation of polyethylene glycol (PEGs) moieties, a strategy applied in drug design to achieve compounds with the ideal properties to be used in biological media and to improve cell permeability. Therefore, combining these features with the required structural modulation for the application in PDI should lead to a novel group of very active PDI agents against viruses and bacteria.

Knowing all of this, and since PDI has been growing as a promising alternative therapy to conventional antiviral and antibacterial treatments, the objective would be to take the advantages of these chlorins and study them as promising new agents for PDI of viruses and bacteria.

The rational design of PS for PDI of microorganisms can determine many of their photophysical properties and has been mostly based on the modification of porphyrins. For instance, protonation or incorporation of halogen atoms in the macrocycle changes the balance between fluorescence and intersystem crossing and can influence many

photophysical parameters. In addition, it has been shown that the location and binding site of the PS, which is highly dependent on the structure and intramolecular charge distribution, is an important factor in microbial PDI. The presence of a positive charge in the PS structure seems to be important to target Gram-negative bacteria, but negatively charged molecules may be effective for Gram-positive bacteria. Besides, they seem to have a superior activity towards microbial species and a relative selectivity over host mammalian cells, enabled by increased binding and penetration through the negatively charged bacteria outer barrier (**Figure 5.1**) (Xu *et al.*, 2016; Yuan *et al.*, 2017).

Another example is that in order to be efficient as photosensitizing agents for viral PDI, the photosensitizers must bind specifically to vital viral components. However, there is a difference in target selectivity depending on the mechanism involved: sugar moieties are usually attacked by radicals (generated via type I process) and guanine residues are the targets of singlet oxygen (generated via type II process). The positive charges on the PS molecule appear to promote a tight electrostatic interaction between the positively charged PS and the negatively charged sites at the viral capsids and envelopes, orientating the PS toward sites, which are critical for the stability and metabolism of a particular microorganism. This kind of association increases the efficiency of the photoinactivation process (Costa *et al.* 2012).

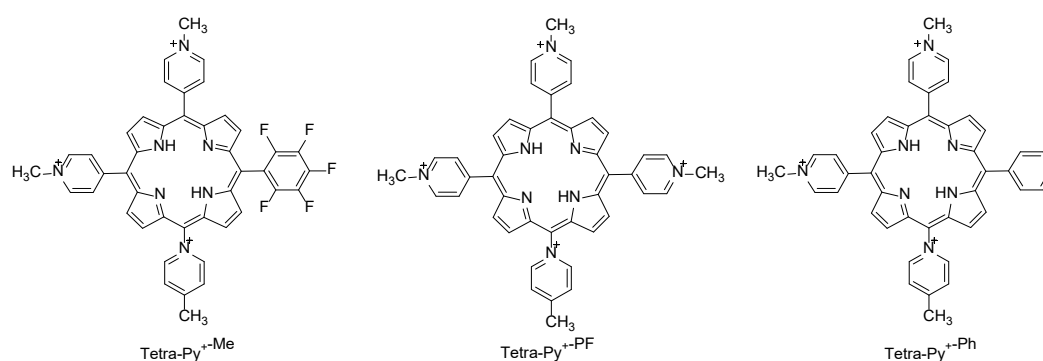


Figure 5. 1 – Chemical structures of investigated photosensitizers.

However, the intrinsic characteristics of the unnatural cationic groups do not endow the derivatives with good biocompatibility. So another important issue in designing

efficient photosensitizers is their lipophilicity and solubility in biocompatible media. Thus, hydrophilic substituents are frequently inserted into the macrocycle in order to develop clinically relevant photosensitizers, like PEG moieties or native basic amino acids, (for example L-lysine, L-histidine and L-arginine), which can be covalently conjugated with amino porphyrins as cationic auxiliary groups (Jiang *et al.*, 2016).

Based on this, some structures, along with a strategic route for their synthesis, can be proposed (**Figure 5.2** and **Scheme 5.1**, respectively) that not only gather all the usual PS characteristics but also other factors that affect their efficiency as PS for PDI.

Factors like chemical and structural stability with the introduction of a fused ring, which prevent back oxidation to the porphyrin state and photobleaching; the heavy atom effect” from the abundance of Fluor atoms in *ortho* and *meta* positions of the pentafluorophenyl groups in the *meso* position of the macrocycle; the possibility to easily functionalize them on the *para* position of the same groups; and enhanced lipophilicity through possible PEGylation or ester (fused-ring) reduction. The next step would be to modulate these structures in order to adjust them as PS agents for PDI against viruses and bacteria, which would include the incorporation of the previously stated characteristics, such as positive charges in their structure, and to study their antimicrobial activity and mechanism of action. Initially, the potential *in vitro* cytotoxicity of the compounds would be investigated and only those compounds that show no relevant cellular toxicity would be further investigated.

Up to now, the synthesized chlorins have shown promising results as PS agents for PDT against cancer cell lines (like OE19), with $50 \text{ nM} < \text{IC}_{50} < 250 \text{ nM}$ and so, it is only logical to explore their action as PS for PDI against viruses and bacteria.

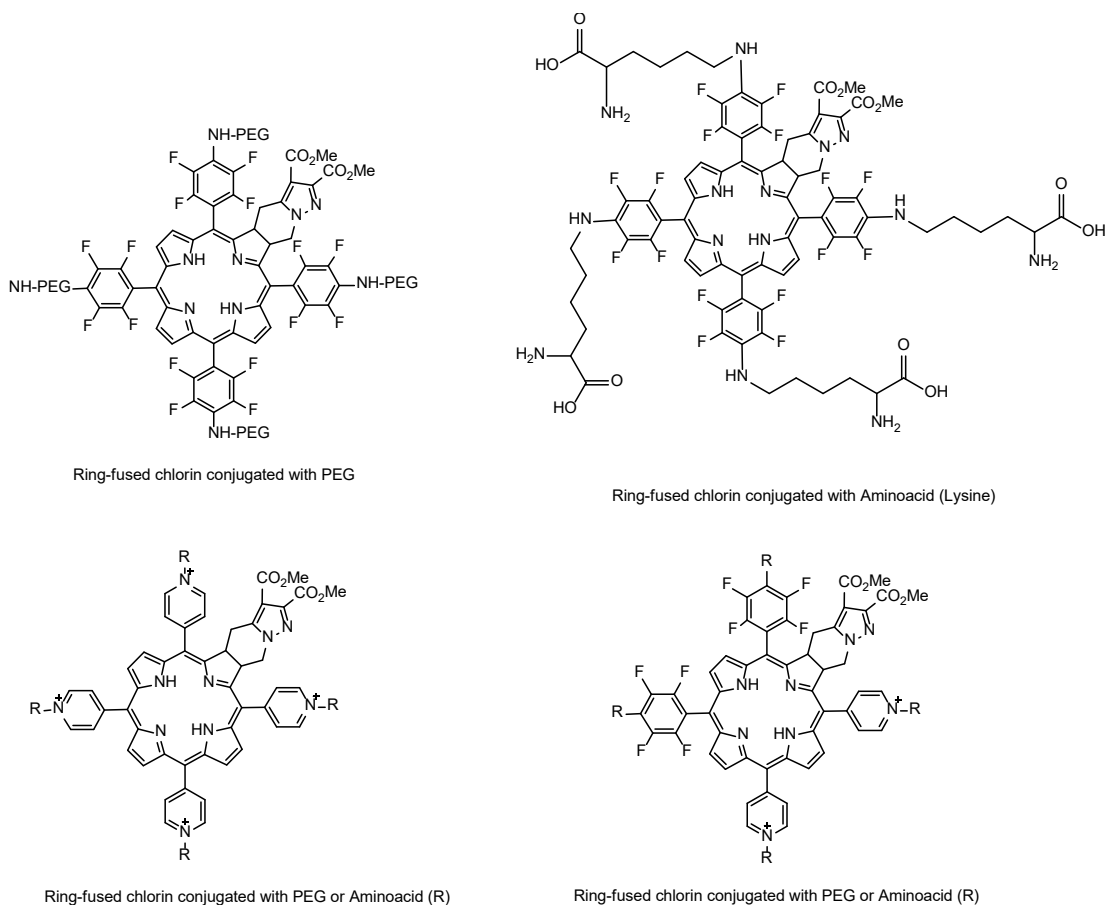
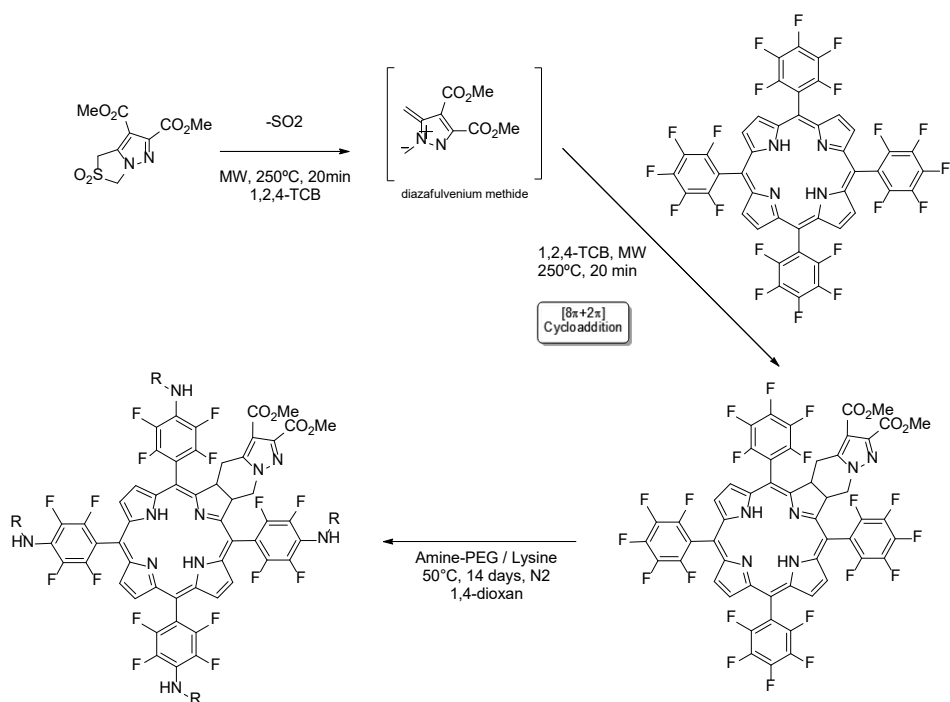


Figure 5. 2 – Some of the proposed structures



Scheme 5.1 – Example of the proposed synthetic route for one of the compounds

References

- ✓ Abrahamse, H.; Hamblin, M. R. New Photosensitizers for Photodynamic Therapy. *Biochemical Journal* 2016, 473 (4), 347–364. DOI:10.1042/Bj20150942
- ✓ Ackroyd, R.; Kelty, C.; Brown, N.; Reed, M. The History of Photodetection and Photodynamic Therapy. *Photochemistry and Photobiology* 2007, 74 (5), 656–669. DOI:10.1562/0031-8655(2001)0740656THOPAP2.0.CO2
- ✓ Agostinis, P.; Berg, K.; Cengel, K. A.; Foster, T. H.; Girotti, A. W.; Gollnick, S. O.; Hahn, S. M.; Hamblin, M. R.; Juzeniene, A.; Kessel, D.; et al. Photodynamic Therapy of Cancer: An Update. *CA: A Cancer Journal for Clinicians* 2011, 61 (4), 250–281.
- ✓ Allison, R. R. Photodynamic Therapy: Oncologic Horizons. *Future Oncology* 2014, 10 (1), 123–124.
- ✓ Allum, W. H.; Blazeby, J. M.; Griffin, S. M.; Cunningham, D.; Jankowski, J. A.; Wong, R. Guidelines for the Management of Oesophageal and Gastric Cancer. *Gut* 2011, 60 (11), 1449–1472. DOI:10.1136/Gut.2010.228254
- ✓ Altman, S. A.; Randers, L.; Rao, G. Comparison of Trypan Blue Dye Exclusion and Fluorometric Assays for Mammalian Cell Viability Determinations. *Biotechnology Progress* 1993, 9 (6), 671–674. DOI:10.1021/bp00024a017
- ✓ Anand, S.; Ortel, B. J.; Pereira, S. P.; Hasan, T.; Maytin, E. V. Biomodulatory Approaches to Photodynamic Therapy for Solid Tumors. *Cancer Letters* 2012, 326 (1), 8–16. DOI:10.1016/J.Canlet.2012.07.026
- ✓ Parusel, A. B. J.; Grimme, S. DFT/MRCI Calculations on the Excited States of Porphyrin, Hydroporphyrins, Tetrazaporphyrins and Metalloporphyrins. *Journal of Porphyrins and Phthalocyanines (JPP)* 2001, 5 (3), 225–232. DOI:10.1002/jpp.310
- ✓ Armarego, W. L. F.; Perrin, D. D. Purification of Laboratory Chemicals, Fourth Edition, Butterworth-Heinemann, Oxford: MA, USA, 1997
- ✓ Arnaut, L. G. *Advances in Inorganic Chemistry*. R.S.G VanEldik.: 2011
- ✓ Aschner, M. et al. (Ed) *Cell Culture Techniques*, Humana Press Inc.: New Jersey, 2011
- ✓ Berlanda, J.; Kiesslich, T.; Engelhardt, V.; Krammer, B.; Plaetzer, K. Comparative in Vitro Study on the Characteristics of Different Photosensitizers Employed in PDT. *Journal of Photochemistry and Photobiology B: Biology* 2010, 100 (3), 173–180. DOI:10.1016/j.jphotobiol.2010.06.004
- ✓ Bonnett, R. Photosensitizers of the Porphyrin and Phthalocyanine Series for Photodynamic Therapy. *Chemical Society Reviews* 1995, 24 (1), 19. DOI:10.1039/CS9952400019
- ✓ Brown, S. B.; Brown, E. A.; Walker, I. The Present and Future Role of Photodynamic Therapy in Cancer Treatment. *The Lancet Oncology* 2004, 5 (8), 497–508. DOI:10.1016/S1470-2045(04)01529-3
- ✓ Bruckner, C.; McCarthy, J. R.; Daniell, H. W.; Pendon, Z. D. ; Ilagan, R. P.; Francis, T. M.; Ren, L.; Birge, R. R.; Frank, H. A. *Chemical Physics* 2003, 294, 285-303.
- ✓ Brückner, C.; Luciano, M. Modifications of Porphyrins and Hydroporphyrins for Their Solubilization in Aqueous Media. *Molecules* 2017, 22 (6), 980. DOI:10.3390/molecules22060980
- ✓ Brückner, C.; Dolphin, D. 2,3-Vic-Dihydroxy-Meso-Tetraphenylchlorins from the Osmium Tetroxide Oxidation of Meso-Tetraphenylporphyrin. *Tetrahedron Letters* 1995, 36 (19), 3295–3298. DOI: 10.1016/0040-4039(95)00524-G

- ✓ Brückner, C.; Dolphin, D. B, β - β '-dihydroxylation of Meso-Tetraphenylchlorins and Metallochlorins. *Tetrahedron Letters* 1995, 36 (52), 9425–9428. DOI: 10.1016/0040-4039(95)02052-7
- ✓ Byrne, A. T.; O'Connor, A. E.; Hall, M.; Murtagh, J.; O'Neill, K.; Curran, K. M.; Mongrain, K.; Rousseau, J. A.; Lecomte, R.; McGee, S.; et al. Vascular-Targeted Photodynamic Therapy with BF₂-Chelated Tetraaryl-Azadipyromethene Agents: A Multi-Modality Molecular Imaging Approach to Therapeutic Assessment. *British Journal of Cancer* 2009, 101 (9), 1565–1573. DOI:10.1038/Sj.Bjc.6605247
- ✓ Calvete, Mário J. F.; Gomes, Ana. T. P. C.; Moura, Nuno M. M. *Rev. Virtual Quim.* 2009; 1, 92-103.
- ✓ Carmichael, J.; DeGraff, W.G.; Gazdar, A. F.; Minna, J. D.; Mitchell, J. B. Evaluation of a Tetrazolium-Based Semiautomated Colorimetric Assay: Assessment of Chemosensitivity Testing, *Cancer Res* 1987, 47, 936–942.
- ✓ Castano, A. P.; Mroz, P.; Hamblin, M. R. Photodynamic Therapy and Anti-Tumour Immunity. *Nature Reviews Cancer* 2006, 6 (7), 535–545. DOI:10.1038/Nrc1894
- ✓ Cavaleiro, J. A. S.; Smith, K. M. *Rev. Port. Quím.*, 1989, 31, 29
- ✓ Cavaleiro, J. A. S.; Neves, M. G. P. M.; Tomé, A. C.; Silva, A. M. S.; Faustino, M. A. F.; Lacerda, P. S.; Silva, A. M. G. Porphyrin Derivatives: Synthesis and Potential Applications. *Journal of Heterocyclic Chemistry* 2000, 37 (3), 527–534. DOI:10.1002/jhet.5570370310
- ✓ Cole, S. P. C. Rapid Chemosensitivity Testing of Human Lung Tumor Cells Using the MTT Assay. *Cancer Chemotherapy and Pharmacology* 1986, 17 (3). DOI:10.1007/BF00256695
- ✓ Costa, J. I. T.; Tomé, A. C.; Neves, M. G. P. M. S.; Cavaleiro, J. A. S. 5,10,15,20-Tetrakis(pentafluorophenyl)porphyrin: A Versatile Platform to Novel Porphyrinic Materials. *Journal of Porphyrins and Phthalocyanines* 2011, 15 (11n12), 1116–1133. DOI:10.1142/S1088424611004294
- ✓ Costa, L.; Faustino, M. A. F.; Neves, M. G. P. M. S.; Cunha, Â.; Almeida, A. Photodynamic Inactivation of Mammalian Viruses and Bacteriophages. *Viruses* 2012, 4 (7), 1034–1074. DOI:10.3390/V4071034
- ✓ Da Silva, E. F. F.; Pedersen, B. W.; Breitenbach, T.; Toftegaard, R.; Kuimova, M. K.; Arnaut, L. G.; Ogilby, P. R. Irradiation- and Sensitizer-Dependent Changes in the Lifetime of Intracellular Singlet Oxygen Produced in a Photosensitized Process. *The Journal of Physical Chemistry B* 2011, 116 (1), 445–461. DOI:10.1021/Jp206739y.
- ✓ Davila, M. L. Photodynamic Therapy. *Gastrointestinal Endoscopy Clinics of North America* 2011, 21 (1), 67–79. DOI:10.1016/J.Giec.2010.09.002
- ✓ Denizot, F.; Lang, R. Rapid Colorimetric Assay for Cell Growth and Survival. *Journal of Immunological Methods* 1986, 89 (2), 271–277. DOI:10.1016/0022-1759(86)90368-6
- ✓ Desjardins, A.; Flemming, J.; Sternberg, E. D.; Dolphin, D. Nitrogen Extrusion from Pyrazoline-Substituted Porphyrins and Chlorins Using Long Wavelength Visible Light. *Chemical Communications* 2002, No. 22, 2622–2623. DOI:10.1039/B208368J
- ✓ Dias, N.M., Nicolau, A., Carvalho, G., Mota, M., & Lima, N. Miniaturization and application of the MTT assay to evaluate metabolic activity of protozoa in the presence of toxicants. *Journal of basic microbiology* 1999, 39 (2), 103-8.

- ✓ Fan, X.; Ouyang, N.; Teng, H.; Yao, H. Isolation and Characterization of Spheroid Cells from the HT29 Colon Cancer Cell Line. *International Journal of Colorectal Disease* 2011, 26 (10), 1279–1285. DOI:10.1007/s00384-011-1248-y
- ✓ Ferlay, J.; Soerjomataram, I.; Dikshit, R.; Eser, S.; Mathers, C.; Rebelo, M.; Parkin, D. M.; Forman, D.; Bray, F. Cancer Incidence and Mortality Worldwide: Sources, Methods and Major Patterns in GLOBOCAN 2012. *International Journal of Cancer* 2014, 136 (5), E359–E386. DOI:10.1002/ijc.29210
- ✓ Freimoser, F. M., Jakob, C. A., Aebi, M., & Tuor, U. The MTT [3-(4,5-Dimethylthiazol-2-yl)-2,5-Diphenyltetrazolium Bromide] Assay Is a Fast and Reliable Method for Colorimetric Determination of Fungal Cell Densities. *Applied and Environmental Microbiology* 1999, 65 (8), 3727–3729.
- ✓ Freshney, R. *Culture of Animal Cells: A Manual Of Basic Technique*, John Wiley & Sons Inc.: New Jersey, 2005
- ✓ Gao, Y.; Pan, J. G.; Huang, Y. J.; Ding, S. Y.; Wang, M. L. Microwave-Assisted Synthesis of Fluorine Substituted Porphyrins and Kinetics of Formation of Zinc Porphyrin Complexes in Acetic Acid. *Journal of Porphyrins and Phthalocyanines* 2015, 19 (12), 1251–1255. DOI:10.1142/S1088424615501096
- ✓ Gouterman, M. Spectra of Porphyrins. *Journal of Molecular Spectroscopy* 1961, 6, 138–163. DOI:10.1016/0022-2852(61)90236-3
- ✓ GOUTERMAN, M. Optical Spectra and Electronic Structure of Porphyrins and Related Rings. In *The Porphyrins*; Elsevier, 1978; pp 1–165. DOI:10.1016/B978-0-12-220103-5.50008-8
- ✓ Gouterman, M.; Wagnière, G. H.; Snyder, L. C. Spectra of Porphyrins. *Journal of Molecular Spectroscopy* 1963, 11 (1–6), 108–127. DOI:10.1016/0022-2852(63)90011-0
- ✓ Hamid, R.; Rotshteyn, Y.; Rabadi, L.; Parikh, R.; Bullock, P. Comparison of Alamar Blue and MTT Assays for High through-Put Screening. *Toxicology in Vitro* 2004, 18 (5), 703–710. DOI:10.1016/j.tiv.2004.03.012
- ✓ Hatz, S.; Poulsen, L.; Ogilby, P. R. Time-Resolved Singlet Oxygen Phosphorescence Measurements from Photosensitized Experiments in Single Cells: Effects of Oxygen Diffusion and Oxygen Concentration. *Photochemistry and Photobiology* 2008, 84 (5), 1284–1290. DOI:10.1111/J.1751-1097.2008.00359.X.
- ✓ Hopper, C. Photodynamic Therapy: A Clinical Reality In The Treatment Of Cancer. *Lancet Oncology*: 2000, 1: 212–219
- ✓ Huang, Y.-Y.; Vecchio, D.; Avci, P.; Yin, R.; Garcia-Diaz, M.; Hamblin, M. R. Melanoma Resistance to Photodynamic Therapy: New Insights. *Biological Chemistry* 2013, 394 (2). DOI:10.1515/Hsz-2012-0228
- ✓ Huang, Z.; Chen, Q.; Shakil, A.; Chen, H.; Beckers, J.; Shapiro, H.; Hetzel, F. W. Hyperoxygenation Enhances the Tumor Cell Killing of Photofrin-Mediated Photodynamic Therapy[¶]. *Photochemistry and Photobiology* 2007, 78 (5), 496–502. DOI:10.1562/0031-8655(2003)0780496HETTCK2.0.CO2
- ✓ Huang, Z.; Xu, H.; Meyers, A. D.; Musani, A. I.; Wang, L.; Tagg, R.; Barqawi, A. B.; Chen, Y. K. Photodynamic Therapy for Treatment of Solid Tumors — Potential and Technical Challenges. *Technology in Cancer Research & Treatment* 2008, 7 (4), 309–320. DOI:10.1177/153303460800700405

- ✓ Hunter, C. A.; Sanders, J. K. M. The Nature of π - π Interactions. *Journal of the American Chemical Society* 1990, 112 (14), 5525–5534. DOI:10.1021/ja00170a016
- ✓ Hyland, M. A.; Morton, M. D.; Brückner, C. Meso-Tetrakis(pentafluorophenyl)porphyrin-Derived Chromene-Annulated Chlorins. *The Journal of Organic Chemistry* 2012, 77 (7), 3038–3048. DOI:10.1021/jo3001436
- ✓ Jiang, L.; Gan, C. R. R.; Gao, J.; Loh, X. J. A Perspective on the Trends and Challenges Facing Porphyrin-Based Anti-Microbial Materials. *Small* 2016, 12 (27), 3609–3644. DOI:10.1002/Sml.201600327
- ✓ Juarranz, Á.; Jaén, P.; Sanz-Rodríguez, F.; Cuevas, J.; González, S. Photodynamic Therapy of Cancer. Basic Principles and Applications. *Clinical and Translational Oncology* 2008, 10 (3), 148–154. DOI:10.1007/S12094-008-0172-2.
- ✓ Juzeniene, A.; Juzenas, P.; Ma, L.-W.; Iani, V.; Moan, J. Effectiveness of Different Light Sources for 5-Aminolevulinic Acid Photodynamic Therapy. *Lasers in Medical Science* 2004, 19 (3), 139–149. DOI:10.1007/S10103-004-0314-X
- ✓ Karch, J.; Molkentin, J. D. Regulated Necrotic Cell Death. *Circulation Research* 2015, 116 (11), 1800–1809. DOI:10.1161/CIRCRESAHA.116.305421.
- ✓ Kasha, M.; Rawls, H. R.; Ashraf El-Bayoumi, M. The Exciton Model in Molecular Spectroscopy. *Pure and Applied Chemistry* 1965, 11 (3–4). DOI:10.1351/pac196511030371
- ✓ Keepers, Y. P.; Pizao, P. E.; Peters, G. J.; van Ark-Otte, J.; Winograd, B.; Pinedo, H. M. Comparison of the Sulforhodamine B Protein and Tetrazolium (MTT) Assays for in Vitro Chemosensitivity Testing. *European Journal of Cancer and Clinical Oncology* 1991, 27 (7), 897–900. DOI:10.1016/0277-5379(91)90142-Z
- ✓ Kessel, D. More Adventures in Photodynamic Therapy. *International Journal of Molecular Sciences* 2015, 16 (12), 15188–15193. DOI:10.3390/ijms160715188
- ✓ Kessel, D.; Morgan, A.; Garbo, G. M. Sites and Efficacy of Photodamage by Tin Etiopurpurin *In Vitro* Using Different Delivery Systems. *Photochemistry and Photobiology* 1991, 54 (2), 193–196. DOI:10.1111/j.1751-1097.1991.tb02006.x
- ✓ Kessel, D.; Reiners, J. J. Apoptosis and Autophagy After Mitochondrial or Endoplasmic Reticulum Photodamage. *Photochemistry and Photobiology* 2007, 83 (5), 1024–1028. DOI:10.1111/J.1751-1097.2007.00088.X
- ✓ Kushibiki, T.; Hirasawa, T.; Okawa, S.; Ishihara, M. Responses of Cancer Cells Induced by Photodynamic Therapy. *Journal of Healthcare Engineering* 2013, 4 (1), 87–108. DOI:10.1260/2040-2295.4.1.87
- ✓ Kvíčala, J.; Beneš, M.; Paleta, O.; Král, V. Regiospecific Nucleophilic Substitution in 2,3,4,5,6-Pentafluorobiphenyl as Model Compound for Supramolecular Systems. Theoretical Study of Transition States and Energy Profiles, Evidence for Tetrahedral SN2 Mechanism. *Journal of Fluorine Chemistry* 2010, 131 (12), 1327–1337. DOI:10.1016/j.jfluchem.2010.09.003
- ✓ Regiel-Futyra, A.; Dąbrowski, J. M.; Mazuryk, O.; Śpiewak, K.; Kyzioł, A.; Pucelik, B.; Brindell, M.; Stochel, G. Bioinorganic Antimicrobial Strategies in the Resistance Era. *Coordination Chemistry Reviews* 2017, 351, 76–117. DOI:10.1016/J.Ccr.2017.05.005
- ✓ Langdon, S. *Cancer Cell Culture: Methods and Protocols*, Humana Press Inc: New Jersey, 2004

- ✓ Lascelles, J. (1964). *Tetrapyrrole Biosynthesis and its Regulation*. Nova York., A. Benjamim, Inc
- ✓ Lehninger, R. A. L; Nelson, D.L; Cox, M. M. (2000). *Princípios de Bioquímica*. São Paulo.Sarvier, São Paulo.
- ✓ Lindsey, J. S.; Hsu, H. C.; Schreiman, I. C. Synthesis of Tetraphenylporphyrins under Very Mild Conditions. *Tetrahedron Letters* 1986, 27 (41), 4969–4970. DOI:10.1016/S0040-4039(00)85109-6
- ✓ Lindsey, J. S.; Schreiman, I. C.; Hsu, H. C.; Kearney, P. C.; Marguerettaz, A. M. Rothmund and Adler-Longo Reactions Revisited: Synthesis of Tetraphenylporphyrins under Equilibrium Conditions. *The Journal of Organic Chemistry* 1987, 52 (5), 827–836. DOI:10.1021/jo00381a022:
- ✓ Lindsey, J. S.; Wagner, R. W. Investigation of the Synthesis of Ortho-Substituted Tetraphenylporphyrins. *The Journal of Organic Chemistry* 1989, 54 (4), 828–836. DOI:10.1021/jo00265a021
- ✓ Liu, Y.; Peterson, D. A.; Kimura, H.; Schubert, D. Mechanism of Cellular 3-(4,5-Dimethylthiazol-2-Yl)-2,5-Diphenyltetrazolium Bromide (MTT) Reduction. *Journal of Neurochemistry* 2002, 69 (2), 581–593. DOI:10.1046/j.1471-4159.1997.69020581.x
- ✓ Liu, W. M.; Dalgleish, A. G. MTT Assays Can Underestimate Cell Numbers. *Cancer Chemotherapy and Pharmacology* 2009, 64 (4), 861–862. DOI:10.1007/s00280-009-1047-0
- ✓ Lodish, H.; Berk, A.; Kaiser, C. A.; Krieger, M.; Scott, M. P.; Bretscher, A.; Ploegh, H.; Matsudaira, P.; Uzman, A. *Molecular Cell Biology, Sixth Edition. Biochemistry and Molecular Biology Education* 2010, 38 (1), 60–61. DOI:10.1002/bmb.20373
- ✓ Louis, K. S.; Siegel, A. C. Cell Viability Analysis Using Trypan Blue: Manual and Automated Methods. In *Methods in Molecular Biology*; Humana Press, 2011; pp 7–12. DOI:10.1007/978-1-61779-108-6_2
- ✓ Machado, A. E. da H. *Terapia Fotodinâmica: Princípios, Potencial de Aplicação E Perspectivas*. *Química Nova* 2000, 23 (2), 237–243. DOI:10.1590/S0100-40422000000200015
- ✓ Maestrin, A. P. J.; Ribeiro, A. O.; Tedesco, A. C.; Neri, C. R.; Fábio, S. A novel chlorin derivative of Meso-tris(pentafluorophenyl)-4-pyridylporphyrin: synthesis photophysics and photochemical properties. *Journal of Brazilian Chemical Society* 2004, 15 (6), 923–930.
- ✓ Masters, J. *Animal Cell Culture: A Practical Approach*, Oxford University Press: Oxford, 2000
- ✓ Milgrom, L. R.; Smith, R. A. The Colours of Life: An Introduction to the Chemistry of Porphyrins and Related Compounds. *Journal of Chemical Education* 1997, 75 (4), 420.
- ✓ Mitton, D.; Ackroyd, R. A Brief Overview of Photodynamic Therapy in Europe. *Photodiagnosis and Photodynamic Therapy* 2008, 5 (2), 103–111. DOI:10.1016/J.Pdpdt.2008.04.004
- ✓ Mosmann, T. Rapid Colorimetric Assay for Cellular Growth and Survival: Application to Proliferation and Cytotoxicity Assays. *Journal of Immunological Methods* 1983, 65 (1–2), 55–63. DOI:10.1016/0022-1759(83)90303-4
- ✓ Muthiah, C.; Taniguchi, M.; Kim, H.-J.; Schmidt, I.; Kee, H. L.; Holten, D.; Bocian, D. F.; Lindsey, J. S. Synthesis and Photophysical Characterization of Porphyrin, Chlorin and Bacteriochlorin Molecules Bearing Tethers for Surface Attachment. *Photochemistry and Photobiology* 2007, 83 (6), 1513–1528. DOI:10.1111/j.1751-1097.2007.00195.x
- ✓ Nascimento, B. F. O. *Synthetic Studies of Nitrogen-Containing Heterocycles Under Microwave Irradiation*; Universidade De Coimbra: Coimbra, 2013

- ✓ Nascimento, B. F. O.; Rocha Gonsalves, A. M. d'A.; Pineiro, M. MnO₂ instead of Quinones as Selective Oxidant of Tetrapyrrolic Macrocycles. *Inorganic Chemistry Communications* 2010, 13 (3), 395–398. DOI:10.1016/J.Inoche.2009.12.032
- ✓ Nemykin, V. N.; Hadt, R. G. Interpretation of the UV–vis Spectra of thmeso(Ferrocenyl)-Containing Porphyrins Using a TDDFT Approach: Is Gouterman's Classic Four-Orbital Model Still in Play? *The Journal of Physical Chemistry A* 2010, 114 (45), 12062–12066. DOI:10.1021/jp1083828
- ✓ Nishie, H.; Kataoka, H.; Yano, S.; Kikuchi, J.; Hayashi, N.; Narumi, A.; Nomoto, A.; Kubota, E.; Joh, T. A next-Generation Bifunctional Photosensitizer with Improved Water-Solubility for Photodynamic Therapy and Diagnosis. *Oncotarget* 2016, 7 (45). DOI:10.18632/oncotarget.12366
- ✓ Nyman, E. S.; Hynninen, P. H. Research Advances in the Use of Tetrapyrrolic Photosensitizers for Photodynamic Therapy. *Journal of Photochemistry and Photobiology B: Biology* 2004, 73 (1–2), 1–28. DOI:10.1016/j.jphotobiol.2003.10.002
- ✓ O'Connor, A. E.; Gallagher, W. M.; Byrne, A. T. Porphyrin and Nonporphyrin Photosensitizers in Oncology: Preclinical and Clinical Advances in Photodynamic Therapy. *Photochemistry and Photobiology* 2009, 85 (5), 1053–1074. DOI:10.1111/J.1751-1097.2009.00585.X
- ✓ Ormond, A.; Freeman, H. Dye Sensitizers for Photodynamic Therapy. *Materials* 2013, 6 (3), 817–840. DOI:10.3390/ma6030817
- ✓ Ortel B, Shea CR, Calzavara-Pinton PG: Molecular mechanisms of photodynamic therapy. *Frontiers in Bioscience* 14, 4157-4172
- ✓ Papazisis, K. .; Geromichalos, G. .; Dimitriadis, K. .; Kortsaris, A. . Optimization of the Sulforhodamine B Colorimetric Assay. *Journal of Immunological Methods* 1997, 208 (2), 151–158. DOI:10.1016/S0022-1759(97)00137-3
- ✓ Pappas, D. *Practical Cell Analysis*; John Wiley & Sons, Ltd: New York, 2010
- ✓ Parusel, A. B. J.; Grimme, S. DFT/MRCI Calculations on the Excited States of Porphyrin, Hydroporphyrins, Tetrazaporphyrins and Metalloporphyrins. *Journal of Porphyrins and Phthalocyanines (JPP)* 2001, 5 (3), 225–232. DOI: 10.1002/jpp.310
- ✓ Paszko, E.; Vaz, G. M. F.; Ehrhardt, C.; Senge, M. O. Transferrin Conjugation Does Not Increase the Efficiency of Liposomal Foscan during in Vitro Photodynamic Therapy of Oesophageal Cancer. *European Journal of Pharmaceutical Sciences* 2013, 48 (1–2), 202–210. DOI:10.1016/J.Ejps.2012.10.018
- ✓ Patani, G. A.; LaVoie, E. J. Bioisosterism: A Rational Approach in Drug Design. *Chemical Reviews* 1996, 96 (8), 3147–3176. DOI:10.1021/cr950066q
- ✓ Pereira, N. A. M.; Fonseca, S. M.; Serra, A. C.; Pinho e Melo, T. M. V. D.; Burrows, H. D. [8π+2π] Cycloaddition of Meso-Tetra- and 5,15-Diarylporphyrins: Synthesis and Photophysical Characterization of Stable Chlorins and Bacteriochlorins. *European Journal of Organic Chemistry* 2011, 2011 (20–21), 3970–3979. DOI:10.1002/Ejoc.201100465
- ✓ Pereira, N. A. M.; Laranjo, M.; Casalta-Lopes, J.; Serra, A. C.; Piñeiro, M.; Pina, J.; Seixas de Melo, J. S.; Senge, M. O.; Botelho, M. F.; Martelo, L.; et al. Platinum(II) Ring-Fused Chlorins as Near-Infrared Emitting Oxygen Sensors and Photodynamic Agents. *ACS Medicinal Chemistry Letters* 2017, 8 (3), 310–315. DOI:10.1021/Acsmedchemlett.6b00476

- ✓ Pereira, N. A. M.; Laranjo, M.; Pineiro, M.; Serra, A. C.; Santos, K.; Teixo, R.; Abrantes, A. M.; Gonçalves, A. C.; Sarmiento Ribeiro, A. B.; Casalta-Lopes, J.; et al. Novel 4,5,6,7-tetrahydropyrazolo[1,5-A]pyridine Fused Chlorins as Very Active Photodynamic Agents for Melanoma Cells. *European Journal of Medicinal Chemistry* 2015, 103, 374–380. DOI:10.1016/J.Ejmech.2015.08.059
- ✓ Pereira, N. A. M.; Laranjo, M.; Pina, J.; Oliveira, A. S. R.; Ferreira, J. D.; Sánchez-Sánchez, C.; Casalta-Lopes, J.; Gonçalves, A. C.; Sarmiento-Ribeiro, A. B.; Piñeiro, M.; et al. Advances on Photodynamic Therapy of Melanoma through Novel Ring-Fused 5,15-Diphenylchlorins. *European Journal of Medicinal Chemistry* 2018, 146, 395–408. DOI:10.1016/J.Ejmech.2017.12.093
- ✓ Pereira, N. A. M.; Serra, A. C.; Pinho e Melo, T. M. V. D. Novel Approach to Chlorins and Bacteriochlorins: $[8\pi+2\pi]$ Cycloaddition of Diazafulvenium Methides with Porphyrins. *European Journal of Organic Chemistry* 2010, 2010 (34), 6539–6543. DOI:10.1002/Ejoc.201001157
- ✓ Pereira, N.; Serra, A. C.; Pineiro, M.; Gonsalves, A. M. d'A. R.; Abrantes, M.; Laranjo, M.; Botelho, F. Synthetic Porphyrins Bearing β -Propionate Chains as Photosensitizers for Photodynamic Therapy. *Journal of Porphyrins and Phthalocyanines* 2010, 14 (5), 438–445. DOI:10.1142/S1088424610002227
- ✓ Pineiro, M.; Pereira, M. M.; Rocha Gonsalves, A. M. d'; Arnaut, L. G.; Formosinho, S. J. Singlet Oxygen Quantum Yields from Halogenated Chlorins: Potential New Photodynamic Therapy Agents. *Journal of Photochemistry and Photobiology A: Chemistry* 2001, 138 (2), 147–157. DOI:10.1016/S1010-6030(00)00382-8.
- ✓ Pinto, S. M. A.; Henriques, C. A.; Tomé, V. A.; Vinagreiro, C. S.; Calvete, M. J. F.; Dąbrowski, J. M.; Piñeiro, M.; Arnaut, L. G.; Pereira, M. M. Synthesis Of meso-Substituted Porphyrins Using Sustainable Chemical Processes. *Journal of Porphyrins and Phthalocyanines* 2016, 20 (01n04), 45–60. DOI: 10.1142/S1088424616300020
- ✓ Plaetzer, K.; Krammer, B.; Berlanda, J.; Berr, F.; Kiesslich, T. Photophysics and Photochemistry of Photodynamic Therapy: Fundamental Aspects. *Lasers in Medical Science* 2008, 24 (2), 259–268. DOI:10.1007/S10103-008-0539-1
- ✓ Pucelik, B.; Paczyński, R.; Dubin, G.; Pereira, M. M.; Arnaut, L. G.; Dąbrowski, J. M. Properties of Halogenated and Sulfonated Porphyrins Relevant for the Selection of Photosensitizers in Anticancer and Antimicrobial Therapies. *PLOS ONE* 2017, 12 (10), e0185984. DOI:10.1371/Journal.Pone.0185984
- ✓ Woodward, R. B.; Hoffmann, R. Die Erhaltung der Orbitalsymmetrie. *Angewandte Chemie International Edition in English*, 1969, 8, 781-853. DOI: 10.1002/ange.19690812102
- ✓ Ricchelli, F. Photophysical Properties of Porphyrins in Biological Membranes. *Journal of Photochemistry and Photobiology B: Biology* 1995, 29 (2–3), 109–118. DOI: 10.1016/1011-1344(95)07155-U
- ✓ Robertson, C. A.; Evans, D. H.; Abrahamse, H. Photodynamic Therapy (PDT): A Short Review on Cellular Mechanisms and Cancer Research Applications for PDT. *Journal of Photochemistry and Photobiology B: Biology* 2009, 96 (1), 1–8. DOI:10.1016/J.Jphotobiol.2009.04.001
- ✓ Samaroo, D.; Vinodu, M.; Chen, X.; Drain, C. M. Meso-Tetra(pentafluorophenyl)porphyrin as an Efficient Platform for Combinatorial Synthesis and the Selection of New Photodynamic Therapeutics Using a Cancer Cell Line. *Journal of Combinatorial Chemistry* 2007, 9 (6), 998–1011.

DOI:10.1021/Cc070067j

- ✓ Senge, M. O. mTHPC – A Drug on Its Way from Second to Third Generation Photosensitizer? *Photodiagnosis and Photodynamic Therapy* 2012, 9 (2), 170–179. DOI:10.1016/J.Pdpdt.2011.10.001
- ✓ (1Senge, M.; Ryan, A.; Letchford, K.; MacGowan, S.; Mielke, T. Chlorophylls, Symmetry, Chirality, and Photosynthesis. *Symmetry* 2014, 6 (3), 781–843. DOI: 10.3390/sym6030781
- ✓ Serra, A.; Pineiro, M.; Santos, C. I.; Rocha Gonsalves, A. M. d'Á.; Abrantes, M.; Laranjo, M.; Botelho, M. F. In Vitro Photodynamic Activity of 5,15-bis(3-Hydroxyphenyl)porphyrin and Its Halogenated Derivatives Against Cancer Cells. *Photochemistry and Photobiology* 2010, 86 (1), 206–212. DOI: 10.1111/j.1751-1097.2009.00622.x
- ✓ Serra, A.; Pineiro, M.; Pereira, N.; Rocha Gonsalves, A.; Laranjo, M.; Abrantes, M.; Botelho, F. A Look at Clinical Applications and Developments of Photodynamic Therapy. *Oncology Reviews* 2008, 2 (4), 235–249. DOI:10.1007/S12156-008-0081-1
- ✓ Serra, A. C.; Pineiro, M.; Rocha Gonsalves, A. M. d'Á.; Abrantes, M.; Laranjo, M.; Santos, A. C.; Botelho, M. F. Halogen Atom Effect on Photophysical and Photodynamic Characteristics of Derivatives of 5,10,15,20-tetrakis(3-Hydroxyphenyl)porphyrin. *Journal of Photochemistry and Photobiology B: Biology* 2008, 92 (1), 59–65. DOI:10.1016/J.Jphotobiol.2008.04.006
- ✓ Sibata, C. H.; Colussi, V. C.; Oleinick, N. L.; Kinsella, T. J. [NO TITLE AVAILABLE]. *Brazilian Journal of Medical and Biological Research* 2000, 33 (8), 869–880. DOI:10.1590/S0100-879X2000000800002
- ✓ Silva, A. M. G.; Tomé, A. C.; Neves, M. G. P. M. S.; Cavaleiro, J. A. S.; Kappe, C. O. Porphyrins in Diels–Alder Reactions. Improvements on the Synthesis of Barrelene-Fused Chlorins Using Microwave Irradiation. *Tetrahedron Letters* 2005, 46 (28), 4723–4726. DOI: 10.1016/j.tetlet.2005.05.047
- ✓ Silva, A. M. G.; Tomé, A. C.; Neves, M. G. P. M. S.; Cavaleiro, J. A. S. Porphyrins in 1,3-Dipolar Cycloaddition Reactions: Synthesis of a Novel Pyrazoline-Fused Chlorin and a Pyrazole-Fused Porphyrin. *Synlett* 2002, 2002 (7), 1155–1157. DOI: 10.1055/s-2002-32581
- ✓ Silva, A. M. G.; Tomé, A. C.; Neves, M. G. P. M. S.; Silva, A. M. S.; Cavaleiro, J. A. S. Meso-Tetraarylporphyrins as Dipolarophiles in 1,3-Dipolar Cycloaddition Reactions. *Chemical Communications* 1999, No. 17, 1767–1768. DOI: 10.1039/A905016G
- ✓ Sinha, B. and Kumar, R. (2008). *Principles of animal cell culture*. Lucknow: IBDC.
- ✓ Smith, K. M.; Lavallee, D. K. A Review of: 'Porphyrins and Metalloporphyrins, Ed., Elsevier Scientific Publishing Company, New York, N.Y., 1975, 910 Pp, \$112.20 (Hardcover), \$36.50 (Paperback).' *Synthesis and Reactivity in Inorganic and Metal-Organic Chemistry* 1978, 8 (1), 97–98. DOI: 10.1080/00945717808057392
- ✓ Pinho e Melo, T. M. V. D.; Soares, M. I. L.; Rocha Gonsalves, A. M. d'Á. New Chemistry of Diazafulvenium Methides: One Way to Pyrazoles. *Tetrahedron Letters* 2006, 47 (5), 791–794. DOI: 10.1016/J.Tetlet.2005.11.094
- ✓ Souza, J. M.; de Assis, F. F.; Carvalho, C. M. B.; Cavaleiro, J. A. S.; Brocksom, T. J.; de Oliveira, K. T. Synthesis of Non-Aggregating Chlorins and Isobacteriochlorins from Meso-Tetrakis(pentafluorophenyl)porphyrin: A Study Using 1,3-Dipolar Cycloadditions under Mild Conditions. *Tetrahedron Letters* 2014, 55 (8), 1491–1495. DOI:10.1016/J.Tetlet.2014.01.049

- ✓ Stockert, J. C.; Blázquez-Castro, A.; Cañete, M.; Horobin, R. W.; Villanueva, Á. MTT Assay for Cell Viability: Intracellular Localization of the Formazan Product Is in Lipid Droplets. *Acta Histochemica* 2012, 114 (8), 785–796. DOI: 10.1016/j.acthis.2012.01.006
- ✓ Sutcliffe, O. B.; Storr, R. C.; Gilchrist, T. L.; Rafferty, P. Cycloadditions to Pyrrolo[1,2-C]thiazoles and Pyrazolo[1,5-C]thiazoles. *Tetrahedron* 2000, 56 (51), 10011–10021. DOI: 10.1016/S0040-4020(00)00956-X
- ✓ Tomé, A. C.; Lacerda, P. S. S.; Neves, M. G. P. M. S.; Cavaleiro, J. A. S. Meso-Arylporphyrins as Dienophiles in Diels–Alder Reactions: A Novel Approach to the Synthesis of Chlorins, Bacteriochlorins and Naphthoporphyrins. *Chemical Communications* 1997, No. 13, 1199–1200. DOI: 10.1039/A702504A
- ✓ Tran, M.; Swavey, S. Porphyrin and Phthalocyanine Photosensitizers as PDT Agents: A New Modality for the Treatment of Melanoma. In *Recent Advances in the Biology, Therapy and Management of Melanoma*; InTech, 2013. DOI:10.5772/54940 255
- ✓ Triesscheijn, M.; Baas, P.; Schellens, J. H. M.; Stewart, F. A. Photodynamic Therapy in Oncology. *The Oncologist* 2006, 11 (9), 1034–1044. DOI:10.1634/Theoncologist.11-9-1034
- ✓ Van Tonder, A.; Joubert, A. M.; Cromarty, A. Limitations of the 3-(4,5-Dimethylthiazol-2-Yl)-2,5-Diphenyl-2H-Tetrazolium Bromide (MTT) Assay When Compared to Three Commonly Used Cell Enumeration Assays. *BMC Research Notes* 2015, 8 (1), 47. DOI:10.1186/s13104-015-1000-8
- ✓ Vichai, V.; Kirtikara, K. Sulforhodamine B Colorimetric Assay for Cytotoxicity Screening. *Nature Protocols* 2006, 1 (3), 1112–1116. DOI:10.1038/Nprot.2006.179
- ✓ Vlasov, V. M. Fluoride Ion as a Nucleophile and a Leaving Group in Aromatic Nucleophilic Substitution Reactions. *Journal of Fluorine Chemistry* 1993, 61 (3), 193–216. DOI:10.1016/S0022-1139(00)80104-9
- ✓ Voigt, W. Sulforhodamine B Assay and Chemosensitivity. In *Chemosensitivity*; Humana Press; pp 039–048. DOI:10.1385/1-59259-869-2:039
- ✓ Whitlock, H. W.; Hanauer, R.; Oester, M. Y.; Bower, B. K. Diimide Reduction of Porphyrins. *Journal of the American Chemical Society* 1969, 91 (26), 7485–7489. DOI:10.1021/Ja01054a044
- ✓ Xu, Z.; Gao, Y.; Meng, S.; Yang, B.; Pang, L.; Wang, C.; Liu, T. Mechanism and In Vivo Evaluation: Photodynamic Antibacterial Chemotherapy of Lysine-Porphyrin Conjugate. *Frontiers in Microbiology* 2016, 7. DOI:10.3389/Fmich.2016.00242
- ✓ Yano, T., Hatogai, K., Morimoto, H., Yoda, Y., & Kaneko, K. Photodynamic therapy for esophageal cancer. *Annals Of Translational Medicine*, 2014, 2(3). DOI:10.21037/3538
- ✓ Yoo, J.-O.; Ha, K.-S. New Insights into the Mechanisms for Photodynamic Therapy-Induced Cancer Cell Death. In *International Review of Cell and Molecular Biology*; Elsevier, 2012; pp 139–174. DOI: 10.1016/B978-0-12-394306-4.00010-1
- ✓ Yuan, Y.; Liu, Z.-Q.; Jin, H.; Sun, S.; Liu, T.-J.; Wang, X.; Fan, H.-J.; Hou, S.-K.; Ding, H. Photodynamic Antimicrobial Chemotherapy with the Novel Amino Acid-Porphyrin Conjugate 4I: In Vitro and in Vivo Studies. *PLOS ONE* 2017, 12 (5), e0176529. DOI:10.1371/Journal.Pone.0176529
- ✓ Zhang, L.-J.; Bian, J.; Bao, L.-L.; Chen, H.-F.; Yan, Y.-J.; Wang, L.; Chen, Z.-L. Photosensitizing Effectiveness of a Novel Chlorin-Based Photosensitizer for Photodynamic Therapy in Vitro and in

Vivo. *Journal of Cancer Research and Clinical Oncology* 2014, 140 (9), 1527–1536.
DOI:10.1007/S00432-014-1717-0

✓ Zhu, S.; Wu, F.; Wang, K.; Zheng, Y.; Li, Z.; Zhang, X.; Wong, W.-K. Photocytotoxicity, Cellular Uptake and Subcellular Localization of Amidinophenylporphyrins as Potential Photodynamic Therapeutic Agents: An in Vitro Cell Study. *Bioorganic & Medicinal Chemistry Letters* 2015, 25 (20), 4513–4517. DOI:10.1016/J.Bmcl.2015.08.072

